NASA TECHNICAL MEMORANDUM

NASA TM X-52209

NASA TM X-52209

CURRENT STATUS OF PLANE CRACK TOUGHNESS TESTING

by William F. Brown, Jr., and John E. Srawley
Lewis Research Center
Cleveland, Ohio

TECHNICAL PAPER proposed for presentation at Annual Meeting of the
American Society for Testing and Materials
Atlantic City, New Jersey, June 29, 1966

NATIONAL AERONAUTICS AND SPACE ADMINISTRATION · WASHINGTON, D.C. · 1966

CURRENT STATUS OF PLANE CRACK TOUGHNESS TESTING

by William F. Brown, Jr., and John E. Srawley

Lewis Research Center
Cleveland, Ohio

TECHNICAL PAPER proposed for presentation at

Annual Meeting of the American Society for Testing and Materials
Atlantic City, New Jersey, June 29, 1966

NATIONAL AERONAUTICS AND SPACE ADMINISTRATION

CONTENTS

CURRENT STATUS OF PLANE CRACK TOUGHNESS TESTING

by William F. Brown, Jr., and John E. Srawley

Lewis Research Center
National Aeronautics and Space Administration
Cleveland, Ohio

INTRODUCTION

This report deals with the design and testing of crack-notched specimens for determination of the resistance of materials to unstable opening-mode crack extension under plane strain conditions. Test methods concerned with subcritical crack extension due to repeated loading or agressive environments are not discussed. It is assumed that the reader will be familiar with the terminology and concepts of linear elastic fracture mechanics used in earlier reports of ASTM Committee E-24 on Fracture Testing of Metals (refs. 1-5). Much of the background has been thoroughly reviewed recently in the various contributions contained in ASTM Special Technical Publication No. 381 (ref. 6).

The plane strain crack toughness K_{Ic} is a material property which is measured in terms of the opening-mode stress intensity factor K_I, expressed in units of $(\text{stress})\times(\text{length})^{1/2}$. The distinction between K_{Ic} and K_I is important, and is comparable to the distinction between strength and stress. To determine a K_{Ic} value a crack-notched specimen of suitable dimensions is increasingly loaded until the crack becomes unstable and extends abruptly. The ratio of K_I to the applied load is a function of specimen design and dimensions which is evaluated by stress analysis, as discussed later. The K_I value corresponding to the load at which unstable crack extension is observed is the K_{Ic} value determined in the test. This property is a function of temperature and strain rate.

The plane strain crack toughness of a given sample of material is characterized by the distribution of K_{Ic} values determined on specimens taken from the sample. The dispersion of this distribution is often considerable, and the K_{Ic} levels of engineering materials may be more realistically represented by lower confidence limits rather than mean values.

Under certain conditions the K_{Ic} level of a material can be used to estimate the load that a structural member containing a crack of specified dimensions could sustain without fracture. Strength estimates based on K_{Ic} assume a high degree of constraint to plastic flow of the material at the crack tip, corresponding to a state of plane strain. Under different conditions, such as those pertaining to a through-thickness crack in a thin plate, the ability of the material to resist unstable extension of the crack can be substantially greater than indicated by the K_{Ic} level. The effective toughness then depends upon the degree of relaxation of crack front constraint due to the proximity of the plate surfaces.

The effective toughness of a material will not be less than its K_{Ic} level under any practical conditions, and it is therefore appropriate to regard K_{Ic} as a basic index of intrinsic crack toughness. It has been established that the K_{Ic} levels of a number of structural materials are essentially independent of specimen design and dimensions when the specifications for valid K_{Ic} testing are met.

It is necessary to develop specifications for valid K_{Ic} testing because real materials do not deform in the elastic-brittle manner

assumed in linear elastic fracture mechanics. Nevertheless, when a sufficiently large crack-notched specimen is tested, the behavior is sufficiently close to elastic brittle because the crack tip plastic region remains small relative to the significant specimen dimensions. The conditions for valid K_{Ic} testing comprise both minimum limits for specimen dimensions and a maximum limit on deviation from linearity of the load-displacement record. These limits are established on the basis of test data obtained for the purpose, as discussed in subsequent sections. It should be clearly understood, however, that a certain degree of arbitrariness is unavoidable in specifying these limits. As the amount of useful data increases it should be possible to reduce the degree of arbitrariness in setting the conditions for valid K_{Ic} testing.

FUNDAMENTALS OF SPECIMEN DESIGN AND TESTING

The purpose of this section is to review certain basic factors in the design and testing of K_{Ic} specimens. To understand the important factors in the design of practical K_{Ic} test specimens it is useful to start out by considering a configuration that is as simple as possible.

The simplest configuration to consider is the axially-symmetric circular crack located inside a body sufficiently large that the effects of its bounding surfaces on the stress field of the crack are negligible. Initially, before load is applied to the body, the crack is regarded as ideally sharp and free from any self-equilibrating stress field (such as might exist in a practical specimen from the residual effects of artificially generating the crack). The "specimen" is tested by steadily increasing the gross tensile stress, σ, which is applied

remote from and normal to the crack plane. The opening mode stress intensity at every point around the crack border is given by:

$$K_I = 2\sigma\,(a/\pi)^{1/2} \qquad (1)$$

where $2a$ is the effective crack diameter. When σ is small compared with the yield strength of the material, σ_{YS}, the effective crack diameter is not appreciably different from the actual crack diameter $2a_o$. Strictly, however, the effective crack diameter is taken to be formally equal to $2a_o + K_I^2/3\pi\sigma_{YS}^2$, where the supplemental term is Irwin's estimate of the plane strain plastic zone correction term for matching an equivalent elastic crack to an elastic-plastic crack (ref. 7).

To conduct a satisfactory K_{Ic} test it is necessary to provide for autographic recording of the applied load versus the output from a transducer which accurately senses some quantity which can be related to extension of the crack. The basic measurement for this purpose is the relative displacement of two points located symmetrically on opposite sides of the crack plane. Assuming that such a measurement could be made on a buried-crack specimen, the displacement per unit load would be constant as long as the effective crack diameter remained constant, but would increase if $2a$ increased. Hence, the load-displacement plot would be linear as long as there was no appreciable change in $2a$. In the ideal case in which $2a_o$ is large compared with the quantity $(K_{Ic}/\sigma_{YS})^2$, the load-displacement plot would be linear up to the point at which the specimen fractured abruptly, as in Figure 1a. The value of K_{Ic} could then be calculated from the maximum load and the measured crack diameter, using equation (1).

It follows from equation (1) that if $2a_o$ were less than about $1.5(K_{Ic}/\sigma_{YS})^2$, the applied stress would exceed σ_{YS} before the stress intensity reached K_{Ic}. The specimen would then undergo gross plastic deformation before fracture, and the load-displacement plot would be obviously nonlinear, as in Figure 1b. It is likely that fracture would nevertheless occur rather abruptly without much crack extension prior to maximum load, but since the crack stress field could no longer be matched by that of an equivalent elastic crack with an acceptable degree of accuracy, the K_I value which could be calculated formally from the maximum load should not be regarded as a valid K_{Ic}.

The crack diameter is the characteristic dimension of the simple specimen under discussion. This characteristic dimension has to exceed a certain size, proportional to $(K_{Ic}/\sigma_{YS})^2$, in order for a valid K_{Ic} measurement to be made. The quantity $(K_{Ic}/\sigma_{YS})^2$ is a characteristic property of the material having dimensions of length which is, in some respects, a better measure of crack toughness than K_{Ic}. The useful lower limit of the crack diameter cannot be deduced, at present, from theoretical considerations alone; it must be established empirically from the results of a large number of trial K_{Ic} tests.

In a test in which $2a_o$ is greater than, but close to, the useful lower limit, the load-displacement record might be somewhat nonlinear near to the point of maximum load, as in Figure 1c. In fact, records of this sort are often encountered in valid tests of practical specimens. The nonlinearity is partly due to slight, irregular extension of the crack during the last stages of loading and partly due to plastic

deformation around the crack border (which can be regarded formally as a virtual crack extension). If the extent of the nonlinearity is not excessive, then it can be ignored and the K_{Ic} value can be calculated from the maximum load and the measured crack diameter $2a_o$. The question of how much nonlinearity is excessive needs to be specified precisely, of course, and it is consistent with the Irwin formalism to require that the allowable nonlinearity should not exceed that which would correspond to an increase of the initial crack diameter by the amount of the formal plane strain plastic zone correction term, in round figures: $0.1(K_{Ic}/\sigma_{YS})^2$. It is shown later that this requirement leads to an equivalent limitation on the amount by which the reciprocal slope of the secant OP in Figure 1c may exceed the reciprocal of the initial loading slope OQ if the test is to be regarded as valid.

Measurements of K_{Ic} with circular crack specimens are straightforward in principle. The same is true of related types of practical specimens, such as the crack-notch round bar (conceptually the inverse of the circular crack) or the surface crack specimen. Such specimens, however, are comparatively inefficient in respect of the volume of material and the magnitude of test load required for measurement of K_{Ic} of a given material. A number of different types of specimens of rectangular cross-section with through-thickness cracks, referred to briefly as plate specimens, have been developed, and are more efficient but conceptually more complicated. In the first place, the dimensions of the specimens in relation to the crack dimensions are not large enough that the effects of the specimen boundaries on the crack stress

field can be neglected. This circumstance leads to more complicated expressions for K_I which are arrived at by either mathematical or experimental stress analysis, as discussed in the section on "K Calibrations of Specimens". Secondly, the most efficient use of these plate specimens depends upon the proper exploitation of the phenomenon of popin of the crack front which is observed when K_I reaches the K_{Ic} level of the material in plate specimens of nearly marginal thickness, as will now be explained.

Popin K_{Ic} Measurements with Flat Plate Specimens

The simplest type of plate specimen has a central, through-thickness crack of initial length $2a_o$, and is tested like the circular crack specimen, by applying a uniformly distributed tensile load remote from the crack and normal to the crack plane. It can be regarded as a central, longitudinal slice of thickness B from a circular crack specimen, except that the crack fronts are assumed to be straight. If the width W is large compared to $2a_o$, then the opening mode stress intensity at every point along the crack fronts is:

$$K_I = \sigma(\pi a)^{1/2} \qquad (2)$$

where σ is the gross applied stress and $2a$ is the effective crack length.

If $2a_o$ and B are both large compared with $(K_{Ic}/\sigma_{YS})^2$, then the test record, Figure 2a, will be similar to that for a large circular crack specimen. If progressively thinner specimens are tested, however, a thickness range will be reached within which a specimen does not

fracture completely at the load corresponding to K_{Ic} ; instead, the abrupt advance of the crack front proceeds at the center but is suppressed at the free faces of the specimen. A tongue of fracture extends from the crack front, as shown schematically above Figure 2b, and is then temporarily halted until the load is increased further. The test record, Figure 2b, shows a popin step where the displacement increases without any commensurate increase in load. This popin phenomenon was first exploited by Boyle et al (ref. 8), however, it should be noted that Boyle's specimens had sharp, machined notches that were not crack-tipped; consequently, the popins were more pronounced than they would have been if crack-notch specimens had been used, and the K_{Ic} values reported were somewhat higher.

The extent of the popin diminishes with decrease of specimen thickness, and the popin step in the test record becomes correspondingly less pronounced until it becomes impossible to detect the popin load with any degree of confidence, as in Figure 2c. The popin phenomenon in a plate specimen is connected with the nature of the crack tip plastic zone in such a specimen, and it is useful to keep in mind certain aspects of this plastic zone. Figure 3 shows a formal representation of the shape of a crack tip plastic zone in a plate specimen, based on Mises yield limit lines for plane stress and plane strain as given by McClintoch and Irwin (ref. 9). The plastic zone shape which would be obtained by a more complicated elastic-plastic analysis would differ somewhat from this, and would depend on the strain-hardening characteristics of the material. The differences, however, are not important for the present discussion.

In a sufficiently thick specimen, plane strain conditions prevail in the middle part of the thickness, while plane stress conditions prevail near the faces. The plastic zone extends much further ahead of the crack near the faces than it does near midthickness, and the free surface influence extends into the thickness of the specimen for a distance which is proportional to $(K_I/\sigma_{YS})^2$. It is clear, therefore, that when the thickness is less than some critical value that is proportional to $(K_{Ic}/\sigma_{YS})^2$, the constraint-relieving influence of the free faces will extend entirely through the thickness before the stress intensity reaches K_{Ic} . This relief of constraint tends to suppress opening mode crack extension because of the increased possibilities of plastic deformation, and the effect of any opening mode crack extension which does occur is masked by the effect of the concommitant plastic deformation. The result is a gradual, rather than abrupt, change in slope of the load-displacement record, as in Figure 2c.

The lower limit of thickness for reliable popin K_{Ic} measurement cannot be predicted at present from theoretical considerations alone; it must be established from a sufficient number of trial K_{Ic} tests. Results that have been obtained for this purpose are discussed in the later section on "Specimen Size Requirements". While these results are not considered to be sufficient for final determination of the thickness limit, they lead to the tentative conclusion that the thickness should not be less than about $2.5(K_{Ic}/\sigma_{YS})^2$. Results are also presented which lead to a similar conclusion regarding the crack length.

The wide center-cracked plate specimen thus has two independent characteristic dimensions, crack length and thickness, which must exceed certain sizes, proportional to the characteristic material property $(K_{Ic}/\sigma_{YS})^2$, in order that a valid K_{Ic} measurement can be made. A further improvement in specimen efficiency can be made by decreasing the specimen width W so that $2a_o/W$ is not a small fraction. When this is done equation (2) no longer applies accurately; however, an appropriate stress analysis has been conducted, as discussed under "K Calibrations of Specimens". If $2a_o/W$ exceeds a certain value a third independent characteristic dimension has to be considered, namely the uncracked length, or ligament length, $W/2 - a_o$. Clearly, if the crack tip is too close to the free edge of the specimen, then the plastic zone size will be comparable to the ligament length and it will no longer be possible to match the stress field with that of an equivalent elastic crack. Once again, the lower limit for $W/2 - a_o$ should be related to the characteristic material dimension $(K_{Ic}/\sigma_{YS})^2$, and the numerical proportion must be determined from trial K_{Ic} tests. At the present time there is insufficient data for anything more than an informed guess at this proportion.

These three independent characteristic dimensions have to be considered in designing any of the various types of plate specimens that are discussed in this report. The different types of plate specimens are shown schematically in Figure 4, in approximate proportion for equal K_{Ic} measurement capacities, assuming that the thickness is adequate. These specimens are considered in detail in the sections which follow.

K CALIBRATIONS OF SPECIMENS

The crack tip stress intensity factor K_I in a test specimen is equal to the applied load multiplied by some function of the specimen dimensions, including the crack length, which depends on the specimen design. An established relation connecting K_I with the specimen dimensions and applied load for a particular design of specimen is called a K calibration for conciseness. Various methods of mathematical or experimental stress analysis are used to obtain K calibrations, and all the methods involve certain simplifying assumptions about the specimen configuration or the distribution of applied load or both. In making use of the resulting K calibrations it is advisable to be aware of these assumptions in order to avoid errors in K_{Ic} measurement that might result from incompatability of the K calibration with the design of the specimen and loading arrangements. This section is concerned with some pertinent aspects of various methods for K calibration and, in addition, includes the results of some extended or improved K calibrations that have become available since the preparation of reference 10.

Adjustment of Two-Dimensional K Calibrations

Apart from the crack-notch round bar, all the specimens considered in this section are plate specimens with through-thickness cracks. The cracks are assumed to have straight leading edges normal to the plate faces. Because of the difficulty of complete three-dimensional stress analysis, the K calibration procedures that are used, whether mathematical or experimental, treat these plate specimens as essentially two-dimensional. Some investigators adjust the two-dimensional K

calibrations by multiplying by the factor $(1 - \nu^2)^{-1/2}$, where ν is Poisson's ratio. The magnitude of this adjustment factor is 1.05 when ν is 0.3. The adjustment is intended to improve the accuracy with which a two-dimensional K calibration would apply to a real plane strain crack toughness specimen, and was used by the present authors in an earlier review paper (ref. 10). It is by no means clear, however, that the adjustment factor should be as large as $(1 - \nu^2)^{-1/2}$, although there is general agreement that it should not be less than unity. In view of this uncertainty, the present authors now prefer the simpler alternative of using the two-dimensional K calibrations directly, without adjustment. Any error resulting from this practice will be small (probably less than 5 percent) and conservative in that K_{Ic} will be underestimated rather than overestimated.

Methods for K Calibration

The most commonly used experimental method of K calibration is that due to Irwin and Kies (ref. 11) in which measurements are made of the compliance (reciprocal of the stiffness) of a specimen having a narrow machined slot which is incrementally extended between successive measurements. The machined slot is used to simulate a crack primarily because it is not feasible to produce plane cracks of sufficient size and accuracy. It is apparent, however, that the compliance of a crack of given length will not be exactly the same as that of a finite-width slot of the same length. The experimental data are treated by expressing the specimen compliance as a function of crack length, and then obtaining the derivative of this function with respect to crack length. While it

is obvious that the compliance of a specimen with a slot will be somewhat greater than that of a specimen with an equally long crack, it does not follow that the derivative of the compliance with respect to the length will always be greater for the slot than for a crack. Since it is not known how to correct for the slot width, it is advisable to take the equivalent crack length as equal to the slot length but uncertain to the extent of the slot width. This uncertainty will be minimal if the specimen is made large and the slot narrow. It is always an advantage to use as large a specimen as possible for compliance measurements because the displacements will be proportionately large and can be measured with correspondingly good accuracy.

To conduct a compliance calibration with good accuracy it is necessary to use sensitive, accurate gages, and to pay careful attention to detail (refs. 12 and 13). More accurate results can be obtained with compliant specimens, such as bend bars, than with stiff specimens such as notched rounds. It should also be appreciated that the accuracy of the K calibration is likely to be less than that of the compliance measurements because of the differentiation operation required for reducing the experimental data. The error-magnifying effect of differentiation should be less the larger the number of compliance measurements involved for a given range of crack lengths.

The main advantage of the compliance calibration method is that the actual configuration and load distribution of a K_{Ic} test specimen can be closely modelled by the K calibration specimen. In a mathematical crack stress analysis the specimen has to be idealized into a sufficiently

simple model. For instance, the complicated stress distribution around a loading pin has to be replaced by a simpler equivalent stress distribution assumed, on the basis of St Venant's principle, to have the same effect on the crack stress field (refs. 14, 15, 16). With careful attention to the design of both specimen and mathematical model, and apart from the fact that the model is usually two-dimensional, the inaccuracy due to the idealization can be made as small as desired. To achieve high accuracy, however, may entail some sacrifice in compactness of the specimen design. For example, the length of a pin-loaded tension specimen might have to be greater than would otherwise be thought necessary.

The mathematical methods of crack stress analysis are capable of very high precision when used in conjunction with large digital computers. All the K calibrations which follow were obtained by such methods, and are considered to be accurate, in themselves, to within at least 1 percent (with the possible exception of the crack-notched round bar). The accuracy with which any of the K calibrations applies to a specific, detailed specimen design depends, however, on the compatability of the design with the mathematical model on which the K calibration is based.

Center-Cracked Plate Under Uniform Tension

The commonly used Irwin-Westergaard tangent relation for the finite-width center-cracked plate does not properly satisfy the boundary conditions for the specimen, as discussed in reference 17. Mathematical stress analyses of this case have been conducted recently by Forman and Kobayashi (ref. 18), by M. Isida (unpublished), and by Alexander Mendelson

(also unpublished). The results of these studies are in excellent agreement with one another, and can be expressed by a single curve as in Figure 5 -- the individual results would not be distinguishable from the curve on the scale of this figure.

The results of Isida were used by the authors in a least-squares-best-fit procedure to obtain the following compact expression which fits the results to within 0.5 percent over the range of $2a/W$ from 0 to 0.7:

$$Y = K_I BW/Pa^{1/2} = 1.77 + 0.227(2a/W) - 0.510(2a/W)^2 + 2.7(2a/W)^3$$

Over the range of $2a/W$ between 0 and 0.6 the following very simple expression is accurate to within 1 percent:

$$Y = 1.77(1 - 0.1(2a/W) + (2a/W)^2)$$

Polynomial expressions of K calibrations are particularly convenient for incorporation into data-reduction computer programs.

Figure 5 shows that the tangent expression gives K_I values that are lower than those given by the recent K calibration, and that the difference increases with $2a/W$. It is generally agreed that the new calibration is more accurate, and it is recommended that it should be used in place of the tangent expression.

Double-Edge-Cracked Plate

The recommendations made in reference 17 (Table 3) have not been superseded by any recent work. The accuracy is probably within one percent.

Single-Edge Cracked Plate Specimens

There are several forms of single-edge cracked plate specimens for K_{Ic} testing, and these can be classified according to the manner in

which they are loaded, for instance: pin-loading in tension (compact specimens that are extremely eccentrically-loaded in tension are called crackline loaded specimens in this report); four-point bending and three-point bending. Boundary collocation studies of all these variations have been reported (refs. 14, 15, 16, 19), and the K calibrations will be discussed in turn.

Single-Edge Cracked Plates in Tension

In an earlier report by the authors (ref. 10) the K calibration given was derived from experimental compliance measurements on specimens that were pin-loaded through the centerline (ref. 13). It is now considered that the boundary collocation K calibration by Bernard Gross (ref. 14, since extended to cover a larger range of the relative crack length a/W) is more accurate. In this mathematical treatment it is assumed that the tensile load is uniformly distributed across the width of the specimen at a distance not less than the width. This assumption is consistent with pin-loading of the actual specimen if the distance between loading pin centers is not less than three times the specimen width.

The K calibration for uniform tension is represented by the following equation to within 0.4 percent for all values of a/W up to 0.6:

$$Y = K_I BW/Pa^{1/2} = 1.99 - 41.24(a/W) + 18.70(a/W)^2 - 38.48(a/W)^3 + 53.85(a/W)^4$$

A curve representing this relation is shown in Figure 6. The earlier experimental results of reference 13 are in agreement with Figure 6

within 1 percent in the range of a/W between 0.2 and 0.4, but deviate increasingly as a/W is increased beyond 0.4.

Calibrations for single-edge cracked specimens that are eccentrically loaded in tension can be derived by superposition from the results for axial tension and pure bending, as discussed in reference 15; however, such specimens appear to have considerably less practical interest than the more compact crackline specimens discussed later.

Single-Edge Cracked Bend Specimens

Boundary collocation K calibrations for single-edge cracked plate specimens in pure bending and in three-point bending are reported in references 15 and 16 respectively, and have since been extended to cover a larger range of a/W. Figure 7 shows curves representing the results for pure bending and for three-point bending with ratios of support span to specimen depth, S/W, of 4 and 8.

The K calibrations are represented by fourth degree polynomials of the following form to within 0.2 percent for all values of a/W up to 0.6:

$$Y = K_I BW^2/6Ma^{1/2} = A_0 + A_1(a/W) + A_2(a/W)^2 + A_3(a/W)^3 + A_4(a/W)^4$$

where M is the applied bending moment, and the coefficients A_2 have the following values:

	A_0	A_1	A_2	A_3	A_4
Pure bending	+1.99	-2.47	+12.97	-23.17	+24.80
Three point					
$S/W = 8$	+1.96	-2.75	+13.66	-23.98	+25.22
$S/W = 4$	+1.93	-3.07	+14.53	-25.11	+25.80

It is considered that the K calibration for pure bending can be applied to four-point bending if the ratio of the minor span to specimen depth is not less than 2. If the ratio of the major, support span to specimen depth S/W is less than about 4, in either three-point or four-point bending, then it is difficult to avoid substantial errors from specimen indentation and friction at the supports. Even with larger ratios of S/W than 4 it is necessary to take precautions to minimize such errors, as discussed in a later section.

Crackline Loaded Single-Edge Cracked Specimens

It appears that this type of specimen, defined earlier, can be made more compact than any other that could be used for K_{Ic} testing, and it is therefore of particular interest where economy of material or space for exposure of material (as in a nuclear reactor) is of prime importance. There are many possible design variations, and it is not yet clear what the optimum design should be. An early design, due to M. J. Manjoine (ref. 20) has been the subject of considerable study and development, including boundary collocation K calibration (refs. 21, 22, 23). A somewhat different line of development has been pursued by E. Ripling (ref. 24) and Ripling's K calibration has been independently confirmed by boundary collocation analysis (ref. 19).

For illustrative purposes a set of K calibration curves for compact crackline loaded specimens are shown in Figure 8. These are derived from unpublished work by Bernard Gross and show the effect of varying the relative specimen half-height H/W, as well as the relative crack length a/W. For $H/W = 0.444$ and $a/W = 0.38$, the specimen shown in

Figure 8 corresponds essentially to the original Manjoine design. On the basis of considerations regarding crack length and thickness given elsewhere in this report, and assuming a simple, two pin method of loading the specimen, the present authors have tentatively concluded that a specimen with a/W and H/W each equal to about 0.6 would be close to optimum. Tests are scheduled to evaluate such a specimen design in the near future.

A further development due to Mostovoy (ref. 25) concerns the use of tapered crackline loaded specimens, in which the height varies with distance from the loading line. By appropriate tapering, the K calibration relation can be made almost independent of a/W over a substantial range. This is experimentally convenient for fatigue crack propagation studies, and might also have some advantage in K_{Ic} testing. There is clearly a great deal of further development to be expected in the application of crackline loaded specimens, and for this reason it would not be advisable to attempt to be more specific about their use at the present time.

Circumferentially Cracked Round Bar

A stress analysis for this type of specimen was conducted recently by H. F. Bueckner (ref. 26), who considers the accuracy of the resulting K calibration to be within 1 percent (in the range of diameter ratio d/D between 0.5 and 0.9). Earlier K calibrations are not so accurate, and differ considerably from Bueckner's, as shown in Table 8 of reference 26. It is generally agreed that Bueckner's results are the most accurate available, and it is recommended that they should be used.

Figure 9 shows Bueckner's results in the form of values of $Y = (K_I D^{3/2})/P$ plotted against D/d. This form was chosen because the relation between the two variables is represented within 1 percent by the linear equation: $Y = 1.72(D/d) - 1.27$, over the range of d/D between 0.5 and 0.8. If necessary, the linear fitting equation can be used to extrapolate Bueckner's results for values of d/D at least as low as 0.4. Such extrapolated values are consistent with Table 5 of reference 17, and with the associated discussion given in that reference. For the purpose of comparison, Figure 9 also shows the results ascribed to Irwin in reference 26, which are those that are most commonly used.

SPECIMEN SIZE REQUIREMENTS

Before proceeding with a discussion of specimen size requirements, it is appropriate to remind the reader of the assumptions inherent in the application of elastic fracture mechanics to engineering alloys and practical specimen types.

The accuracy with which K_{Ic} describes the fracture behavior of real materials depends on how well the stress intensity factor represents the conditions of stress and strain inside the fracture process zone. In this sense K_I gives an exact representation only in the limit of zero plastic strain. However, for many practical purposes a sufficient degree of accuracy may be obtained if the crack front plastic zone is small in comparison with the vicinity around the crack in which the stress intensity factor yields a satisfactory approximation of the

exact elastic stress field.* The loss in accuracy associated with increasing the relative size of the plastic zone is gradual, and it is not possible at the present time to prescribe limits on the applicability of elastic fracture mechanics by means of theoretical considerations. Obviously, the question of what constitutes a satisfactory degree of accuracy will depend on the application, and in any case the useful limits of K_{Ic} testing in terms of specimen size requirements can only be established by suitable experiments.

In designing such experiments, it may be reasoned as follows: the region around the crack tip in which the elastic stresses are adequately described by a K analysis will increase with crack size and other pertinent specimen dimensions. Thus, the usefulness of K as a descriptive parameter regarding the fracture process should increase as the region of plastic strain at the crack front decreases in size compared with these dimensions. The region around the crack tip in which the elastic stresses will be adequately described by K will vary with the specimen geometry. For this reason, and because the crack front plastic zone is complex in shape, it is unlikely that any single parameter can be used to accurately establish the minimum specimen size required for a K_{Ic} determination of a particular alloy. However, as discussed in a previous section of this report, it is appropriate to assume that $(K_{Ic}/\sigma_{YS})^2$ is a characteristic dimension of the plastic zone that should be useful in

---

*A detailed discussion of this point by H. W. Liu (ref. 27) is recommended for additional reading.

estimating specimen dimensions. The pertinent dimensions of plate specimens for K_{Ic} testing are crack length, thickness, and ligament (uncracked) length. It is assumed that a necessary condition for a K_{Ic} test to be valid is that each of these dimensions should exceed a certain multiple of $(K_{Ic}/\sigma_{YS})^2$, these multiples to be determined by an adequate number of trial K_{Ic} tests. By means of such tests, it should be possible to establish practically useful "working limits" for specimen dimensions. The lower limits of these dimensions for which K_{Ic} remains constant can then be expressed in terms of $(K_{Ic}/\sigma_{YS})^2$.

Since the above approach is different from that used previously in determining specimen size requirements, it is advisable to briefly review the past recommendations as summarized in the 5th Fracture Committee Report (ref. 5) and in a paper by the present authors (ref. 10). Requirements on the specimen thickness B were formulated by Boyle, Sullivan and Krafft (ref. 8) in terms of the plane stress plastic zone correction term: $r_y = \frac{1}{2\pi}\left(\frac{K_{Ic}}{\sigma_{YS}}\right)^2$, and it was suggested that B/r_y should be at least four in order that a distinct popin could be observed. This requirement was based on information derived from tests on sharply-notched 7075-T6 aluminum alloy specimens, before the substantial effect of crack sharpness on the measured plane strain fracture toughness had been appreciated (see SPECIMEN PREPARATION AND TESTING). While the work of Boyle et al is helpful as a guide in formulating further experiments, the use of data from notched specimens without cracks to establish specimen size requirements is misleading.

Hitherto, requirements on the crack length and ligament size have not been stated directly. Instead, it has been assumed that a specimen would be of sufficient size if the ratio of net or nominal stress to the yield strength did not exceed some particular value. For symmetrically loaded plate tensile specimens it may be inferred from the 5th Fracture Committee Report that the net stress should be less than 80 percent of the yield strength* for a valid K_{Ic} test (ref. 5). In the case of single edge cracked tension and bend specimens, the present authors assumed previously that the nominal stress at the crack tip should be less than the yield strength (ref. 10). These limiting stress ratios were then used in conjunction with the appropriate K calibrations to calculate an optimum value of crack length to specimen width, and also to derive K_{Ic} measurement capacities for various specimen types (ref. 10). This procedure resulted in optimum crack length to width ratios that were different for different specimen types and which now appear to be too low.

It appears that basing specimen design requirements on a particular value of the net or nominal stress to yield strength ratio is open to the following objections. First, the so-called nominal stress is an arbitrary quantity and is defined differently for different types of specimens. Also, the use of the nominal stress criterion leads to a

---

*In this connection it should be noted that the limiation of the net stress in terms of the yield strength given in this report was derived from tests on thin, center-slotted panels of tough alloys (K_c tests). The crack lengths at fracture instability, and therefore the K_c values, were very difficult to determine accurately (ref. 28).

ratio of required crack length to plastic zone size which decreases with decreasing ratio of crack length to specimen width. This is inconsistent with the rationale of linear elastic fracture mechanics.

What follows will illustrate how the problem of specimen design may be approached through suitable experiments designed to establish the required limits on the ratios between the three pertinent plate specimen dimensions and $(K_{Ic}/\sigma_{YS})^2$. A necessary requirement of this approach is that the "true" mean K_{Ic} of the material must be accurately established by testing specimens of sufficient crack length, thickness, and ligament size. Once the true mean K_{Ic} is established in this way, a systematic series of trial K_{Ic} tests is made to determine how far a given dimension may be reduced without significant change in the K_{Ic} values obtained. Tests of this type are time consuming and expensive, but no other satisfactory procedure is evident at this time. The experiments to be described are confined to tests on three heats of maraging steel (see Table I) used for the NASA-NRL Cooperative Program. The limited information so far available from this program is indicative but not conclusive regarding specimen size requirements.

Crack Length Requirement

The effect of crack length on the apparent K_{Ic} is shown in Figure 10 for single edge crack bend and tension specimens of 0.45 inch thick, 242 ksi yield strength maraging steel, cracked in the WR direction.* The bend specimens were either one or two inches wide and the

*For nomenclature concerning the direction of crack propagation see reference 2, page 391.

single edge crack tension specimens were 1.5, 3 or 4.5 inches wide. All specimens exhibited load displacement curves with negligible nonlinearity and fractured completely at popin. Except for the shortest crack lengths, it is apparent that there is no trend of K_{Ic} with crack length. The grand average of all 0.45 inch thick specimens is 86.2 ksi - $in^{1/2}$. It can be shown* that the average K_{Ic} (90.8 ksi - $in^{1/2}$) for the group of bend specimens having crack lengths of about 0.17 inch is significantly higher than the grand average. The tension specimens with the shortest crack lengths also had an average K_{Ic} (98.2 ksi - $in^{1/2}$) significantly higher than the grand average. The average K_{Ic} for all other crack lengths was 84.5 ksi - $in^{1/2}$ and this is considered to be the true value. As can be seen from Figure 10, the value of $a_o/(K_{Ic}/\sigma_{YS})^2$ is less than 2 for crack lengths of 0.17 inch and about 2.5 for crack lengths of 0.32 inch.

Additional information concerning the influence of crack length may be obtained from a series of bend tests made on 259 yield strength maraging steel (fig. 11). Specimens 1/4 inch and 1/2 inch thick, having a wide range of crack lengths were cut from a single one-inch thick plate of this steel. Load versus electric potential records exhibited distinct popin indications for all crack lengths investigated. While the data from these tests is very limited it does indicate that the apparent K_{Ic} value increases at $a_o/(K_{Ic}/\sigma_{YS})^2$ ratios less than about 2.5.

---

*The statistical test used was based on the ratio of the difference in averages to the range for the sample (see ref. 29, section 2.2.1).

Further data regarding the influence of crack length is shown in Figure 12 for a 285 ksi yield strength maraging steel. Various types of 1/4 inch thick specimens were machined from a single one-inch thick plate of this steel. Load-potential records showed distinct popin indication for all crack lengths, and within the scatter no trend of K_{Ic} with crack length is noted. The shortest crack length specimens of this series had a ratio of $a_o/(K_{Ic}/\sigma_{YS})^2$ of about 3.8. A ratio of 2.5 would correspond to a crack length of about 0.085 inch.

The results discussed above indicate that the apparent K_{Ic} may overestimate the true value if the crack length is less than some limit which may depend on the material. For the steels investigated, this limit appears to correspond to a ratio of $a_o/(K_{Ic}/\sigma_{YS})^2$ of about 2.5. However, it should be emphasized that additional data on other types of alloys are necessary to set a firm lower limit on this ratio.

Thickness Requirement

The influence of specimen thickness is illustrated in Figure 13 for the 242 ksi yield strength maraging steel. The group of 18 single edge crack specimens and the group of 23 bend specimens, both 0.45 inch thick, represent all data from Fig. 10 having sufficient crack length. The one inch wide bend specimens with thicknesses from 0.1 inch to 0.35 inch were machined from the broken halves of the 0.45 inch thick tension specimens. The two smallest thicknesses, 0.1 and 0.15 inch yielded load displacement records having well defined popin steps preceded by negligible deviation from linearity. The bend specimens at 0.25 and 0.35 inch thickness ruptured completely at popin. Using the same statistical procedure as employed in analysis of the crack length data, the K_{Ic} for each group of smaller thicknesses was tested to determine whether it was significantly greater

than the average for the 0.45 inch thick specimens. The differences were significant at the 5 percent level for thicknesses 0.25 inch and lower but, not for a thickness of 0.35 inch. On the basis of this analysis it is concluded that specimens of this material thinner than 0.35 inch are likely to give significantly higher K_{Ic} values than thicker specimens. This thickness partition corresponds to a ratio of $B/(K_{Ic}/\sigma_{YS})^2$ of about 2.5.

Additional data illustrating the thickness effect is shown in Figure 14 for 259 yield strength maraging steel. Single edge cracked and center cracked tension specimens and bend specimens of three thicknesses were machined from a single one-inch thick plate. Two widths and several crack lengths were investigated for the bend specimens while a single size was used for the tension specimens. All specimens were cracked in the RW direction. Electric potential measurements were made during the course of these tests and typical load-potential records are shown in the insets of Figure 14. The effect of reducing the specimen thickness was to produce load-potential records which were more difficult to interpret, and tests at 1/8-inch thickness gave records which exhibited no clear popin indication. Attempts to select popin loads from these records on the basis of deviations from linearity (indicated by arrow in Fig. 14) gave K_{Ic} values which significantly exceeded the average established by tests at the two larger thicknesses. These data also suggest that a ratio of $B/(K_{Ic}/\sigma_{YS})^2$ somewhere between 2 and 3 is necessary for valid K_{Ic} determination. Similar tests on 7075-T6 aluminum alloy gave essentially the same result.

Further data for maraging steel at a yield strength level of 285 ksi is shown in Figure 15. Specimens of various types covering a wide range of thickness were machined from a single one-inch thick plate and cracked in the RW or RT direction. Well defined popin indications on load-potential records were obtained at all thicknesses investigated and within the scatter no trend of K_{Ic} with thickness is noted. The thinnest specimens of this series had a $B/(K_{Ic}/\sigma_{YS})^2$ of about 3.5. A ratio of 2.5 would correspond to a thickness of 0.090 inch.

The data reported here regarding the effect of thickness indicate that the apparent K_{Ic} value may increase below a certain limiting thickness even though distinct popin indications are obtained. In other cases the effect of reducing the thickness is to render the popin indication so indistinct as to make unambiguous interpretation of the record extremely difficult. A limiting value of $B/(K_{Ic}/\sigma_{YS})^2$ for a valid K_{Ic} test on the alloys investigated appears to be about 2.5. However, it should be emphasized that the limiting value of this ratio may vary from alloy to alloy and further tests of this type are needed to establish a conservative lower limit.

Ligament Requirement

In order to investigate the effect of ligament length $(W-a_o)$, a series of bend tests was made for 242 ksi yield strength, maraging steel specimens having a constant crack length but varying width, as shown in Figure 16. The crack length selected (0.43 inch) for this series of tests was adequate for a valid K_{Ic} determination, as can be seen from Figure 10. All specimens ruptured completely at popin and within the scatter of the data

there is no trend of K_{Ic} with $(W-a_o)$. The results do not clearly define an upper limit on $(W-a_o)$, but examination of the load-displacement records for this series of tests showed that the deviation from linearity preceding rupture was very small for all specimens except those having the smallest ligament. The deviations from linearity for the latter specimens were distinctly greater which would tend to indicate that the limiting ligament length is not much less than the smallest value investigated. While more information of this type is certainly needed, the data do indicate that higher a_o/W values can be used than were previously suggested.

Summary of Suggested Size Requirements

On the basis of the information presented it is suggested that both the crack length and thickness should be greater than some multiple of $(K_{Ic}/\sigma_{YS})^2$ for a valid K_{Ic} test. The data available so far indicate that this multiple should not be less than about 2.5. This value, however, should be regarded as a preliminary estimate pending development of adequate data on a variety of alloys. Apparently the ligament length can be somewhat smaller than the crack length; however, ratios of crack length to width greater than about 0.5 are undesirable because the K calibration curve for single edge cracked tension and bend tests (see Figs. 6 and 7) rises very steeply at the high a/W values. Under these circumstances small errors in measured crack length can have undesirable large effects on the calculated K_{Ic} values.

Specimen dimensions consistent with the requirement that neither a nor B should be less than 2.5 $(K_{Ic}/\sigma_{YS})^2$ are considerably greater than hitherto considered necessary (refs. 5, 8, 10). For example, a crack-notch bend specimen about 2 inches thick and 4 inches deep would be required

for a material having a K_{Ic} of 160 ksi-in$^{1/2}$ and a yield strength of 180 ksi. The specimen dimensions for lower strength materials of high toughness, such as HY-80 steel, would probably be quite impractical. However, under some circumstances, K_{Ic} testing is useful for evaluation of lower strength materials. There are widely used structural materials with yield strengths below 100 ksi having K_{Ic} values sufficiently low that plane strain fracture toughness measurements can be made with specimens of practical sizes. Furthermore, if a sufficiently large specimen is used that is designed to "match" the expected applications, the fact that the specimen is not large enough to provide an acceptable K_{Ic} value is, in itself, an assurance that the material is tough enough for the application. The word "match" is used here in the sense that the specimen has a thickness appropriate to the application and a crack length consistent with inspection capability, reliability and service circumstances.

Variability of K_{Ic} Results

It was pointed out in the INTRODUCTION that the plane strain crack toughness of a given sample of material is characterized by the distribution of K_{Ic} values determined on specimens taken from the sample. The data obtained on the NASA-NRL Cooperative Program and presented in Figures 10 through 16 for three heats of maraging steel is sufficient to permit a judgement concerning the variability of K_{Ic} results. A statistical analysis of the maraging steel data, shown in Table II, gives the mean value $\bar{X}$, standard deviation S, the coefficient of variation $S/\bar{X}$ for all valid K_{Ic} information. Added to this table are some results obtainrd on 1/2-inch thick 7075-T651 aluminum alloy plate.

It will be noted that the coefficients of variation did not differ significantly among the various alloy conditions tested and are within the range that might be expected for a mechanical property relating to the fracture of metallic alloys. For example, a statistical analysis of impact data obtained by Driscoll for SAE 4340 (Ref. 30) was given in Ref. 3. This analysis showed a coefficient of variation of 0.041 and 0.044 for tests on two types of impact machines. These values are not considered to be significantly different from those given for the coefficient of variation of K_{Ic} in Table II.

PRACTICAL SPECIMEN TYPES

This section deals with specific recommendations regarding the dimensions of the various types of K_{Ic} test specimens, their load requirements, and various other considerations that enter into the choice of a specimen type for a particular application. Detailed drawings of the various types of specimens are given in appendix B. In addition, this section included some comments on the use of surface crack specimens and precracked Charpy specimens.

Recommended Specimen Dimensions and Corresponding Load Requirements

Table III is a summary of recommended minimum specimen dimensions for six different types of plate specimens and for the crack-notched round bar, based on the discussion in the preceding section. For consistency it is assumed that the depth of the annular crack-notch in the round bar, $(D - d)/2$, is equivalent to the crack length in the edge-crack plate specimens and therefore equal to $2.5(K_{Ic}/\sigma_{YS})^2$. The ratio of total crack length to

specimen width in the plate specimens, and the ratio d/D in the round bar, is taken as 0.5.* This choice is a compromise between the desire to extend the K_{Ic} measurement limit for a given specimen as far as possible, and the recognition that the K_{Ic} measurement accuracy deteriorates with increasing relative crack length. The last column in the table gives the ratios of required load to yield strength corresponding to the dimensions listed, assuming that the characteristic material dimensions $(K_{Ic}/\sigma_{YS})^2$ is equal to one inch. For other values of this characteristic material dimension, the specimen dimensions whould be proportional to $(K_{Ic}/\sigma_{YS})^2$, and the required load proportional to $(K_{Ic}/\sigma_{YS})^4$.

To determine suitable specimen dimensions for an unfamiliar material it is first necessary to decide the highest level of $(K_{Ic}/\sigma_{YS})^2$ that the material is likely to exhibit. Figure 17 is provided to help the reader in this respect. In this figure the lower part of the curve which bounds the "Region of Current K_{Ic} Measurements" is based on the highest values of K_{Ic} that have been measured for steels with yield strengths between 180,000 and 3000,000 psi. The horizontal dashed line represents the highest level of $(K_{Ic}/\sigma_{YS})^2$ that has been reached to date. The figure shows $(K_{Ic}/\sigma_{YS})^2$ versus the ratio of yield strength to Young's modulus,

*Previous practice has been to use a d/D of 0.707 for the notched round on the basis that this gives the highest K for a given notch (net area) stress. The authors assume that additional K_{Ic} measurement capacity can be gained with negligible loss in accuracy by using a d/D = 0.5. However, it should be noted that no experiments have been performed to check the validity of this assumption.

σ_{YS}/E, so that nonferrous alloys could be plotted for comparison. There is insufficient information to provide upper bound curves for nonferrous alloys, but all nonferrous alloy results known to the authors lie well below the bounding curve for steels. It is recommended that specimen dimensions for unfamiliar materials should be based on values of $(K_{Ic}/\sigma_{YS})^2$ taken from the bounding curve in Figure 17 whenever the dimensions of the available material stock permit. These specimen dimensions will usually be more than adequate. If it is necessary to use smaller dimensions, then the adequacy of the dimensions can only be decided after the tests have been conducted.

Considerations in Selecting Specimens for Particular Applications

On the basis of the foregoing recommendations concerning specimen dimensions and load requirements, it would appear that bend (or possibly crack line loaded specimens) would be the only ones of interest for K_{Ic} determination. However, under some circumstances other considerations than "efficiency" can determine the selection of a particular specimen type or crack length to width ratio.

Bend specimens certainly do have a wide range of application, and are suited to testing plates or forgings because directionality effects can readily be investigated by suitable orientation of the specimen with respect to the fiber. Tests in the short transverse direction frequently present difficulties due to the limited thickness available; however, in some cases extension pieces can be welded to the test section. If the tests must be conducted in a limited lateral space, such as might be

encountered in reactor tubes or a cryostat, the single edge crack tensile specimen offers the advantage of requiring a minimum amount of space normal to the loading direction. It should be noted that single edge crack tension specimens shorter than those recommended here have been used by some investigators (Ref. 31). The K calibrations given in this report are not applicable to such short specimens because of interaction between the stress fields of the loading holes and that of the crack. This interaction makes an analytical stress analysis extremely difficult, and K calibrations for short specimens must be determined by experimental compliance measurements which are in themselves subject to several uncertainties (see Section on "K Calibrations of Specimens").

The center cracked and double edge cracked plate specimens are of considerable interest from a theoretical standpoint since they are loaded in pure tension, and provide a base line for the development of other specimen types. Their high load and material requirements exclude them from consideration in most practical applications of K_{Ic} testing. However, they do provide a means for determining crack extension resistance curves as discussed previously by the present authors (Ref. 10), and of investigating the fracture mode transition in terms of the notch strength as a function of thickness change.

While a crack length to width ratio of 0.5 has been recommended for the plate specimens listed in Table III, there is no reason why smaller values could not be used in special circumstances providing there is adequate crack length. For example, in testing weldments it is frequently desirable to locate the tip of the crack in some particular region of the

metal structure and to relate the popin load to the K_{Ic} value of this region.

The circumferentially cracked round bar has received considerable attention in the past as a specimen for use in studying the influence of notch sharpness. In investigations of this type it has the advantage that notches of a particular contour may be produced to close tolerances by cylindrical grinding or lathe turning. As described in the 4th Fracture Committee Report (Ref. 4), this specimen provided with a very sharp notch, may be used to screen alloys regarding their fracture behavior in thick sections. However, aside from its high load and material requirement the cracked round bar is not well suited for K_{Ic} testing unless the particular application dictates the use of this type of specimen (e.g., an investigation of the effects of cracks at the base of screw threads). While machined circumferential notches are relatively easy to produce to close tolerances in the notch round specimen fatigue cracking is difficult to control so that the crack front is concentric with the loading axis. In addition, special precautions are necessary to reduce eccentricity of loading during testing in order to avoid undesirable scatter. In the absence of eccentricity the fracture properties of this specimen will be largely controlled by the region on the crack circumference having the lowest toughness. The fact that a cracked round bar fractures without shear lips is sometimes taken to mean that the specimen may be used to determine K_{Ic} values at much higher ratios of K_{Ic}/σ_{YS} than would be possible using plate specimens. This, of course, is not true since the absence of shear lips does not assure the absence of extensive plastic deformation in this or any other specimen.

Surface Crack Specimen

The surface crack specimen was developed originally for the purpose of simulating flaws of a type which are frequently encountered in service (Refs. 32, 33), and is particularly valuable for this purpose. Subject to the conditions which apply to all K_{Ic} test specimens, measurements of K_{Ic} can be made with surface crack specimens, but they are by no means limited to this purpose. Tests of surface crack specimens provide direct information on the effects of realistic flaws on fracture strength in circumstances which are not amenable to a plane strain fracture mechanics analysis; for instance, where the net stress in the presence of the largest expected flaw size is between yield and tensile strength.

While it is not efficient to use surface crack specimens for general K_{Ic} testing it may sometimes be necessary to do so. In such cases the required crack lengths (depths) for surface crack specimens of particular crack geometry should be no less than that for other types of plate specimens. This leads to a thickness requirement for the surface crack specimen which is twice that for other plate specimens, since the surface crack depth should be less than one-half the thickness if the conventional expression for the stress intensity factor is used (Ref. 2). There is only a limited amount of data available which permits the comparison of fracture toughness values determined using surface crack specimens with those obtained from a variety of other specimen types. Some information of this nature available from the NASA-NRL Cooperative Program is illustrated in Figure 18, which shows the effect of crack size for surface crack specimens of 285 ksi yield strength maraging steel (see table I) before fatigue cracking. Electric

potential and acoustic instrumentation was used on all specimens. These measurements indicated no stable crack extension at crack sizes greater than $a/\varphi^2 = 0.02$*, and only very small amounts of crack extension proceeding maximum load at this crack sizes. As discussed in the last section of this report, a large number of tests on this same plate using a variety of other specimen types gave an average K_{Ic} level of 52 ksi - $(in.)^{1/2}$, independent of whether the cracks were propagating in the same direction as those in the surface crack specimens or into the edges of the plate. The level of K_{Ic} for the surface crack specimens closely approaches 52 ksi - $(in.)^{1/2}$ for a/φ^2 ratios above about 0.06. Specimens having a/φ^2 values smaller than 0.06 have crack depths less than $a = 0.09 = 2.5\left(K_{Ic}/\sigma_{YS}\right)^2$.

These results illustrate that apparent K_{Ic} values determined using specimens with insufficient crack size can be too high. The implication here is that the strength of a specimen containing a small flaw could be underestimated by calculations based on the K_{Ic} values obtained from specimens containing larger cracks. Additional data supporting these observations have been obtained by Randall (Ref. 34) from tests on D6a steel (σ_{YS} = 249 ksi). Further in an unpublished statistical analysis, Randall has treated a very large amount of data obtained from tests on surface crack specimens cut from 6Al-4V-Ti forgings. This analysis shows that the fracture strength of specimens containing small cracks tends to be under-estimated by calculations based on K_{Ic} values derived from specimens containing larger cracks.

---

*Where φ^2 is a crack shape parameter as discussed in reference 2.

The main conclusion to be made after examining a substantial amount of surface crack specimen data is that considerable additional testing is needed to define the effects of crack shape and permit further comparisons between K_{Ic} values obtained using surface crack specimens and those obtained from other plate specimen types. For further information, the reader is referred to papers by Kobayaski, Ziv and Hall (Ref. 35) and by Kobayashi (Ref. 36), which give estimates of the stress intensity factor for embedded elliptical cracks that closely approach either free boundaries or coplanar elliptical cracks. The previously memtioned work by Randall (Ref. 34) is part of a continuing program designed to yield additional data on crack shape effects.

Cracked Charpy Specimens

Impact tests of cracked Charpy specimens are frequently employed for screening alloys regarding the effect of metallurgical variables on relative toughness level (e.g., Refs. 37 and 38). In this case the pendulum energy loss divided by the initial uncracked area (W/A) is reported. Some investigations have converted the W/A values directly to $\mathcal{G}_{Ic}$ (or K_{Ic}) or have tested the specimen in slow bending, treating it much the same as a conventional single edge crack bend test.

The limitations inherent in the use of cracked Charpy specimens for K_{Ic} measurement have been discussed previously in detail (Ref. 10) and will only be briefly reviewed here. The basic limitation is of course the specimen size. It should be evident from the preceding discussion of size requirements for bend specimens that the cracked Charpy with a width of 0.394 in. and an $a/W = 0.5$ has a maximum K_{Ic} measurement capacity

of only 0.28 σ_{YS}, whether tested in impact or slow bending. If tested in impact the conversion of pendulum energy loss to $\mathcal{G}_{Ic}$ involves at least three assumptions: (1) all of the energy loss has been converted to fracture energy, (2) the fracture mode corresponds to plane strain conditions throughout the entire specimen cross-section, and (3) the integrated fracture work divided by the fracture area is equal to $\mathcal{G}_{Ic}$, implying no appreciable dependence of $\mathcal{G}_{Ic}$ on crack speed. It is possible to develop procedures to identify and correct for extraneous energy losses. However, for the second assumption to be true requires the testing of sufficiently large specimens to suppress the formation of side boundary plastic regions* which would relax the transverse constraint responsible for the plane strain conditions at the crack front. This requirement would correspond to testing bend specimens of sufficient size that complete fracture occurs at popin, a condition that can be met in Charpy specimen sizes only for very brittle alloys. The use of W/A values for screening alloys regarding their relative K_{Ic} levels is an uncertain procedure if the impact specimen fractures under mixed mode conditions, unless it can be shown that the mixed mode fracture energies and the plane strain fracture energies bear the same relation among the alloy conditions investigated.

*Attempts have been made to suppress the development of these plastic regions by the use of specimens containing brittle boundaries. While this technique may be useful in some cases, it can lead to additional complexities. The possible difficulties associated with suppression of side boundary deformation either by use of face grooves or brittle boundaries are discussed in the section on Specimen Preparation and Testing.

INSTRUMENTATION

The types and basic principles of instrumentation suitable for detecting crack extension in fracture toughness tests have been reviewed previously (Ref. 10). For plane strain toughness testing, methods involving the measurement of displacements, electrical potential and acoustic emission are most suitable. Recent developments concerning these three techniques are described in this section. In addition, calibration curves are presented which permit estimation of the crack extension from records of load versus displacement or load versus potential change. These calibrations are useful in analysis of popin indications.

Displacement Measurements

The relative displacement referred to here is measured between points on either side of the end of the notch in edge cracked specimens, and across the center slot at the specimen centerline in center cracked specimens. Various types of transducers have been used to make these measurements (Ref. 10). A most satisfactory method employs electric resistance strain gages mounted on a suitably designed flexural element which deforms elastically as the crack notch or slot opens. Krafft (Refs. 39, 40) has described the use of gages of this type in displacement measurements on center crack and single edge crack specimens. He prefers a bi-lobed clip gage (Ref. 40) to measure displacements in a low temperature bath and at high strain rates. In general, considerable effort is required to develop gages of a particular type and care must be taken to insure that adequate sensitivity is combined with a high degree of linearity of output with respect to displacements at the measuring points. Linearity

of gage output is essential if ambiguity in interpretation of test records is to be avoided. A particularly troublesome problem affecting the linearity is maintenance of registery at the measuring points and any satisfactory design should provide for positive positioning during the entire course of a test.

A simple double cantilever beam gage has been developed by one of the authors (Ref. 41) which appears quite suitable for general K_{Ic} testing and combines high sensitivity with linearity of output. The flexures are cantilever arms arranged in the design shown in Figure 19. These arms are made from solution-treated beta titanium, which has a high ratio of yield strength to modulus. Epoxy bonded foil resistance strain gages are fixed to either side of each arm and connected in the bridge arrangement shown. Grooves in the ends of the cantilevers contact knife edges which are machined into edge-cracked specimens on either side of the crack-slot. For center cracked specimens it has been found satisfactory to attach small knife edges by means of screws to the specimen surface at the centerline on either side of the crack-slot. This method of locating the gage has proven very satisfactory in that the gage is positively positioned during the entire test, and yet released without damage when the specimen ruptures. However, precision machining of the grooves in the beams and knife edges in the specimen is essential for satisfactory operation of the gage. When calibrated by a supermicrometer, this gage is linear within 0.0001 inch over the range of 0.200 to 0.250 inch. The sensitivity is about 37.5 mv per volt per inch, giving a magnification factor of about 750X for an X-Y recorder sensitivity of 0.5 mv/in and a

bridge excitation of 10 volts. Conventional resistance strain gage power supplies and wiring techniques may be employed. By use of a commercially available converter, the output of the strain gage bridge may be used to drive the strain axis of the stress-strain recorder of a testing machine.

Calibration curves relating the displacements to relative crack extension are shown in Figures 20 to 22 for several commonly used fracture toughness specimens. These plots give the dimensionless quantity vEB/P as a function of the ratio of crack length to specimen width. The symbols are defined on the graphs. These calibration curves were obtained using a gage length of 0.20 inch, and apply to any specimen having the same geometric proportions as the calibration specimens. Strictly speaking the gage length should also be proportioned; however, its value is not critical providing the length is less than the crack length.

Electric Potential Measurement

The necessary equipment is illustrated in Figure 23, which gives a block schematic of the set-up. Experience with this method in tests at room temperature over the past two years has revealed a source of difficulty in the pickup of interfering signals which produce spurious responses of the X-Y recorder. The voltmeter-amplifier has an inherently high rejection for frequencies of 60 cps and above combined with a very low output inpedance, and for these reasons normally encountered AC fields do not pose a special problem. However, devices which radiate a wide band of frequencies such as an apparatus which produces a sputtering or spark type discharge can cause interference. Under most circumstances

satisfactory operation may be insured by suitable shielding of the signal leads as indicated in Figure 23. Note that twisted pair, two-conductor shielded cable is used and that the signal lead shield is connected only at the specimen. No general recommendations can be made concerning the instrument grounds. Substanial currents are frequently encountered circulating in steel building frames and water pipes, and for this reason it may be necessary to use a separate earth-ground isolated from the neutral side of the AC line.

The electronically regulated constant current supply may be replaced by a combination of a storage cell and a current controlling ballast resistance should be high relative to that of the specimen, and resistor in series with the specimen. This should have a low temperature coefficient. While batteries provide a low cost source of current, they lack the convenience of a good power supply. For example, changes in contact resistance will not influence the set output of the regulated power supply, but if sufficient in magnitude will influence the current drawn from the batteries.

Previous recommendations made by the present authors included a description of yokes that clamped to specimen and positioned the potential probes at a small fixed distance from the crack tip. These yokes were, of necessity, rather heavy and consequently inertia forces tended to damage the probe points when a specimen ruptured so that frequent resharpening of the points was necessary. The present practice is to fasten stainless wire at specified positions either side of the notch on the edges of edge-cracked tensile and bend specimens. In the case of center-cracked specimens the wires are fastened to the specimen on either side of the

crack at the centerline. These positions are further from the crack tip than those obtained using the previously described yokes. These new positions result in some loss in sensitivity; however, experience has shown that the sensitivity is more than adequate, and that the measured potentials are less sensitive to small shifts in position of the pickup points. In the case of steel specimens the wires may be spot welded to the specimen (stainless steel wire is convenient for this purpose) and the signal leads to the voltmeter-amplifier simply clipped onto the ends of these wires. For nonferrous metals the wires may be fastened by means of small screws fitting in tapped holes.

Calibration curves relating the ratio (E/E_o) of measured potential to the potential at zero crack length* to the relative crack length are shown in Figures 24 and 25 for the new probe positions. It is important to note that for the probe positions shown, the calibration curves for symmetrically cracked plate specimens (Fig. 25) will yield the average of the crack extension at each crack tip.

Acoustic Emission

Present techniques for detection of crack sounds (Ref. 42) provide no way to relate the acoustic emission to the amount of crack propagation that has occurred. Also it may be difficult to eliminate sources of extraneous noise. At present the acoustic method best serves as a supplement to the

*A procedure for deriving E_o from the measured initial crack length and the calibration curve is described in reference 10.

previously described techniques. For example, the presence or absence of sound indicates whether a deviation in linearity of the load-displacement record is due to crack propagation on a fine scale or to plastic flow at the crack tip.

Comparison of the Methods

Advantages and limitations of various crack extension detection techniques were discussed previously (Ref. 10). However, a brief comparison of the three methods recommended for plane strain toughness testing should be helpful at this point. The acoustic method has the greatest inherent sensitivity to crack extension and responds only to actual crack movement. However, both the electric potential and displacement gage techniques have more than sufficient sensitivity for plane strain toughness testing. An electric potential measurement is not appreciably influenced by crack tip plastic flow except insofar as this changes the shape of the crack. Therefore non-linearities in the load-potential record are almost entirely due to crack movement. The crack opening displacement, on the other hand, will be influenced by both crack tip plastic flow and crack extension. Nonlinearity in a load-crack opening displacement record therefore can be a reflection of either of these influences.

With the above thoughts in mind, it would seem desirable to use the displacement gage method in combination with a measurement of electric potential or acoustic emission. If only one technique is employed the most generally satisfactory will be that of measuring the crack opening displacement since it requires the least amount of complicated electronic

gear and is most easily adapted to a variety of testing situations, particularly when tests are to be conducted at other than room temperature.

CRITERIA FOR ANALYSIS OF LOAD-DISPLACEMENT RECORDS

As discussed in the first section of this report, the K_{Ic} value is computed on the basis of the load corresponding to a well-defined unstable advance of the crack. The progress of crack extension with load during a test is generally followed by means of a linear displacement gage such as the one described in the preceding section. The analysis of load-displacement records requires the development of suitable popin criteria and methods of data analysis. However, before discussing these it is helpful to consider some of the complications associated with the problem, and to outline the types of load-displacement records encountered in the NASA-NRL Cooperative Program.

It might be expected that a test specimen which met the size requirements outlined in the section on SPECIMEN SIZE REQUIREMENTS would exhibit a load-displacement record which was easily interpretable in terms of the load corresponding to the onset of unstable fracture under plane strain conditions. However, such ideal behavior is not always realized.

In what follows it will be assumed that the commonly described popin behavior illustrated schematically in Figure 2 is obtained. This type of behavior was observed for the alloys tested thus far in the NASA-NRL Cooperative Program, and therefore characterizes the data shown in the section on SPECIMEN SIZE REQUIREMENTS. However, it is important to realize that this behavior will not be encountered for all engineering alloys. For example, SAE 4340 tempered at temperatures above about 750° F

does not exhibit distinct popin steps but rather a gradually developing crack extension to maximum load, the amount of which decreases with increasing thickness. Only a relatively small amount of information is available concerning alloys exhibiting such characteristics and it is not yet clear as to whether the methods of analysis to be discussed in this section will apply to them.

Types of Load-Displacement Records

Typical load-displacement records are shown in Figure 26 for a series of tests on specimens of various thickness. If the specimen is sufficiently thick and the material homogeneous the load-displacement diagram will be essentially linear to maximum load as shown by record A-1. In this case the K_{Ic} value is equal to the K_I value computed on the basis of the maximum load and the initial crack length. The fracture surface of a specimen yielding this type of record will exhibit little or no shear lips. Material inhomogeneities encountered in most wrought alloys can produce small increments of crack extension at loads close to the maximum as indicated by record A-2. In many instances, the magnitude of this "pre-cracking" will be very small, and K_{Ic} computed on the basis of the maximum load will then represent a useful measure of the fracture toughness for the bulk of the material in the specimen. On the other hand, if the alloy structure is strongly laminated or contains large particles of a randomly dispersed second phase, isolated bursts of crack extension of appreciable magnitude may occur at loads substantially less than the maximum as shown by record A-3. In this record one or more distinct popins are observed well below the maximum load separated by portions of

the curve showing no crack extension. Behavior of this type may indicate considerable variability in the fracture properties of the sample. Thus, an identical specimen taken from another location might rupture completely at a load near that corresponding to the first popin of record A-3. Obviously, the significance of these small steps in the A-3 type record depends on the size and distribution of the structural units which fracture to produce the indications.

If the thickness of the specimen is barely sufficient to produce an A-1 type record, then reducing this thickness by perhaps one-half may result in records of type B shown in Figure 26. These records are also readily interpretable in that they consist of a well-defined large popin followed by several bursts of crack extension that lead to complete rupture with only a moderate increase in the load. The effects of inhomogeneities are again revealed by steps in the load displacement diagram preceding final rupture as indicated by records B-2 and B-3. These steps have the same significance as when observed in type A records.

With further reduction in specimen thickness, the load-displacement records change from the easily interpretable type B to presently uninterpretable types such as C. This change in popin behavior corrosponds to a thickness dependent fracture mode transition. Thus, if the thickness of a specimen giving a type B record is reduced by, say, a factor of about four, distinct popin indications may become completely indefinite, as in the C-1 type record in Figure 26. This record is characterized by an initial smooth deviation from linearity followed by a steeply rising curve made up of segments containing steps which are of the same magnitude

or smaller than the precracking which characterized record typed A-2 and B-2. These small, indefinite steps, coupled with the steep continuous rise in load to final rupture, indicate that crack extension is accompanied by considerable plastic flow. It is not possible to derive a value of K_{Ic} from such a record because sufficient plastic flow accompanies initial crack movement to relax the constraints responsible for plane strain conditions at the crack tip. Occasionally a record of type C-2 is encountered, which is similar to C-1 except for the relatively large step which is preceded by considerable cracking under rising load. This behavior is frequently observed when gross inhomogeneities are present such as the various zones in a welded structure. Under these circumstances the advancing crack front may suddenly break through a brittle region and then be arrested. Such records cannot be analyzed to yield useful K_{Ic} data because of the excess plastic flow accompanying the fracture process preceding the apparent popin.

Between the readily analyzable records of types A and B and the unanalyzable type C lie transitional forms. These exhibit some nonlinearity preceding a popin indication of rather small magnitude which is followed by a large amount of crack extension under rising load. Some of these records can yield useful K_{Ic} data while others should be rejected. It is in this transition region that popin criteria are needed.

Criteria and Data Analysis

Popin criteria and data analysis procedures should be compatible with the principles of linear elastic fracture mechanics, and yet be adaptable to an uncomplicated and objective procedure for analysis of test records.

The limitations of our present knowledge require a cautious approach to this problem. Specifically, it is important to have a method that will insure the discarding of records such as C-1 and C-2 which may yield K_{Ic} values that are too high. In formulating a procedure, attention was given to the large number of trial K_{Ic} tests made during the course of the NASA-NRL Cooperative Program.

The suggested data analysis procedure may be illustrated with the load-displacement records* shown in Figure 27, which are typical of those obtained with bend specimens. The basis for the development of this procedure is given in Appendix A. The first step is to construct the secant OB. The reciprocal slope of OB should be larger than that of the initial linear portion OA by 6 percent in the case of single edge crack tension or bend specimens providing a_o/W is about 0.5, and 2 percent in the case of center- or double-edge-cracked tension specimens, providing $2a_o/W$ is about 0.5. For other values of a_o/W the slope of OB can be obtained by reference to the development given in appendix A.

This secant establishes the upper limit on permissible deviation from linearity Δv_i preceding the popin indication. A popin indication is defined as a temporary maximum in the load displacement curve followed by increase of the displacement without the load rising above this maximum value. To meet the requirement on deviation from linearity this load maximum must lie between the lines OA and OB ($\Delta v_i < ab$). The actual

*A similar procedure can be developed for load-potential records. However, as discussed in the section INSTRUMENTATION, the potential measurement is quite insensitive to crack tip plastic flow and for this reason is not recommended for general K_{Ic} testing.

appearance of the popin indication will depend on the combined stiffness of the specimen and tensile machine. In Figure 27 the record illustrating transitional behavior corresponds to a relatively compliant bend specimen and the load drops abruptly at popin. If the stiffness of the tensile machine were decreased sufficiently, the load would remain essentially constant during popin as indicated by the horizontal line mn. For the present purposes the popin displacement Δv_p is taken equal to the horizontal distance mn between the point of maximum load and the load displacement curve. If Δv_p is at least equal to the maximum permissible deviation from linearity (distance ab), the popin is considered to be satisfactory.

Of the records shown in Figure 27, that representing transitional behavior is acceptable because a popin step of sufficient size could be found that was not preceded by excessive deviation from linearity. The K_{Ic} calculated from such a record is considered valid providing the specimen dimensions meet the requirements outlined in the section on SPECIMEN SIZE REQUIREMENTS and providing proper precautions were followed regarding specimen preparation and testing procedure. Neither records of type C-1 or C-2 are acceptable. In the case of C-1 no step of the required size can be found and in the case of C-2 excessive deviation from linearity procedes popin. In appendix A examples are given of the analysis of actual load-displacement records.

SPECIMEN PREPARATION AND TESTING

This section is concerned with those aspects of specimen preparation and testing which require special attention in order to insure satisfactory

accuracy in plane strain fracture toughness measurements with the practical specimen types detailed in appendix B. A considerable amount of general information of specimen preparation and testing was given previously (Ref. 10), and what follows is an attempt to up-date this material.

Fatigue Crack Starter Notches

The details of starter notches given previously (Ref. 10) have been found generally satisfactory. However, the authors now prefer, where possible, to use a chevron notch starter of the type shown in Figure 28 for edge cracked specimens. This geometry has the advantage of a very high stress concentration at the chevron tip which insures that the fatigue crack can be started in a reasonable length of time at a low stress. The radius at the base of the chevron is 0.01 inch maximum, a value easily achieved with conventional milling or grinding equipment.

The fatigue crack should be extended sufficiently beyond the starter notch that the crack tip stress field is not influenced by the notch shape. No information exists to closely establish the required distance. However, experiments made with both sharp V notches and square ended narrow slots as starters show that large extensions are not necessary. According to Figure 29, the apparent K_{Ic} value for 7075-T6 aluminum alloy is between 38 and 40 ksi-in$^{1/2}$ for single edge notch specimens containing V notches with a 0.00025-inch root radius or slots made with a 0.012-inch thick jeweler's saw. With progressive fatigue crack extension from the starter the apparent K_{Ic} value decreases to a constant value between 28 and 31 ksi-in$^{1/2}$. The amount of fatigue crack extension required to produce a constant K_{Ic} value should be larger the milder the discontinuity

represented by the starter, and this effect is observed in Figure 29, with the sawed slot requiring the greater extension.* It is interesting to note that the magnitude of the popin as revealed by the load-potential records shown in Figure 29 is very large for the sharp machined notch and decreases with increasing fatigue crack extension from this notch. For either the V notch or the sawed slot, a fatigue crack extension of somewhat more than 30 mils appeared to remove the crack front from the influence of the starter configuration. For chevron notches having the specified root radius, a fatigue crack extension of 0.050 inch (beyond the intersection of the chevron with the surface) would be more than adequate. When using tension-tension loading to develop fatigue cracks, application of an initial precompression of about one-half the maximum tensile fatigue stress will be helpful in reducing the number of load cycles necessary to start the crack. Tests in the authors' laboratory indicate this procedure will not influence the K_{Ic} value for specimens fatigue cracked in the proper manner. Some investigators have used water or other corrosive media to assist in starting the crack. This procedure should be useful providing it can be shown that the corrosive media does not influence the final results. In some materials an electric discharge machined slot has proven to be a very effective starter in comparison with a machined slot of the same width.

*A larger scatter is observed for the data from the saw-slotted specimens because the effective radius of a sawed slot varies depending on degree of roughness produced at the slot tip which will be a function of the sharpness of the saw and the pressure applied by the operator.

Fatigue Cracking

The effective "sharpness" of a fatigue crack depends on the maximum stress intensity, K_{max}, imposed during fatigue cracking. The effect of increasing K_{max} beyond a certain level is to increase the apparent K_{Ic} of the material. The magnitude of this effect depends on the alloy, and the fatigue cracking conditions should be such that the crack sharpness is not less than is likely to be encountered in service. In this respect, it is considered that $(K_{max}/\sigma_{YS})^2$ is an important parameter influencing the "sharpness" of the fatigue crack.

From general considerations it would be desirable to use a high stress intensity range, ΔK, for fatigue cracking in order to achieve the highest crack propagation rate commensurate with adequate control of the process. On the other hand, the ratio of $(K_{max}/\sigma_{YS})^2$, where K_{max} is the maximum fatigue stress intensity, should be sufficiently low that further reduction in the ratio would not affect the measured K_{Ic} value.

Some indication of the effect of $(K_{max}/\sigma_{YS})^2$ on the apparent K_{Ic} and on the popin behavior is shown by recent tests made by the authors in which the fatigue cracking load applied to bend specimens was varied. The bend specimens were provided with a chevron notch, and were fatigue cracked in cantilever bending (at 3600 rpm) with the notch located directly over the support. Tension-tension loading was employed, the ratio of minimum to maximum load being one-third for all specimens. Tests were made on 242 ksi yield strength maraging steel, fatigue cracked before or after aging, and on 7075-T651 aluminum alloy. In representing these data, the apparent K_{Ic} values have been plotted against $(K_{max}/\sigma_{YS})^2$,

where K_{max} is the estimated stress intensity factor in fatigue calculated from the maximum applied tension load using the K calibration for three-point bending (see the section of "K CALIBRATIONS OF SPECIMENS"). This way of calculating K in cantilever bending does not account properly for the boundary conditions but provides the best available estimate.

According to Figure 30 the apparent K_{Ic} value for 7075-T651 is essentially independent of $(K_{max}/\sigma_{YS})^2$ for values of this ratio up to about 0.05, and then rises with increasing K_{max}. The magnitudes of the popin indications were considerably larger at the higher K_{max} levels, as indicated by the insets in the figure. In contrast, the apparent K_{Ic} of the maraging steel specimens when aged before cracking, Figure 31, was independent of $(K_{max}/\sigma_{YS})^2$ only up to a value of this ratio of about 0.01. It should be noted that attempts to fatigue crack such specimens at $(K_{max}/\sigma_{YS})^2 = 0.050$ resulted in popin during fatigue cracking, and K_{Ic} results for these specimens are not reported. The data for the same maraging steel when cracked before aging is also shown in Figure 31 but is not sufficient to extablish an upper limit on $(K_{max}/\sigma_{YS})^2$ below which the apparent K_{Ic} would be independent of this ratio. However, the data do indicate the apparent K_{Ic} for specimens cracked before aging begins to level out at $(K_{max}/\sigma_{YS})^2$ of about 0.02. The influence of the fatigue cracking conditions on the popin behavior is illustrated by the load displacement curves shown in Figures 32 and 33 for specimens cracked before and after aging, respectively. As was observed for the 7075-T651 aluminum alloy, there is a pronounced increase in the amount of crack extension at popin with increase of $(K_{max}/\sigma_{YS})^2$ for the maraging steel specimens when cracked in either condition.

The fatigue crack extension Δa in the above described test specimens terminated about 0.050 inch beyond the intersection of the chevron notch with the specimen surface. The total number of cycles necessary to produce these cracks is shown in Figure 34 as a function of the estimated ΔK (equal to 2/3 K_{max}). For the maraging steel cracked either before or after aging the total number of cycles is the same function of ΔK within the limits of scatter. At a given ΔK the aluminum alloy requires considerably fewer cycles than the steel to produce a crack of the same length. Comparing Figure 34 with 31 it is seen that at least 30,000 cycles (8 minutes at 3600 rpm) are required to produce an adequately sharp crack in the maraging steel aged before cracking. In contrast, adequately sharp cracks in the aluminum alloy can be produced in about 10,000 cycles (3 minutes).

In summary, the results of these illustrative experiments show that the fatigue cracking conditions can have a pronounced effect on K_{Ic}. High values of $(K_{max}/\sigma_{YS})^2$ during fatigue can produce exaggerated popin indications and an elevated apparent plane strain crack toughness. These effects may be thought of in terms of crack blunting, in that the same type of behavior is observed for specimens provided with sharp machined notches (compare Figures 32 and 33 with 29). Additional data is clearly needed to better define the influences of the conditions of fatigue crack generation on the plane strain fracture behavior. Until more definitive information is available, it would seem desirable to fatigue crack specimens at the lowest value of $(K_{max}/\sigma_{YS})^2$ commensurate with producing the cracks in an acceptable time. The required number of cycles may be minimized by fatigue

cracking after heat treatment rather than before. This sequence corresponds to the highest ΔK for a particular value of $(K_{max}/\sigma_{YS})^2$. In the absence of additional data it appears that a safe procedure would be to insure that at least 30,000 cycles are consumed in fatigue crack propagation.

Face Grooving

Several years ago Newhouse and Wundt (ref. 43) described a Charpy impact specimen provided with a brittle surface layer produced by nitriding. The purpose of this brittle layer was to suppress the formation of plastic zones at the side boundaries and thereby more closely approach plane strain fracture conditions at the crack front. Wei and Lauta (ref. 44) have made use of carbonitriding in fracture toughness tests. More recently, Freed and Krafft (ref. 45) have suggested that face grooving of plate specimens for K_{Ic} testing would accomplish the same purpose and be applicable to any material. Empirical correction procedures have been proposed by these authors for the application of planar K calibrations to specimens with face grooves.

The effects of face grooving have not been adequately studied, but the complexity is apparent. If the grooves are sufficiently deep, crack initiation will occur at the corners between the crack front and the face grooves where the stress intensity is highest. As the ratio of groove depth to specimen thickness is descreased, the variation of K across the crack front is decreased and the crack front will tend to advance uniformly. What is desired is some optimum groove depth and sharpness that will adequately suppress side boundary plastic zone formation, and yet produce a nearly uniform advance of the crack front.

It is difficult to see how this optimum depth can be determined and it will probably be different for different materials.

If the specimen is sufficiently anisotropic in its fracture characteristics, the fracture can originate at the face grooves and propagate across the thickness of specimen. This possibility, of course, increases with the depth and sharpness of the face grooves.

The effect of face grooving on the load-deflection record is illustrated in Figures 35 and 36 for maraging steel (not listed in table I) at two yield strength levels, tested using 1.5-inch wide, single edge crack specimens. Shallow face grooves (the ratio of gross to net thickness, B/B_N = 1.1 or 1.3) with a 0.005-inch root radius were employed. The gross thickness was 0.180 and 0.160 in. for grooved and ungrooved specimens, respectively. When aged at 850° F for 8 hours (σ_{YS} = 280 ksi), Figure 35, a distinct popin is observed without face grooves and the grooved specimen (B/B_N = 1.1) ruptures completely at a load slightly lower than the ungrooved specimen. The K_{Ic} values for these two specimens are in reasonable agreement according to the method of calculation suggested in reference 45. When aged at 700° F for 8 hours (σ_{YS} = 195 ksi), Figure 36, the ungrooved specimen exhibits no distinct popin and the record would be discarded by applying the criteria presented in the section "CRITERIA FOR ANALYSIS OF LOAD DISPLACEMENT RECORDS." With increasing depth of face groove, the maximum load is progressively lowered and the record chopped off. However, if the criteria of the section "CRITERIA FOR ANALYSIS OF LOAD DISPLACEMENT RECORDS" are applied, all of the records in Figure 36 exhibit excessive deviation from linearity and should be discarded.

On the basis of the results so far available it is not clear whether face grooving can usefully increase the K_{Ic} measurement

capacity of a plate specimen. However, it can produce abrupt rupture under conditions where a distinct popin followed by considerable stable crack extension would characterize an ungrooved specimen of the same net thickness. Instrumentation would still be required in order to judge the validity of a K_{Ic} value derived from a face grooved specimen. However, it is not known whether the same criteria for analysis of load displacements records can be applied to face grooved specimens as have been suggested for ungrooved specimens.

Considering all the complications discussed above, it appears that in order to achieve useful results, the depths, and possibly also the root radii, of the face grooves should be tailored to the material and specimen geometry. In this respect, the use of face grooves is a matter for further research rather than a technique to be generally applied in plane strain fracture toughness testing.

Pin Friction Effects in Bending

Pin friction will tend to increase the measured K_{Ic} value over what would be obtained in the absence of friction. Since there is no satisfactory way of correcting for friction effects in a given test set-up, the best procedure is to minimize the effect of pin friction by proper design of the loading fixture.

The following is a brief description of some results obtained in the authors' laboratory from a series of tests made to determine methods of minimizing friction effects in bending. Strain-gaged bend specimens without notches were employed in these tests. The relative influence of changes in the loading arrangements on the friction effect was judged by comparing the measured stress (obtained from the measured strain and

the elastic modulus) with the value calculated from the applied load using the elementary flexure formula. The effect of friction will, of course, be revealed by a calculated stress higher than the measured stress. It should be noted that this method cannot be used to accurately assess the error in K which would be associated with a particular loading arrangement because the manner of deformation and therefore the contribution of friction to the measured load will be different in a cracked specimen than in a smooth specimen.

Tests of the type just described were made on 7075-T651 aluminum bend specimens* approximately 10 inches long, one inch wide and one-quarter inch thick. The tension and compression surfaces were finish ground, and a one-eighth inch long foil strain gage was bonded to the tension surface at the center of the span. The specimens were loaded in four-point bending with a major span of either eight inches or four inches, and a minor span of two inches. An X-Y plotter provided a load-strain record on loading (to 1500 lbs.) and unloading for each test set-up investigated. The loading portion of these records was quite linear in all cases, and the calculated stresses were compared with the measured stresses on the basis of the maximum applied load. Generally the effect of friction was to produce hysteresis in the load strain diagram; however under some conditions the loading and unloading records were linear and coincident even though the calculated stress was greater than the measured stress.

The most pertinent results obtained are summarized in Table IV, which gives the error in the calculated errors in stresses as compared

---

*The tension modulus of 7075-T6 ($E = 10.3 \times 10^6$ psi) given in reference 46 agrees with that reported by the authors in a previous paper reference 13.

with the measured values for five different test set-ups. If all pins are free to roll on flat hardened steel plates the error in the calculated stress is within the $\pm$ 0.5 percent repeatibility of replicate measurements of the strain. A condition of high friction is represented by the tests in which the minor span pins are fixed in a loading yoke, and the major span pins fixed in "V" blocks clamped to a base plate. The error encountered with this set-up was 3.5 percent.

Bend test fixtures can be constructed to permit sufficient movement of the pins so that frictional effects are negligible. In a plane strain fracture toughness test the required movements of the pins will be small, and it is possible to accommodate these and yet prevent the major span pins from being forcibly expelled on complete fracture of the specimen. An example of modification of an existing bend fixture to permit small pin movements is illustrated in Figure 37. This figure shows a fixture that positions the major span pins against vertical dowels (two on each side), and supports the minor span pins in a loading yoke. The major span is adjustable by means of threaded tie bars. Conditions closely approaching those characteristic of free pins were obtained by (a) covering the vertical dowels with 1/16-inch wall thickness surgical tubing and (b) making the holes in the loading yoke 1/32 inch greater in diameter than the minor span pins. For these conditions the maximum error in the calculated stress (Table IV) was one percent.

The bend test fixture modification described above illustrates the generally useful principle that frictional effects in four-point bending can be minimized by permitting small outward movements of the major span pins and corresponding inward movements of the minor span pins. There

are, of course, several ways of incorporating these requirements in the initial fixture design. A design suggested by Mr. M. Jones of NASA-Lewis is shown in Figure 38. The major and minor span pins are retained in slots by small springs. These slots have a width somewhat greater than the pin diameter in order to permit the necessary pin movements. The springs position the pins against accurately located corners of the slots which establish the major and minor spans. The major span support blocks are adjustable by means of pins fitting into locating holes in the base plate.

Friction effects in three-point bending are difficult to investigate by the types of tests described above. These difficulties arise from the fact that the flexure formula applied to three-point bending leads to inaccuracies in the calculated stresses. The errors involved increase with a decrease in the span to width ratio of the three-point loaded beam and as shown by Frocht (ref. 47) may amount to as much as 12 percent for a span to width ratio of 4:1. While approximate solutions to the stresses in three-point loaded beams have been developed (ref. 48), it is unlikely that tests of the type described above using three-point loading are necessary. Thus, for given specimen dimensions, and equal bend angles, three-point loading should result in no larger friction effects than observed for four-point loading, and a fixture suitable for four-point loading should work equally well in three-point loading.

APPENDIX A

BASIS FOR THE ANALYSIS OF LOAD-DISPLACEMENT RECORDS

The purpose here is to develop a rational method for analyzing load displacement records for (1) excessive deviation from linearity preceding popin and, (2) sufficiency of the popin indication. A typical load-displacement record is shown in Figure A-1 which also shows the various quantities involved in the analysis. Popin is indicated by the load maximum P_p followed by an increasing displacement Δv_p with decreasing load. The displacement v_i is that which would have corresponded to P_p if the record had remained linear up to this point. The additional displacement Δv_i is the combined result of several effects and cannot be analyzed precisely; instead this deviation from linearity will be regarded as though it were entirely due to an increment of crack extension Δa_i .

In order to establish a permissible limit for $\Delta a_i/a_o$ it is assumed that Δa_i should not exceed the formally computed plane strain plastic zone correction term. That is,

$$\Delta a_i \leq r_{Iy} \tilde{=} 0.05 \left(\frac{K_{Ic}}{\sigma_{YS}}\right)^2 .$$

Also, for a valid test it was assumed that:

$$a_o \geq 2.5 \left(\frac{K_{Ic}}{\sigma_{YS}}\right)^2 .$$

Hence, for a satisfactory test

$$\frac{\Delta a_i}{a_o} \leq \frac{1}{50} \qquad \text{(A1)}$$

This condition may be expressed in terms of the displacement by use of experimentally determined calibration curves which relate the

displacement per unit load to the crack length for each particular specimen type. The calibration relation takes the form:

$$\frac{vEB}{P} = F\left(\frac{a}{W}\right)$$

where $F\ (a/W)$ is a function of a/W for single edge cracked specimens which depends on the specimen characteristics.* Consequently, at constant load:

$$\frac{\Delta vEB/P}{vEB/P} = \frac{\Delta v}{v} = \frac{F\left(\frac{a}{W} + \frac{\Delta a}{W}\right) - F\left(\frac{a}{W}\right)}{F\left(\frac{a}{W}\right)}$$

or considering that $\Delta a << a_o$:

$$\frac{\Delta v_i}{v_i} = \frac{1}{F} \frac{dF}{d\left(\frac{a_o}{W}\right)} \frac{\Delta a_o}{W}$$

and therefore:

$$\frac{\Delta v_i}{v_i} = \left[\frac{a_o}{W} \frac{1}{F} \frac{dF}{d\left(\frac{a_o}{W}\right)}\right] \frac{\Delta a_i}{a_o} \qquad \text{(A2)}$$

Combining Equation (1) with Equation (2) gives the allowable limit of deviation from linearity in terms of displacements.

$$\frac{\Delta v_i}{v_i} \leq \frac{1}{50} \frac{a_o}{W} \frac{1}{F} \frac{dF}{d\left(\frac{a_o}{W}\right)} = \frac{H}{50}$$

where H is a calibration factor derived from experimentally determined calibration curves. Plots of this factor are given in Figure A-2 for several specimen types.

The limitation on deviation from linearity may be expressed in terms of the reciprocal slope of a secant line connecting the maximum load

---

*In the case of the center and double edge cracked specimens vEB/P is expressed as a function of $2a/W$.

point P_p at popin to the origin. Thus,

$$\frac{\Delta v_i + v_i}{P_p} \leq \frac{v_i}{P_p}\left[1 + \frac{H}{50}\right] \qquad \text{(A3)}$$

For the recommended range of values of a_o/W between 0.45 and 0.55 the value of $H/50$ might be standardized at 0.06 for single edge crack tension and bend specimens and at 0.02 for the center and double edge crack specimens. This leads to the requirement that a deviation from linearity should represent a reciprocal slope change on a plot of load vs displacement, of not more than 6 percent for the single edge crack specimens and not more than 2 percent for the symmetrically cracked specimens.

The question of how large a popin indication should be required can only be answered in an empirical way at this time. Ideally, the advance of the crack front at popin should include an amount of material at least sufficient to be representative of the bulk fracture properties of the specimen (i.e., substantially greater than the size and spacing of minor phase particles in an alloy and extending beyond the small zone of altered material produced during fatigue cracking). This distance will, of course, be different for different materials and probably will also vary with the fatigue cracking and testing conditions. A good deal of additional experience is necessary before firm guidelines can be established for the required extent of popin. Analysis of the trial K_{Ic} tests made during the NASA-NRL Cooperative Program indicate that a displacement change at popin, Δv_p at least equal to the maximum permissible deviation from linearity at the popin load is a reasonably conservative criterion for a satisfactory popin indication. Application of this criterion will probably ensure that the bulk fracture properties

of the specimen are being measured for most engineering alloys tested using specimens meeting the size requirements outlined in the section SPECIMEN SIZE REQUIREMENTS.

Examples of the analyses of actual load displacement records are illustrated in Figure A-3 which shows results obtained from bend tests on specimens of four thicknesses of SAE 4340H steel (600° F temper, σ_{YS} = 230 ksi) machined from a single one inch plate. In order to permit convenient representation of all records on one figure, an ordinate scale of load divided by thickness P/B has been used.

Referring to Figure A-2, a value of H = 1.75 is obtained for the nominal a_o/W of 0.33 used for these specimens. As discussed above, this leads to a requirement that the deviation from linearity preceding popin shall correspond to an increase in the reciprocal slope of the secant of not more than 3.5 percent. The secant lines in Figure A-3 are drawn in conformance with this requirement and the selected popin loads are indicated for each record. Of the records illustrated, those for specimens of 1/8 inch or thicker meet the requirements on deviation from linearity and magnitude of popin indication. The record for the 1/16 inch thick specimen meets neither of these requirements, and the popin load was selected at the first definite step.

The average K_{Ic} value for duplicate tests at each thickness is also shown on Figure A-3. It will be noted that the 1/4 and 1/2 inch thick specimens give an average K_{Ic} = 52.5 ksi-in.$^{1/2}$ while the thinner specimens give higher values. This trend of K_{Ic} with thickness is in accordance with the observations made in the section on SPECIMEN SIZE REQUIREMENTS which would indicate a thickness of at least 0.14 inch would be necessary for a valid K_{Ic} test on this alloy.

APPENDIX B

SPECIMEN TYPES

The suggested proportions of the various plane strain crack toughness test specimens discussed in the text are shown in Figs. B-1 through B-3. Only one bend specimen is illustrated, Fig. B-2, which has a span to width ratio (S/W) of four and is subjected to three point loading. It is considered inadvisable to use bend specimens with substantially lower values of S/W since the K calibrations for such specimens would likely have dubious accuracy and because the errors introduced by friction increase with decreasing S/W. However, there is no reason why higher values of S/W can not be used. Except for the increased load requirements, there is no disadvantage to four point bending. The preferred range of thickness for plate specimens between W/2 and W/4 does not represent a basic requirement for a valid K_{Ic} test, but is suggested for convenience in arriving at a graded series of specimen sizes.

REFERENCES

1. Anon., "Fracture Testing of High-Strength Sheet Materials," ASTM Bul. 243. Jan. 1960, p. 29, also ASTM Bul. 244, Feb. 1960, p. 18.

2. Anon., "The Slow Growth and Rapid Propagation of Cracks," Materials Research & Standards, Vol. 1, 1961, p. 389.

3. Anon., "Fracture Testing of High-Strength Sheet Materials," Materials Research & Standards, Vol. 1, 1961, p. 877.

4. Anon., "Screening Tests for High-Strength Alloys Using Sharply Notched Cylindrical Specimens," Materials Research & Standards, Vol. 2, 1962, p. 196.

5. Anon., "Progress in Measuring Fracture Toughness and Using Fracture Mechanics," Materials Research & Standards, Vol. 4, 1964, p. 107.

6. Anon: Symposium on Fracture Toughness Testing and Its Applications, ASTM Special Tech. Publ. No. 381, 1965.

7. Irwin, G. R., "Plastic Zone Near a Crack and Fracture Toughness," Proceedings of the Seventh Sagamore Ordnance Materials Research Conference, Report No. MeTE 661-611/F, Syracuse University Research Institute, Aug., 1960, p. IV-63.

8. R. W. Boyle, A. M. Sullivan and J. M. Krafft, "Determination of Plane Strain Fracture Toughness with Sharply Notched Sheets," Welding Journal Research Supplement, Vol. 41, 1962, p. 428s.

9. F. A. McClintoch and G. R. Irwin, "Plasticity Aspects of Fracture Mechanics," Symposium on Fracture Toughness Testing and Its Applications, ASTM Special Tech. Publ. No. 381, 1965, p. 84.

10. J. E. Srawley and W. F. Brown, Jr., "Fracture Toughness Test Methods," Symposium on Fracture Toughness Testing and Its Applications, ASTM Special Tech. Publ. No. 381, 1965, p. 133.

11. G. R. Irwin and J. A. Kies, "Critical Energy Rate Analysis of Fracture Strength," Welding Journal Research Supplement, Vol. 33, 1954, p. 193s.

12. J. D. Lubahn, "Experimental Determination of Energy Release Rate for Notch Bending and Notch Tension," Proc. ASTM, Vol. 59, 1959, p. 885.

13. J. E. Srawley, M. H. Jones and B. Gross, "Experimental Determination of the Dependence of Crack Extension Force on Crack Length for a Single-Edge-Notch Tension Specimen," Technical Note D-2396, NASA, Aug., 1964.

14. B. Gross, J. E. Srawley and W. F. Brown, Jr., "Stress-Intensity Factors for a Single-Edge-Notch Tension Specimen by Boundary Collocation of a Stress Function," Technical Note D-2395, NASA, Aug., 1964.

15. B. Gross and J. E. Srawley, "Stress-Intensity Factors for Single-Edge-Notch Specimens in Bending or Combined Bending and Tension by Boundary Collocation of a Stress Function," Technical Note D-2603, NASA, Jan. 1965.

16. B. Gross and J. E. Srawley, "Stress-Intensity Factors for Three-Point Bend Specimens by Boundary Collocation," Technical Note D-3092, Dec. 1965.

17. P. C. Paris and G. C. Sih, "Stress Analysis of Cracks," Symposium on Fracture Toughness Testing and Its Applications, ASTM Special Tech. Publ. No. 381, 1965, p. 30.

18. R. G. Forman and A. S. Kobayashi, "On the Axial Rigidity of a Perforated Strip and the Strain Energy Release Rate in a Centrally Notched Strip Subjected to Uniaxial Tension," Journal of Basic Engineering, Vol. 86, 1964, p. 693.

19. B. Gross and J. E. Srawley, "Stress-Intensity Factors by Boundary Collocation for Single-Edge-Notch Specimens Subject to Splitting Forces," Technical Note D-3295, NASA, Feb. 1966.

20. M. J. Manjoine, "Biaxial Brittle Fracture Tests," Paper No. 64-Met-3, ASME, May, 1964.

21. R. E. Johnson, Panel discussion, Symposium on Fracture Toughness Testing and Its Applications, ASTM Special Tech. Publ. No. 381, 1965, p. 399.

22. W. K. Wilson, "Analytical Determination of Stress Intensity Factors for the Manjoine Brittle Fracture Test Specimen," Report No. WERL-0029-3, Westinghouse Research Laboratories, Aug. 1965.

23. W. K. Wilson, "Optimization of WOL Brittle Fracture Test Specimen," Report No. 66-1B4-BTLFR-R1, Westinghouse Research Laboratories, Jan. 1966.

24. E. J. Ripling, Panel discussion, Symposium on Fracture Toughness Testing and Its Applications, ASTM Special Tech. Publ. No. 381, 1965, p. 396.

25. S. Mostovoy, P. B. Crosley and E. J. Ripling, "Use of Crack Line Loaded Specimens for Measuring Plane Strain Fracture Toughness," Materials Research Laboratory, Inc., Jan. 1966.

26. H. F. Bueckner, "Coefficients for Computation of the Stress Intensity Factor K_I for a Notched Round Bar," Symposium on Fracture Toughness Testing and Its Applications, ASTM Special Tech. Publ. No. 381, 1965, p. 82.

27. H. W. Lui, "Discussion on Critical Appraisal of Fracture Mechanics," Symposium on Fracture Toughness Testing and Its Applications, ASTM Special Tech. Publ. No. 381, 1965, p. 23.

28. W. F. Brown, Jr., "Comments on K_c Data Used in the 5th Fracture Committee Report," Notes to ASTM Special Committee on the Fracture Testing of High Strength Metallic Materials, April 24, 1964.

29. E. L. Crow, F. A. Davis, and M. W. Maxfield, "Statistics Manual," Report No. 3369, Naval Ordance Test Station, 1960.

30. D. E. Driscoll, "Reproducibility of Charpy Impact Test," Symposium on Impact Testing, ASTM Special Tech. Publ. No. 176, 1955, p. 70.

31. A. M. Sullivan, "New Specimen Design for Plane-Strain Fracture Toughness Tests," Materials Research & Standards, Vol. 4, 1964, p. 20.

32. J. E. Srawley and C. D. Beachem, "The Effect of Small Surface Cracks on Strength," Proceedings of the Seventh Sagamore Ordnance Materials Research Conference, Report No. MeTE 661-611/F, Syracuse University Research Institute, 1960, p. IV-169.

33. J. E. Srawley and C. D. Beachem, "Fracture of High Strength Sheet Steel Specimens Containing Small Cracks" -- ASTM STP 302, Symposium on Evaluation of Metallic Materials in Design for Low Temperature Service, ASTM Special Tech. Publ. No. 302, 1961, p. 69.

34. P. N. Randall, "Severity of Natural Flaws as Fracture Origins," Report No. STL-4439-6006-RU-000 (DDC No. AD-472891), TRW Space Technology Laboratories, Oct. 1965.

35. A. S. Kobayashi, M. Ziv and L. R. Hall, "Approximate Stress Intensity Factor for an Embedded Elliptical Crack Near Two Parallel Free Surfaces," International Journal of Fracture Mechanics, Vol. 1, 1965, p. 81.

36. A. S. Kobayashi, "On the Magnification Factors of Deep Surface Flaws," Structural Development Research Memo No. 16, The Boeing Airplane Co., Dec., 1965.

37. C. E. Hartbower and G. M. Orner, "Metallurgical Variables Affecting Fracture Toughness in High-Strength Sheet Alloys," AFASD TDR-62-868, Man Labs Inc., June, 1963.

38. D. Kalish and S. A. Kulin, "Thermomechanical Treatments Applied to Ultra-High Strength Steels," Final Technical Report, Man Labs, Inc., April 1965. (Available from DDC as AD-614806.)

39. J. M. Krafft, Unpublished note to the ASTM Committee on Fracture Testing of High Strength Metallic Materials, August 29, 1963.

40. J. M. Krafft, "A Rate Spectrum of Strain Hardenability and Fracture Toughness," Report of NRL Progress, 1966, p. 6. (Available from Clearinghouse for Scientific and Technical Information.)

41. D. M. Fisher, R. T. Bubsey and J. E. Srawley, "Design and Use of Displacement Gage for Crack Extension Measurements," (To be submitted for publication to ASTM.)

42. M. H. Jones and W. F. Brown, Jr., "Acoustic Detection of Crack Initiation in Sharply Notched Specimens," Materials Research & Standards, Vol. 4, 1964, p. 120.

43. D. L. Newhouse and B. M. Wundt, "A New Fracture Test for Alloy Steels," Metal Progress, Vol. 78, 1960, p. 81.

44. R. P. Wei and F. J. Lauta, "Measuring Plane-Strain Fracture Toughness with Carbonitrided Single-Edge-Notch Specimens," Materials Research and Standards, Vol. 5, 1965, p. 305.

45. C. N. Freed and J. M. Krafft, "Effect of Side Grooving on Measurements of Plane Strain Fracture Toughness," Report to ASTM Committee E-24, May 12, 1965.

46. Anon., Alcoa Aluminum Handbook, Aluminum Company of America, Pittsburgh, Pennsylvania, 1962.

47. M. M. Frocht, "A Photoelastic Investigation of Shear and Bending Stresses in Centrally Loaded Simple Beams," Bulletin of the Carnegie Institute of Technology, 1937.

48. S. Timoshenko and J. N. Goodier, Theory of Elasticity, Second ed., McGraw Hill Book Co., 1951, p. 99.

TABLE I. - COMPOSITION OF MARAGING STEEL USED IN THE NASA-NRL COOPERATIVE PROGRAM*

Supplier	Heat number	Heat treat	σ_{YS}, ksi	Composition									
				C	Ni	Co	Mo	Ti	Al	Mn	Si	P	S
Republic	3920913 1/2 in. plate	1600° F, 1 hr, AC + 850° F, 3 hr	242	0.020	18.20	8.60	4.70	0.70	0.09	0.06	0.06	0.005	0.002
Republic	3930641 1 in. plate	Age 900° F, 3 hr	259	0.020	18.35	7.18	5.32	0.32	0.04	0.05	0.09	0.006	0.005
Allegh-Lud	24349 1 in. plate	Age 900° F, 3 hr	285	0.030	18.53	8.89	4.64	0.69	0.15	0.021	0.06	0.003	0.010

*All steels were Consumable Electrode Vacuum melted.

TABLE II. - VARIABILITY OF VALID* K_{Ic} RESULTS

Material	Heat treatment	Yield strength, ksi	K_{Ic} Tests			
			Number of tests, n	Mean K_{Ic}, $\bar{x}$, ksi-in.$^{1/2}$	Standard deviation, S, ksi-in.$^{1/2}$	$S/\bar{x}$
Marging steel (300)	900° F/3 h	285	38	51.75	2.47	0.0478
Marging steel (250)	900° F/3 h	259	23	68.4	3.51	0.0515
Marging steel (300)	850° F/3 h	242	44	84.5	4.67	0.0555
Aluminum 7075 (1/2 inch thick)	T651	79	24	26.8	1.32	0.0495

*Valid according to the tentative criteria suggested in this report.

TABLE III. - RECOMMENDED MINIMUM SPECIMEN DIMENSIONS AND RATIOS OF REQUIRED LOAD TO YIELD STRENGTH FOR $(K_{Ic}/\sigma_{YS})^2 = 1$

[For other values of $(K_{Ic}/\sigma_{YS})^2$, the dimensions should be in proportion to this factor, and the loads in proportion to its square.]

Specimen type	Thickness, in.	Crack length, in.	Width or diameter, in.	Specimen length, in.	$\frac{\text{Load}}{\text{yield strength}}$, sq in.
Crack-notched round bar	---	2.5 (D/2-d/2)	10 (D)	40	14.7
Center-crack plate	2.5	5.0 (2a)	10	40	7.5
Double-edge-crack-plate	2.5	2.5	10	40	7.9
Single-edge-crack plate, tension	2.5	2.5	5	20	1.6
Single-edge-crack plate, 4-point bent (8:1::Span:Depth) (2:1::Minor Span:Depth)	2.5	2.5	5	41	0.33
Single-edge crack plate, 3-point bend (4:1::Span:Depth)	2.5	2.5	5	21	0.50
Crackline loaded plate	2.5	---------	---	--	-----

TABLE IV. - RESULTS OF TESTS TO DETERMINE FRICTION EFFECTS ON 4-POINT BENDING

Span to width ratio	Set-up[a]	Percent error
8:1	Free pins	0.5
4:1	Free pins	0.5
8:1	"V" blocks[c]	3.5
8:1	Fixture[b]	1.0
4:1	Fixture	0.5

[a]Minor span: 9/16 in. dia. pins on 2 in. centers.
Major span: 3/4 in. dia. pins on 3 in. or 4 in. centers

[b]See Fig. 37 for details of fixture.

[c]Major span pins in "V" blocks fixed to a base plate and minor span pins fixed in a loading yoke.

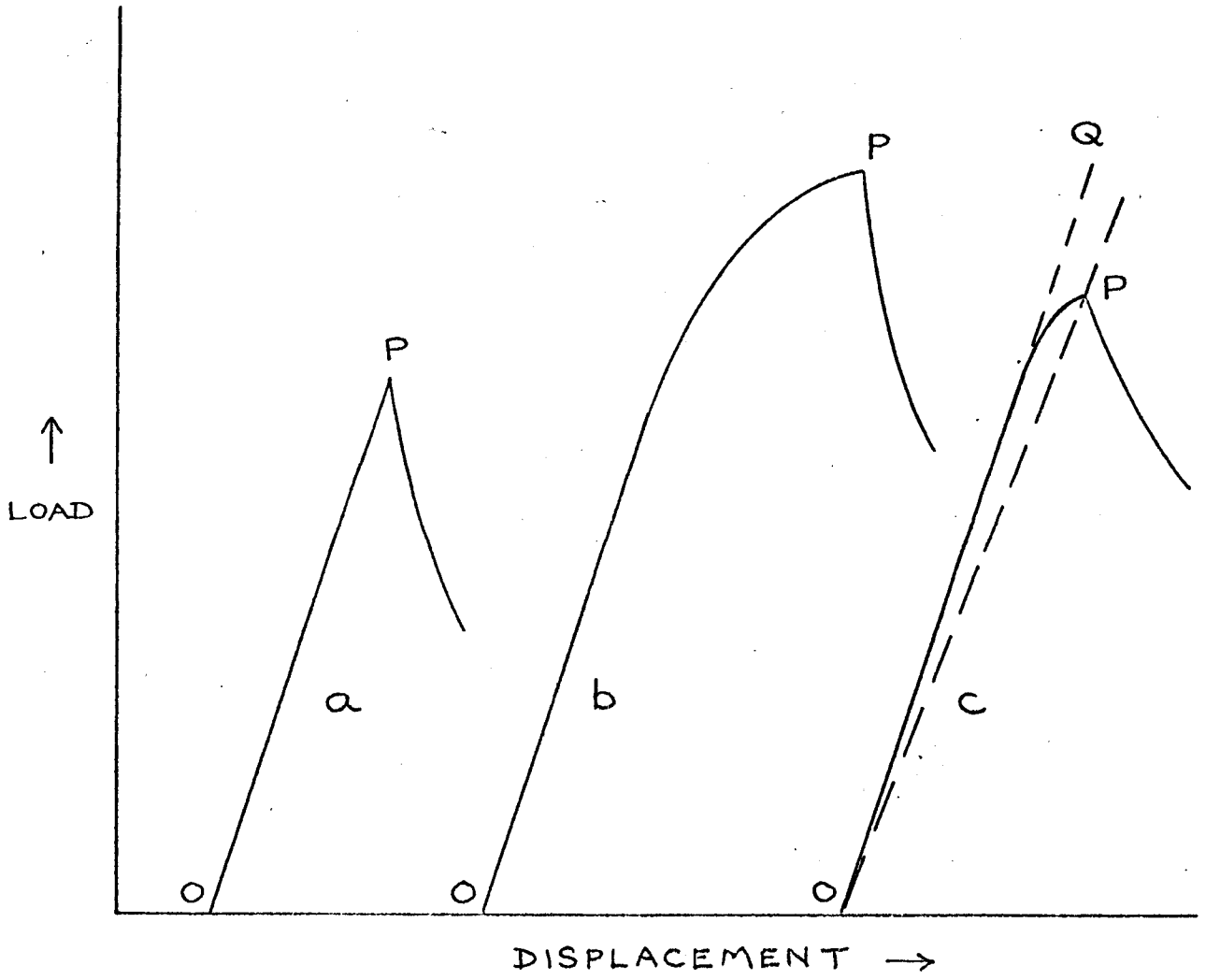

FIG. 1 : HYPOTHETICAL LOAD-DISPLACEMENT PLOTS FOR TESTS OF CIRCULAR CRACK SPECIMENS

Fig 1

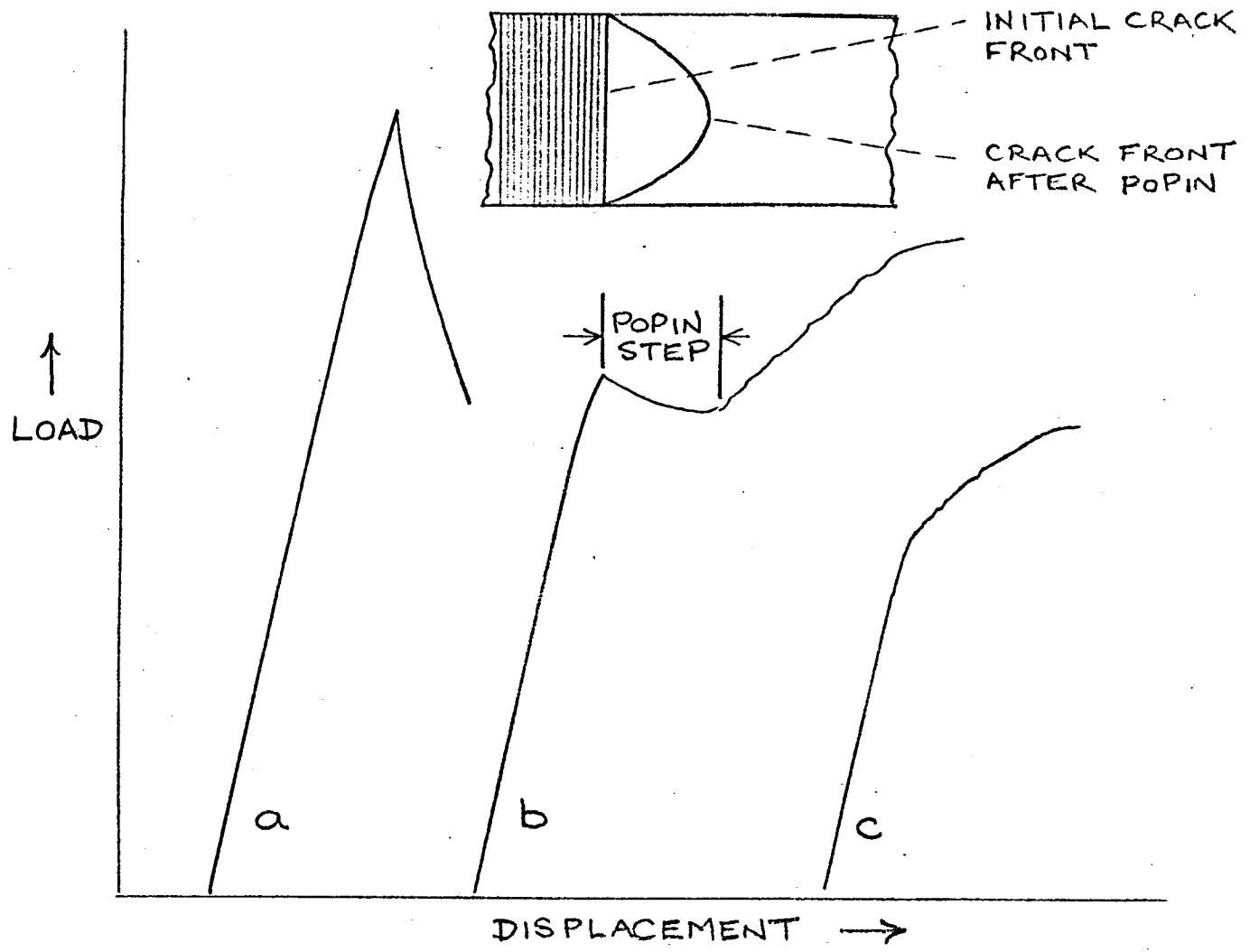

FIG. 2: SCHEMATIC LOAD-DISPLACEMENT PLOTS FOR TESTS OF PLATE SPECIMENS.

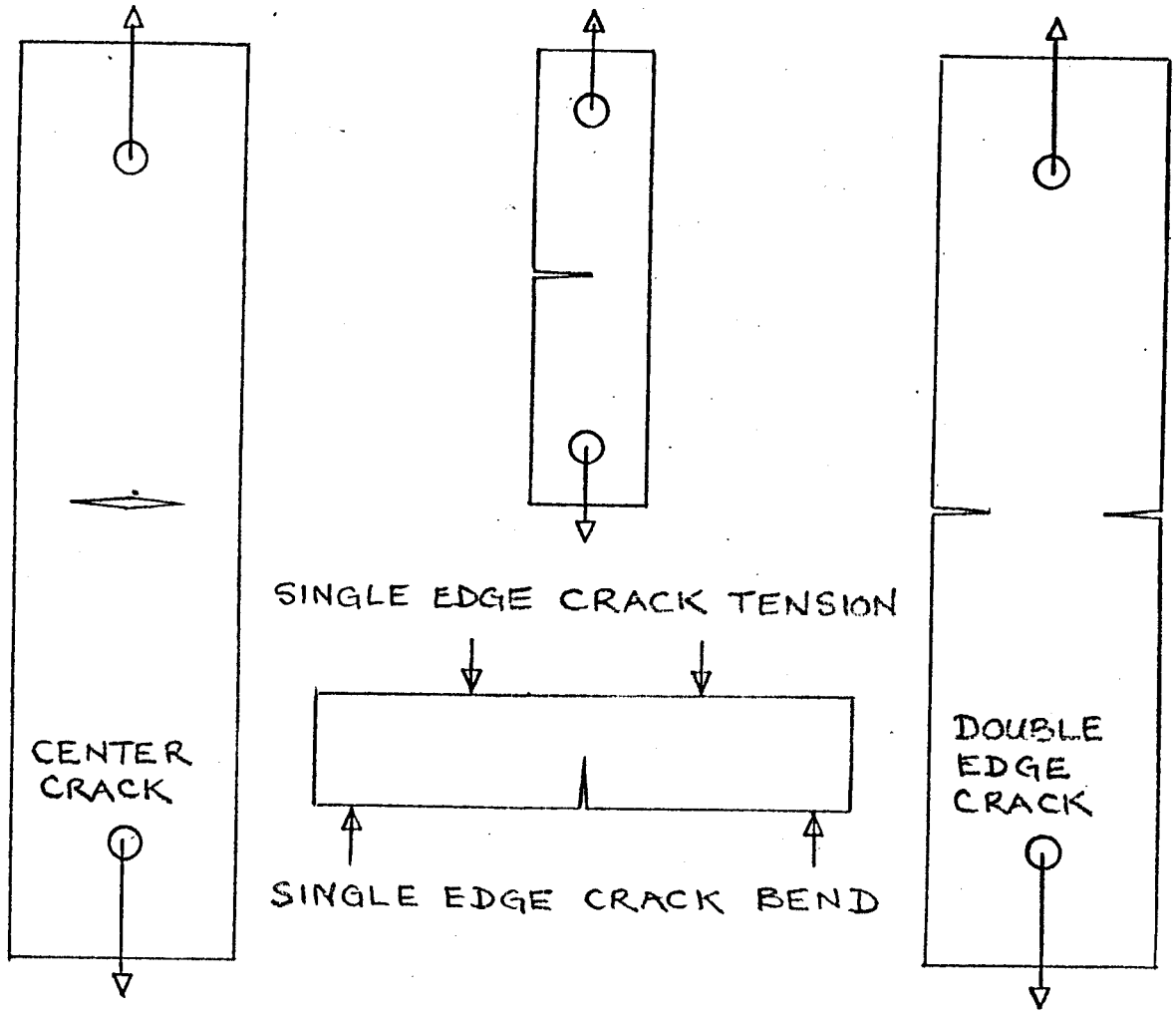

FIG. 4: SOME TYPES OF PLATE SPECIMENS FOR K_{Ic} TESTING

Fig. 4

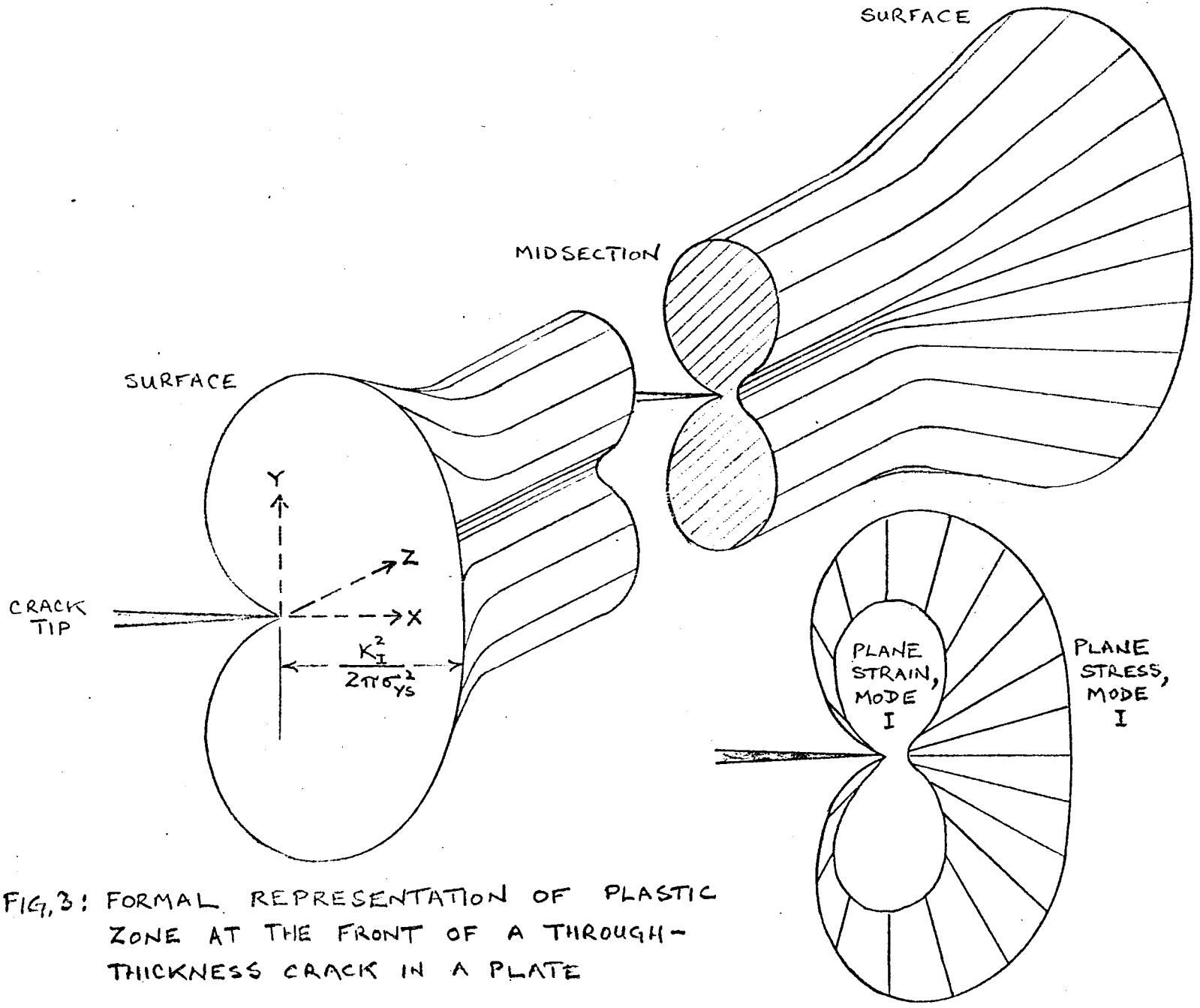

FIG, 3: FORMAL REPRESENTATION OF PLASTIC ZONE AT THE FRONT OF A THROUGH-THICKNESS CRACK IN A PLATE

FIG. 3

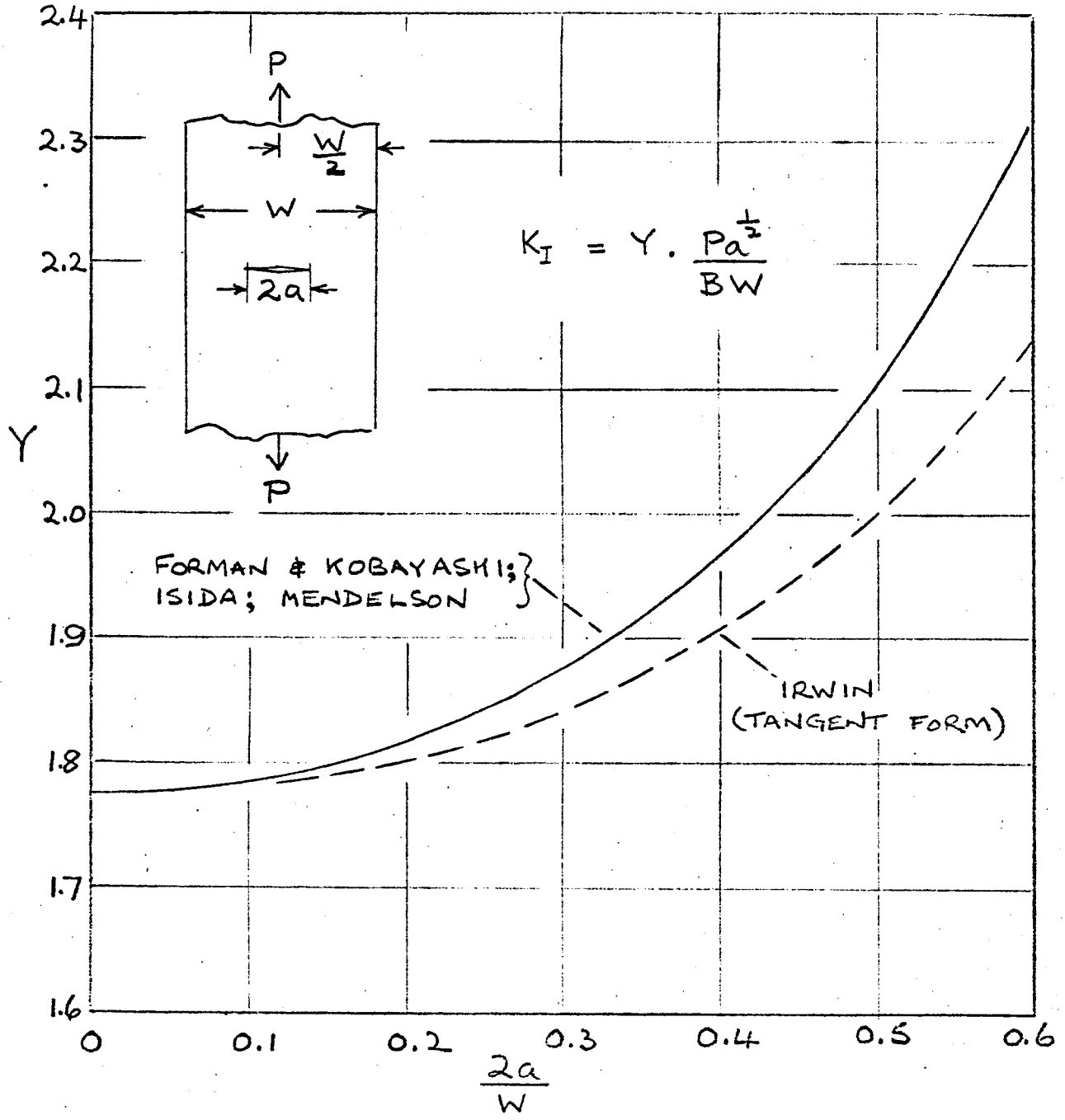

FIG. 5: K CALIBRATIONS FOR THE CENTER-CRACKED PLATE SPECIMEN

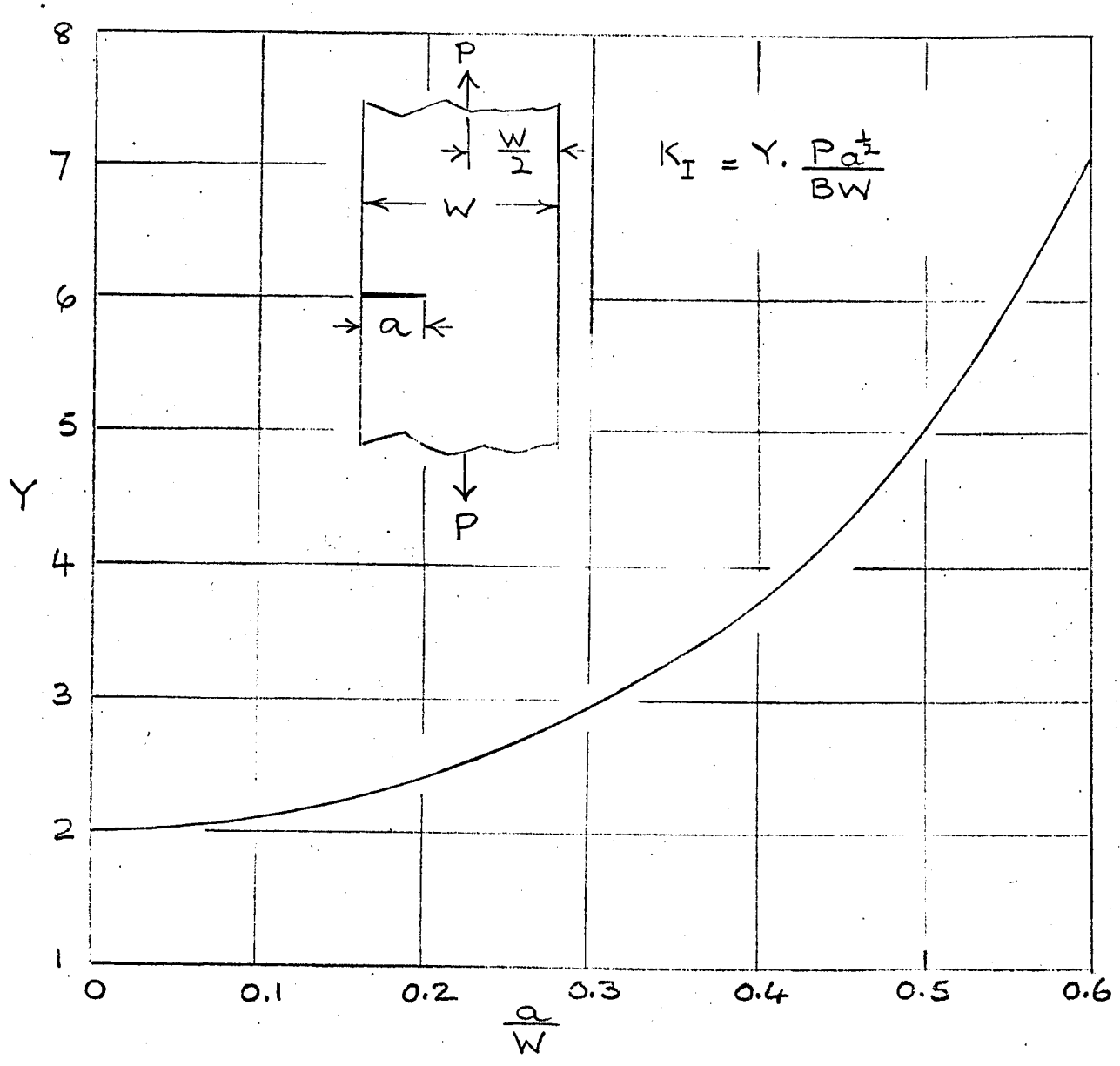

FIG. 6: K CALIBRATION FOR SINGLE-EDGE CRACK TENSION SPECIMEN

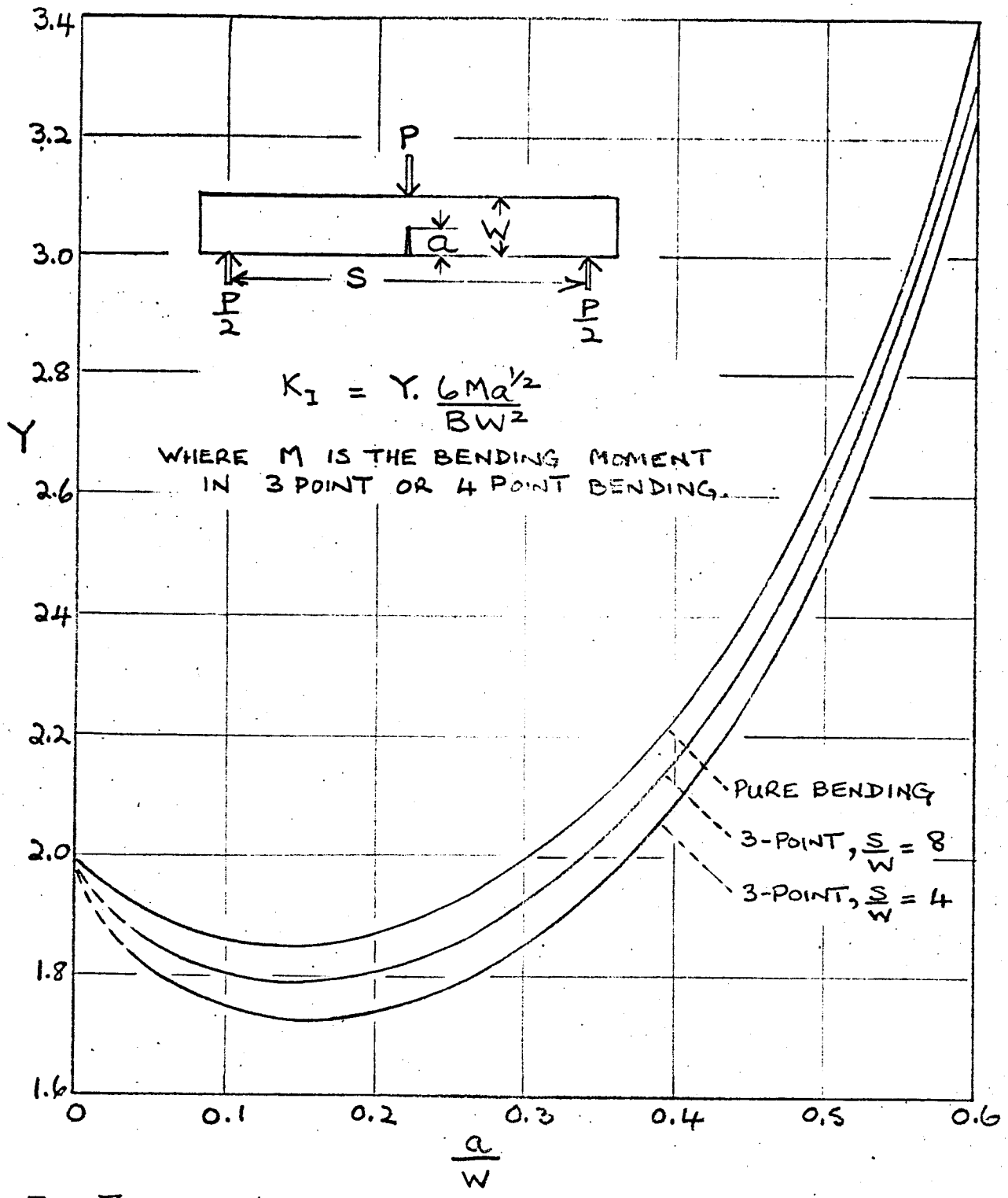

FIG. 7: K CALIBRATIONS FOR BEND SPECIMENS.

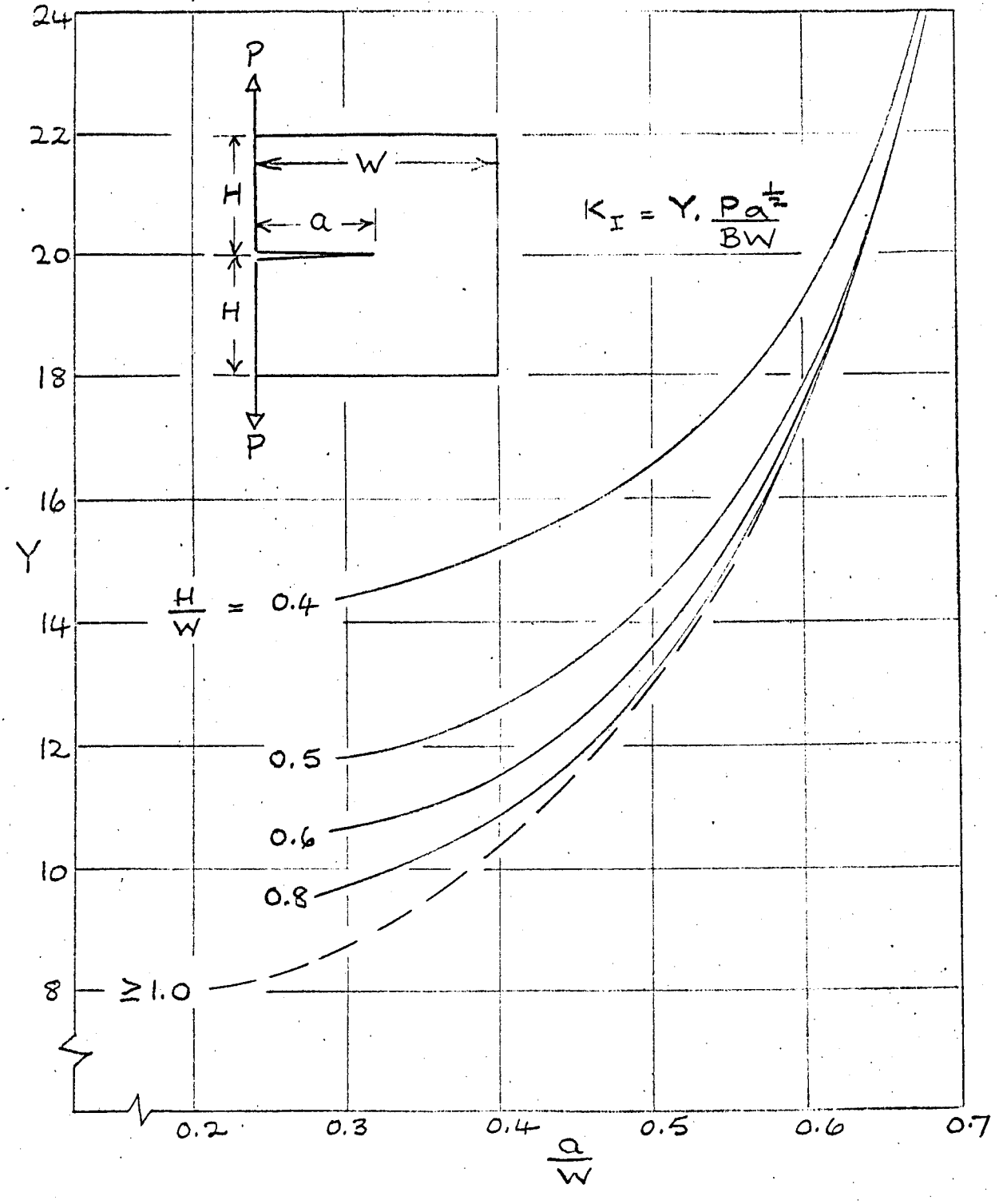

FIG. 8: K CALIBRATIONS FOR COMPACT CRACKLINE LOADED SPECIMENS

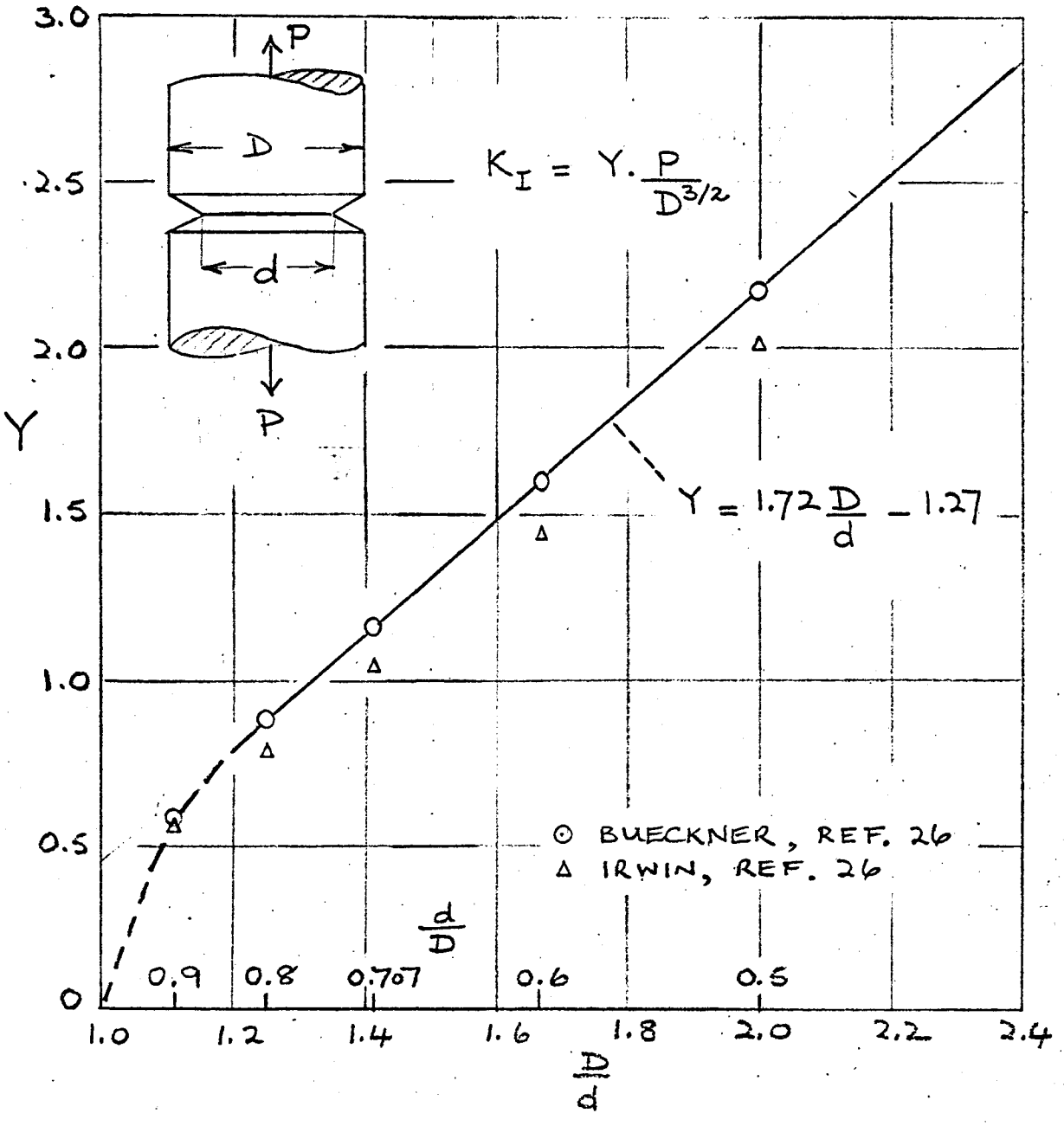

FIG. 9: K CALIBRATION FOR CIRCUMFENTIALLY CRACK-NOTCHED ROUND BAR

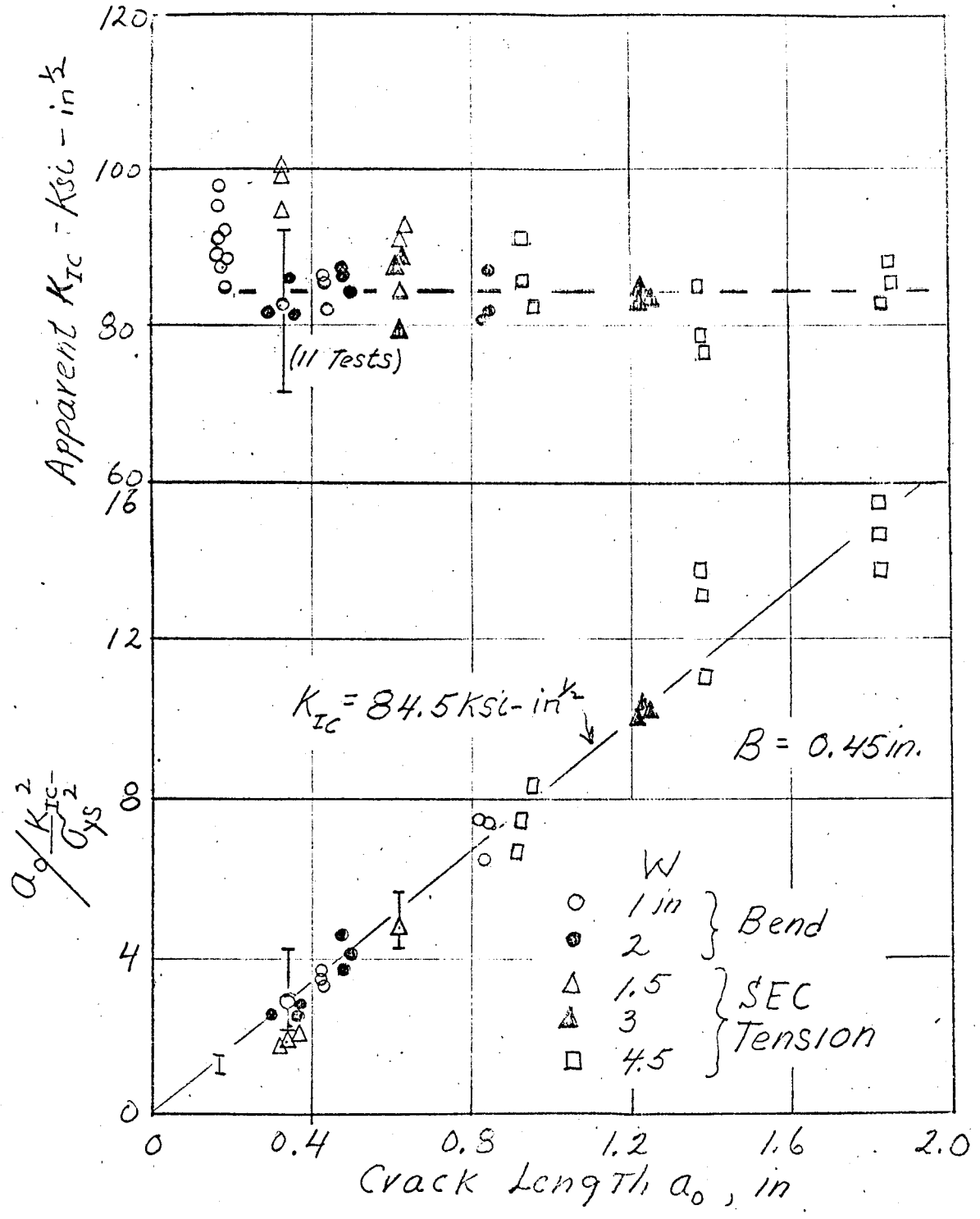

Fig 10: Effect of Crack Length on Apparent K_{IC} for Single Edge Cracked Tension & Bend Tests on 242 yield Strength Maraging Steel

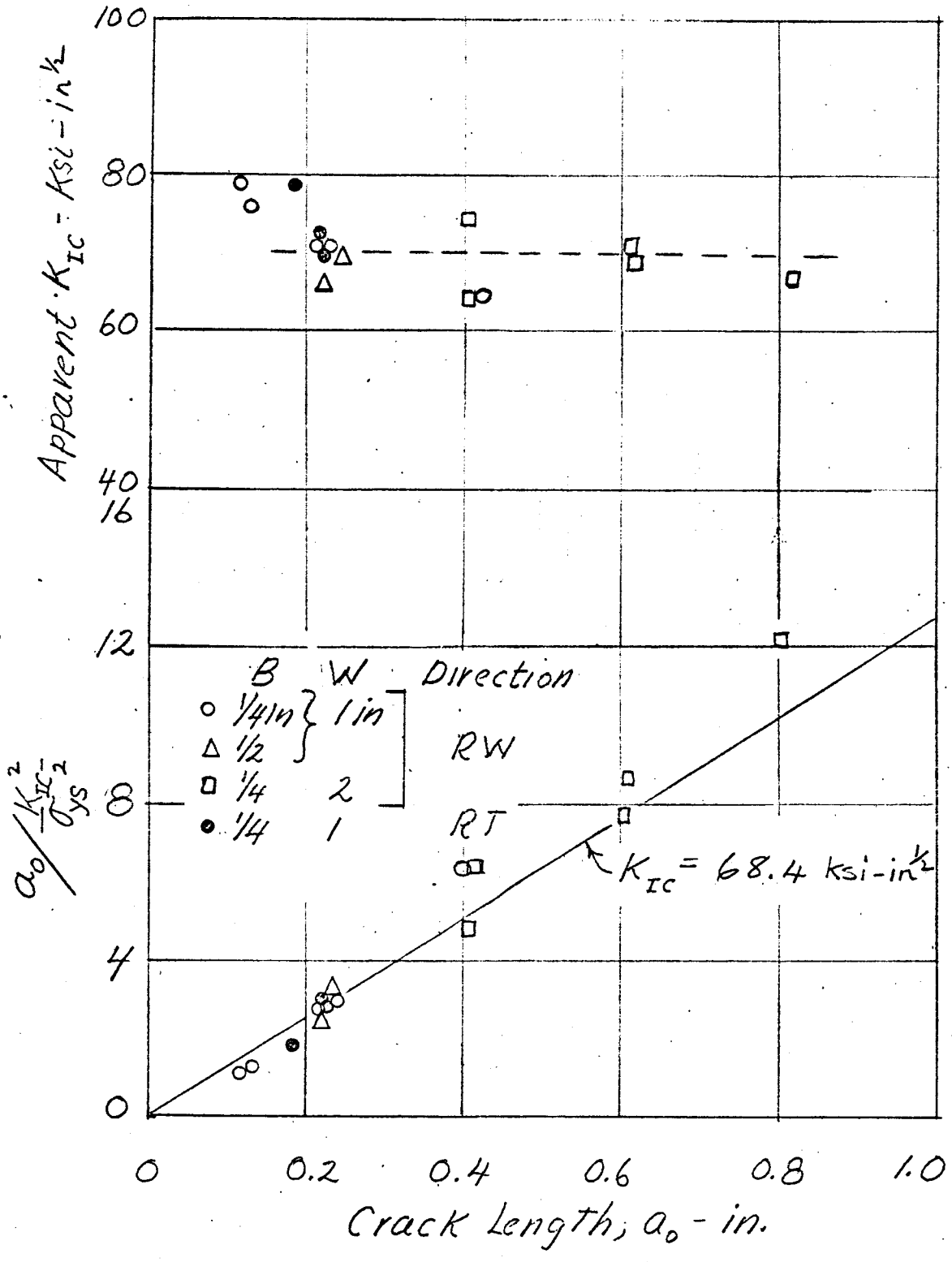

Fig. 11: Effect of Crack Length on Apparent K_{IC} for Bend Tests on 259 ksi Yield Strength Maraging Steel

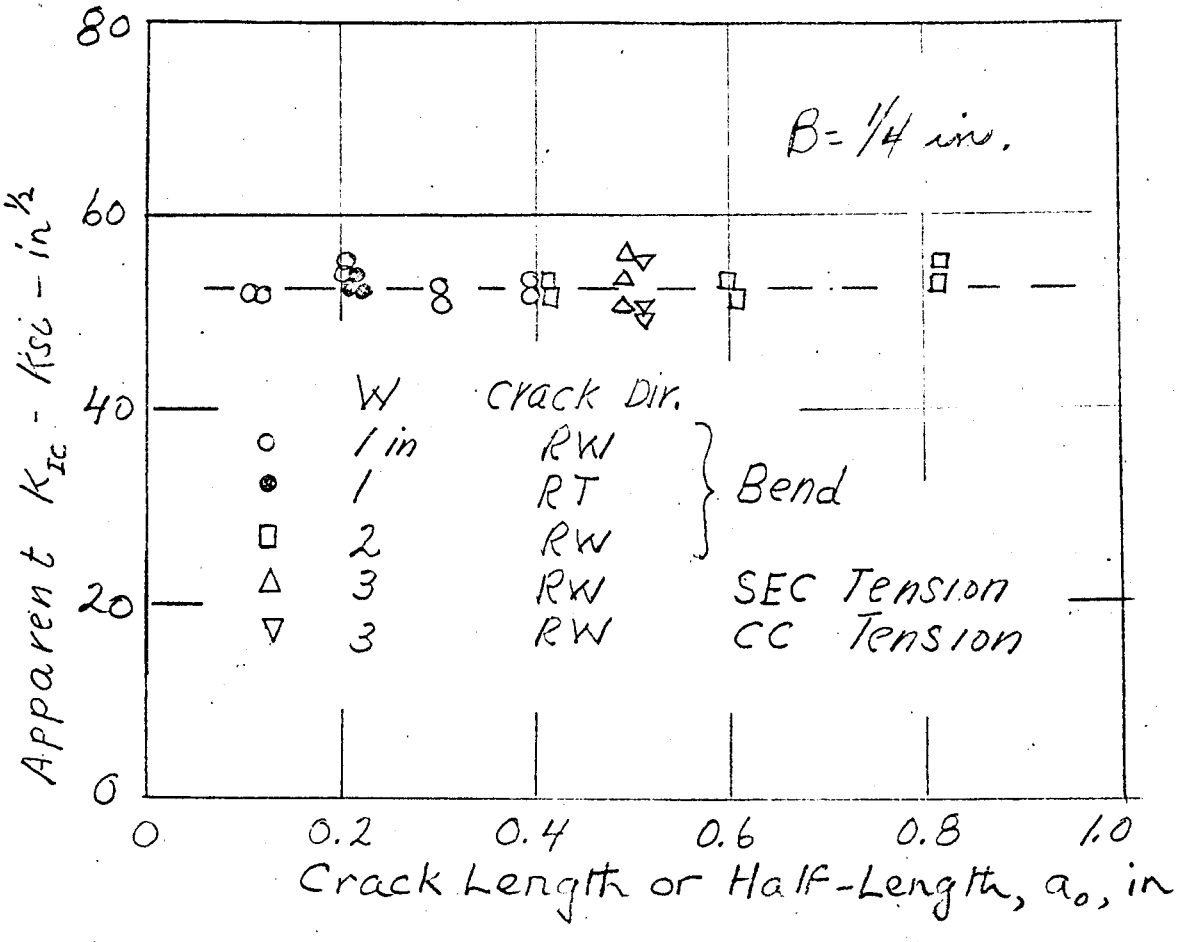

Fig. 12: Effect of Crack Length on Apparent K_{Ic} for 295 ksi Yield Strength Maraging Steel Tested using Several Specimen Types.

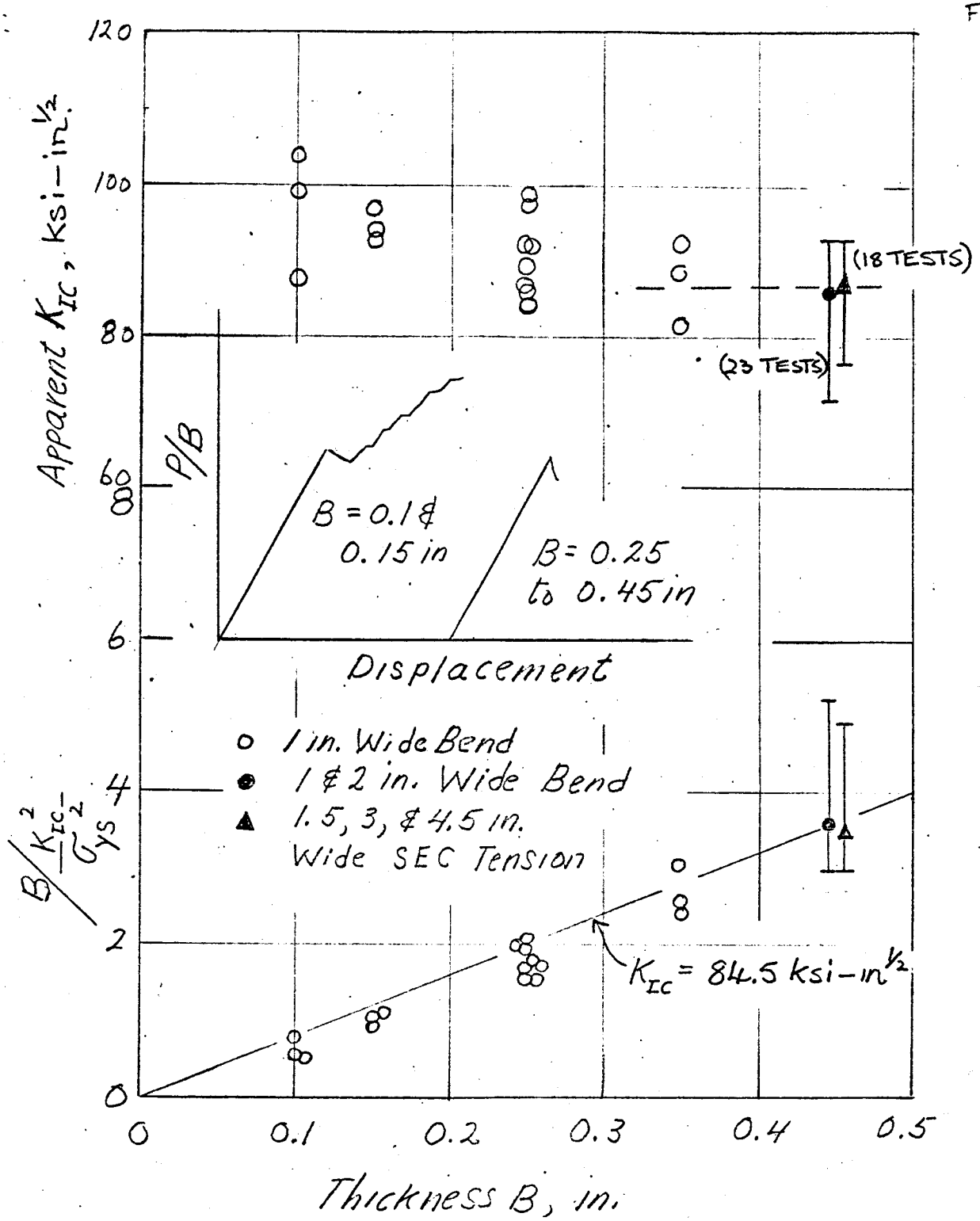

Fig. 13: Effect of Thickness on Apparent K_{IC} For 242 Ksi yield Strength Maraging Steel Tested using Bend & Single Edge Crack Tension Specimens

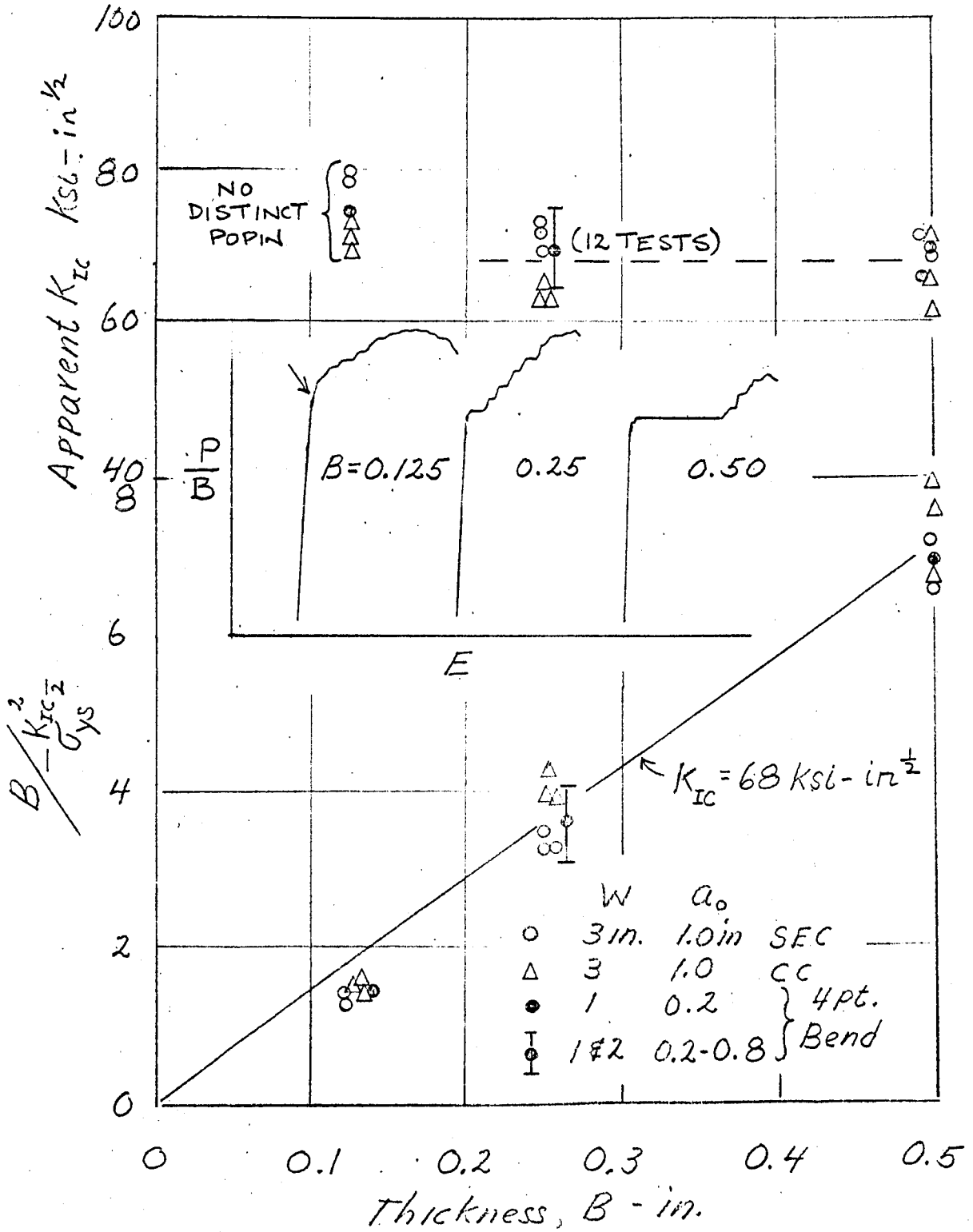

Fig. 14: Effect of Thickness on Popin Behavior & Apparent K_{Ic} For 259 ksi yield Strength Maraging Steel Tested Using Several Specimen Types.

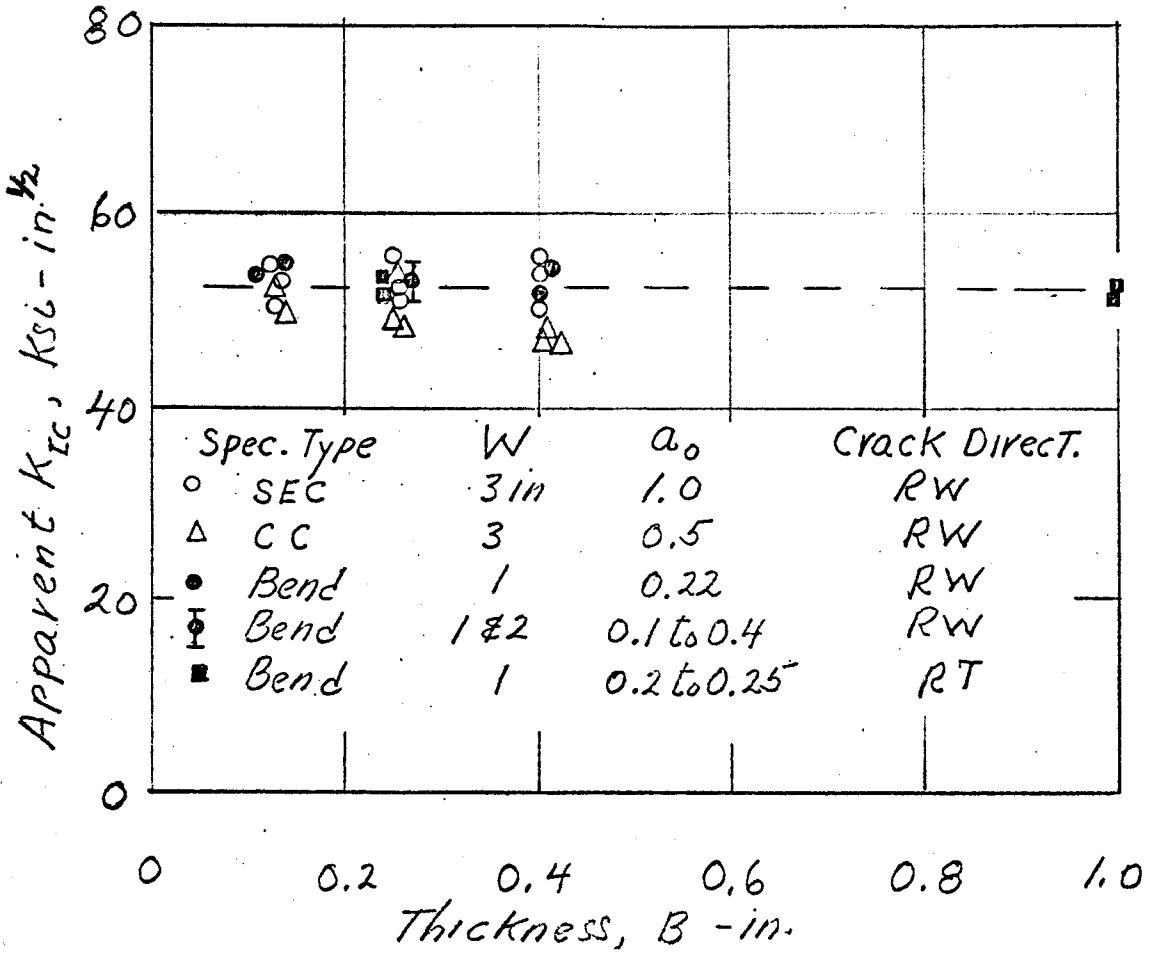

Fig 15: Effect of Thickness on Apparent K_{IC} for 285 ksi Yield Strength Maraging Steel Tested using Several Specimen Types.

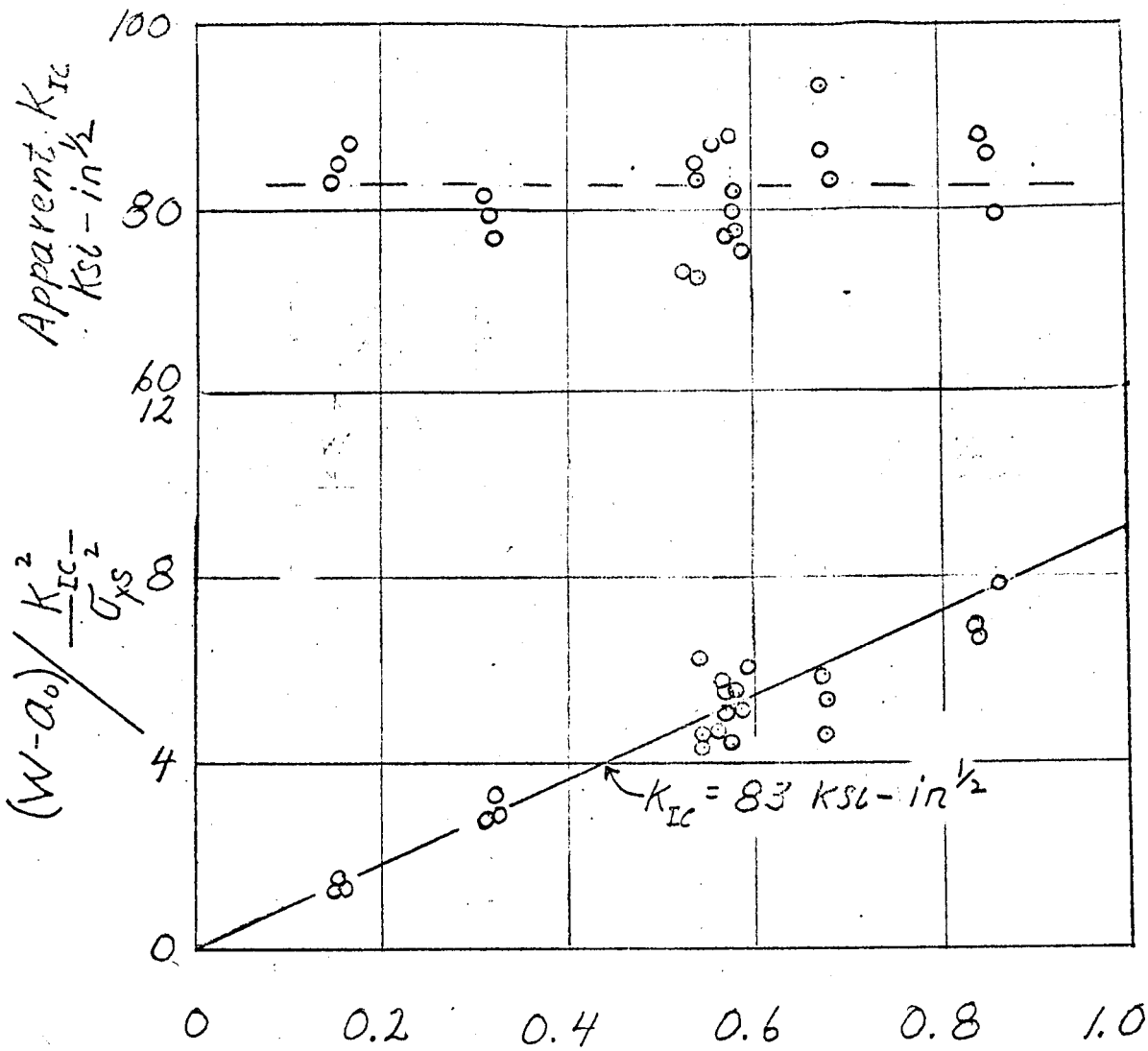

Fig. 16: Effect of Ligament Length on The Apparent K_{Ic} For 242 ksi Yield Strength Maraging Steel Tested in Bending.

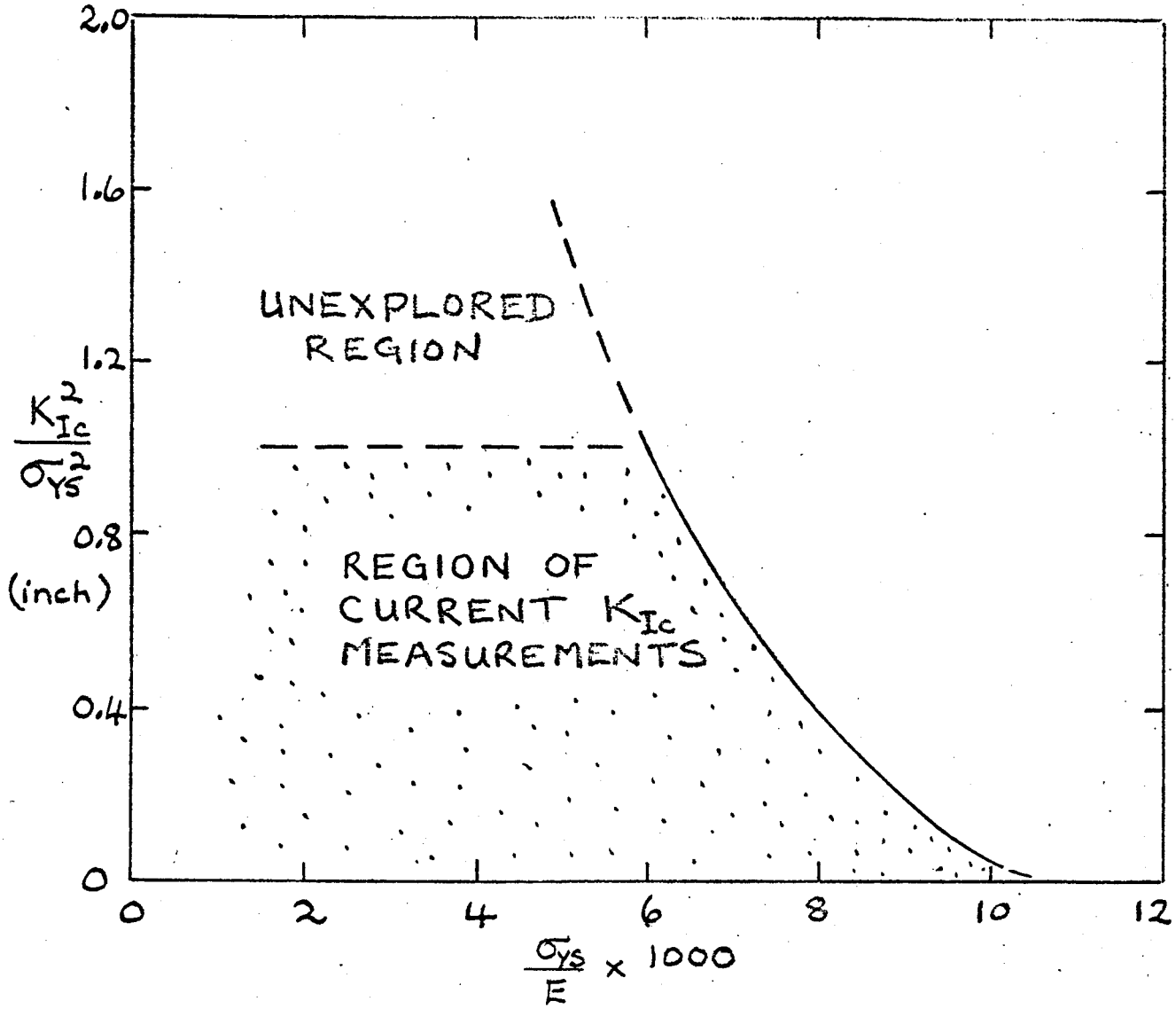

FIG. 17: BOUNDARIES OF THE REGION OF CURRENT PLANE STRAIN CRACK TOUGHNESS TESTS (BASED ON DATA FOR STEELS)

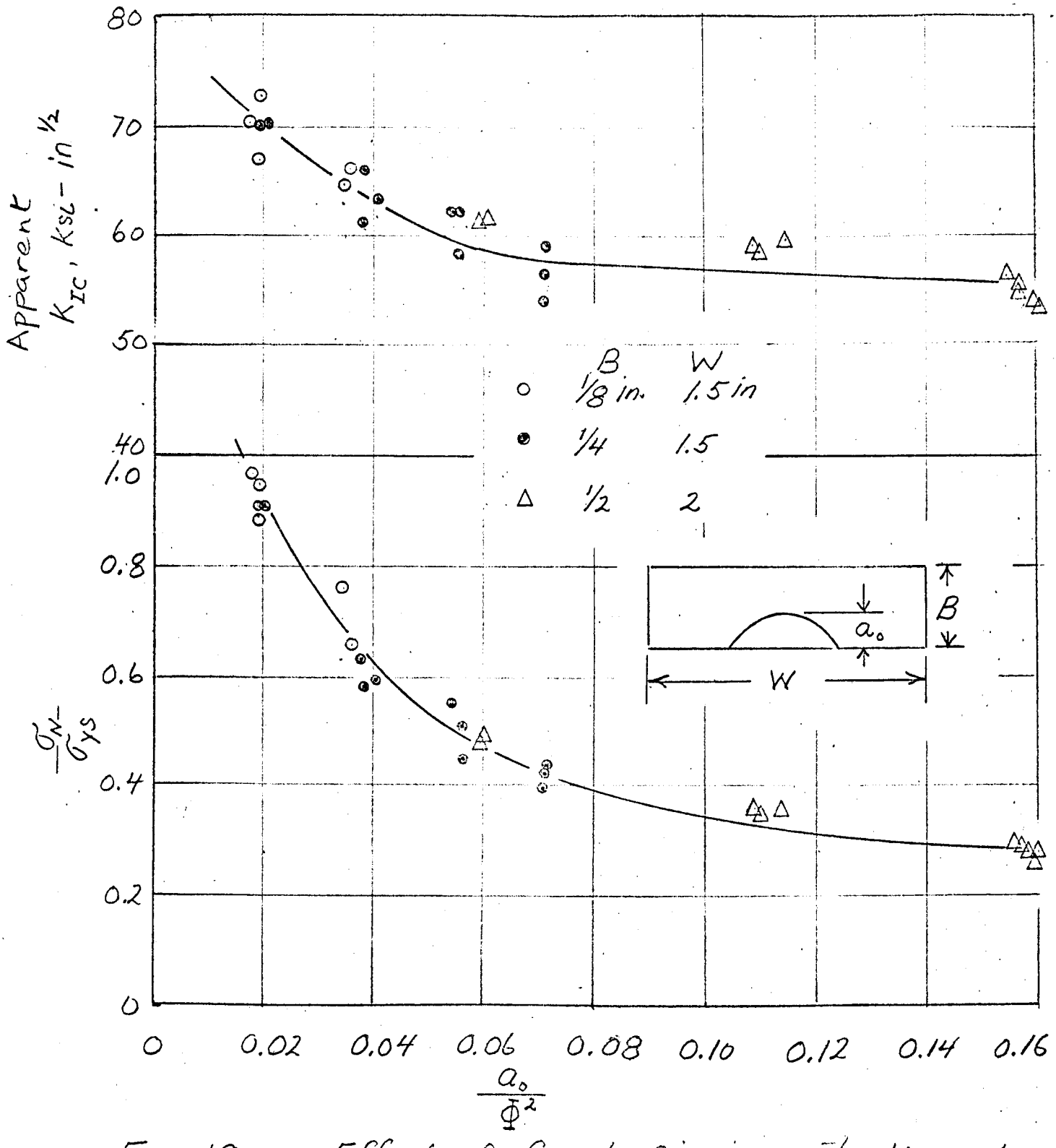

Fig. 18: Effect of Crack Size on The K_{Ic} Value and the Ratio of Net Stress to Yield Strength for 285 ksi Yield Strength Maraging Steel using Surface Cracked Specimens

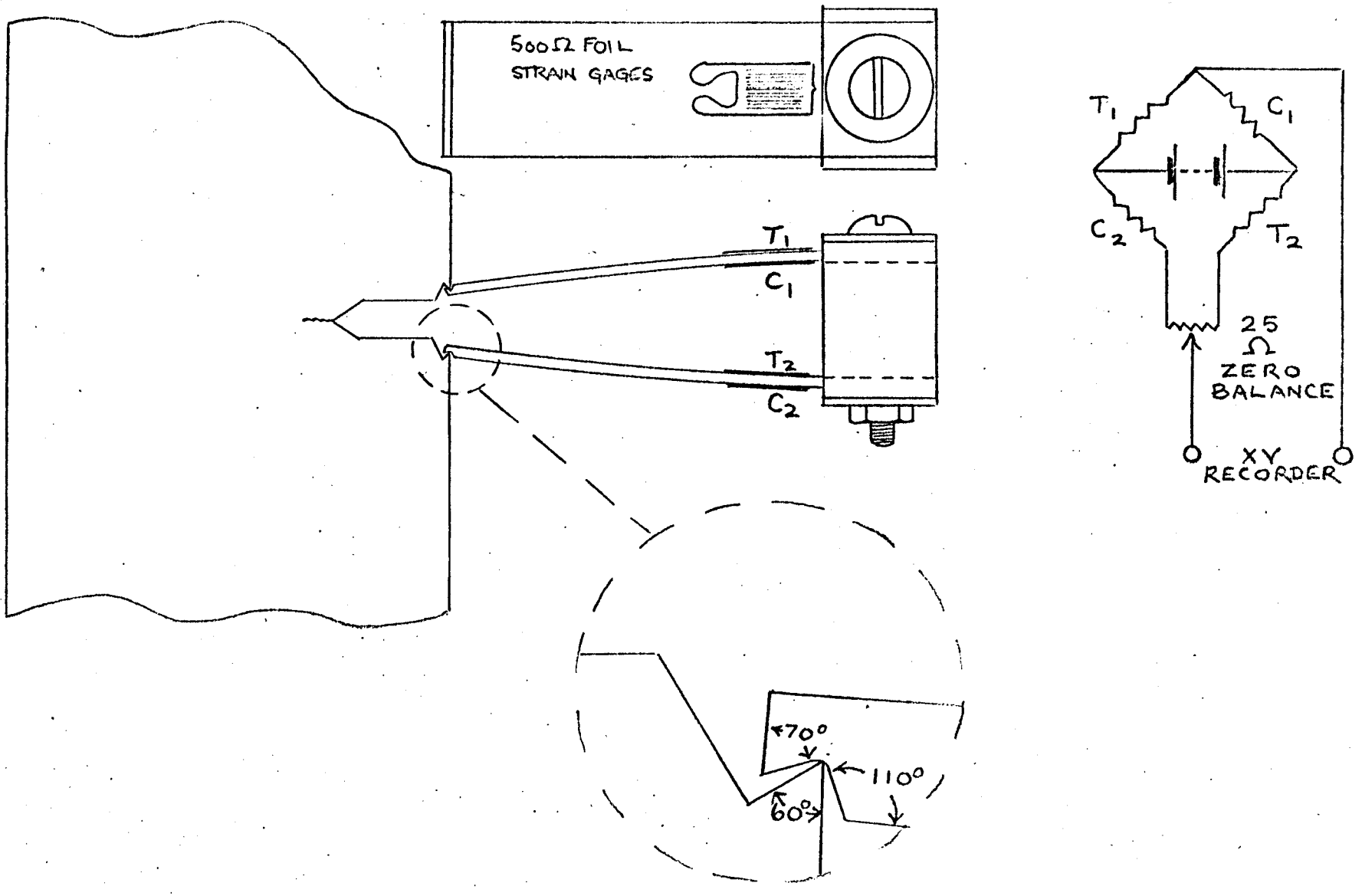

FIG. 19: DOUBLE CANTILEVER BEAM GAGE AND METHOD OF MOUNTING ON CRACK-NOTCHED SPECIMEN FOR DISPLACEMENT MEASUREMENT. DESIGNED BY J. E. SRAWLEY.

FIG. 19

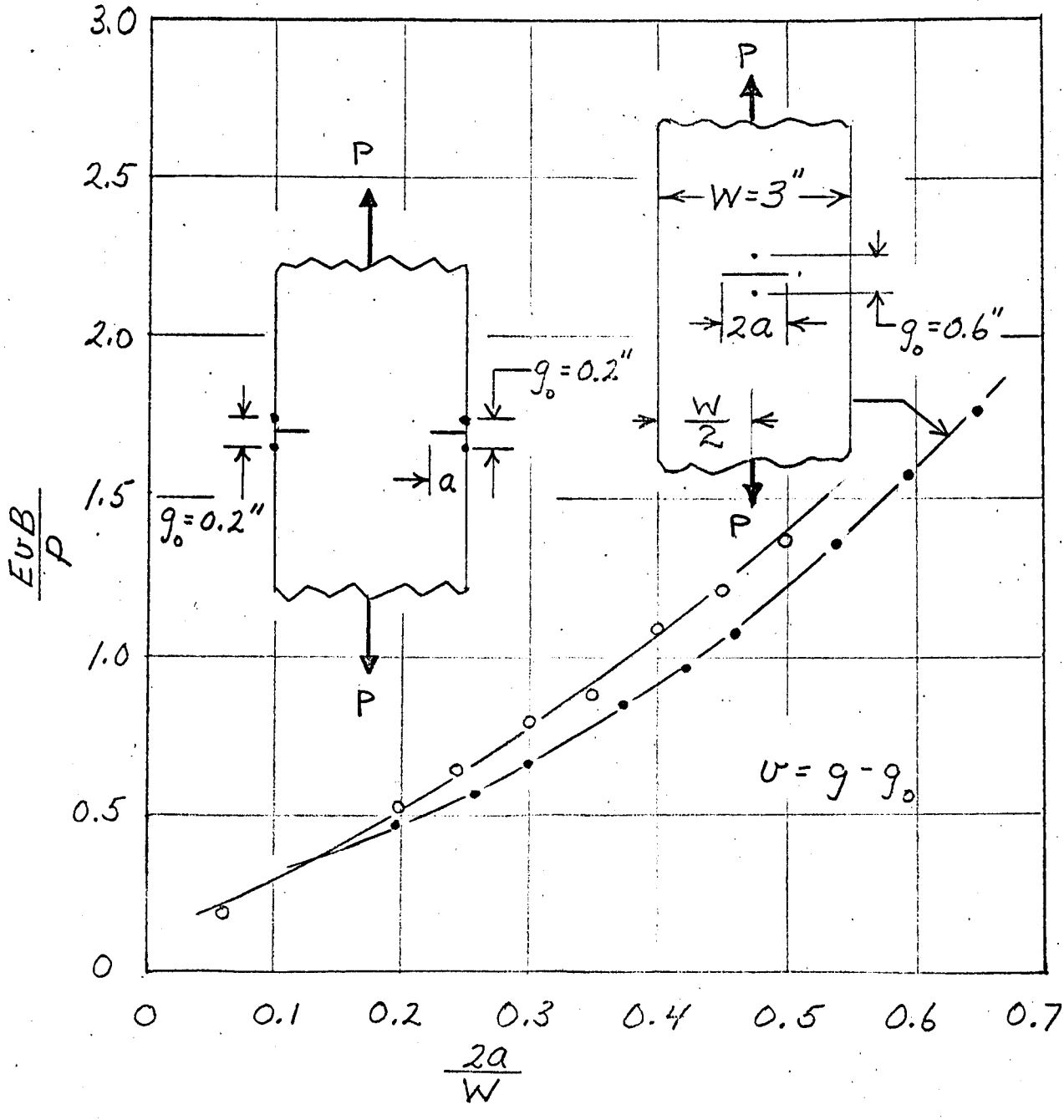

Fig. 20: Calibration Curves for Converting Displacement Measurements to Crack Lengths for Center & Double Edge Crack Specimens.

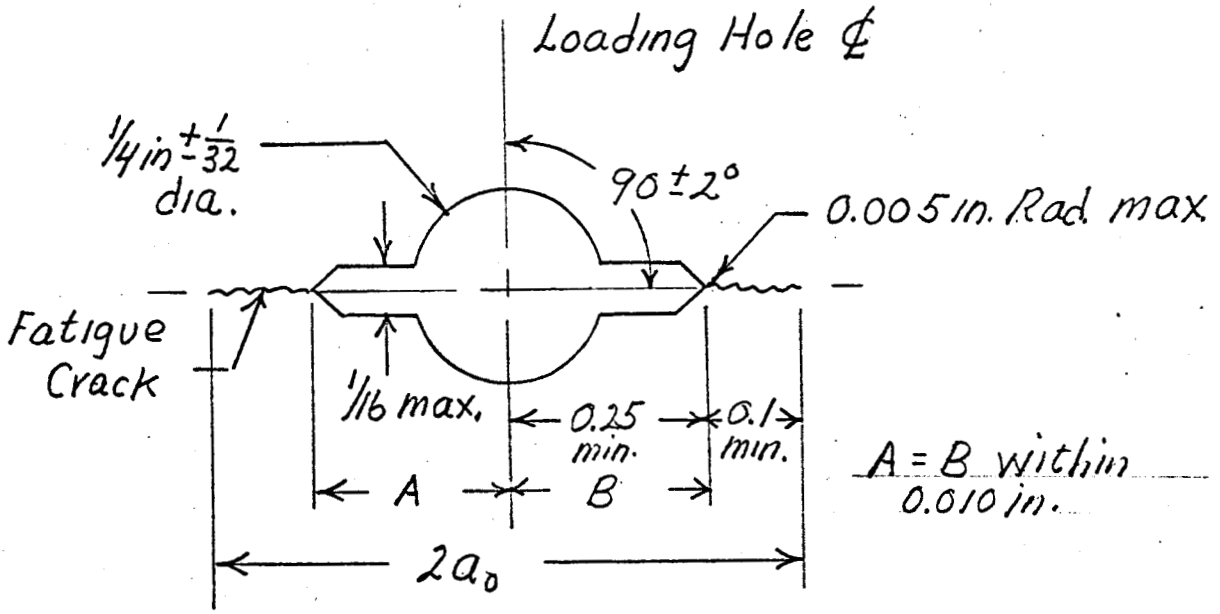

Fig. B4: Fatigue Crack Starter for Center Cracked Plate Specimens

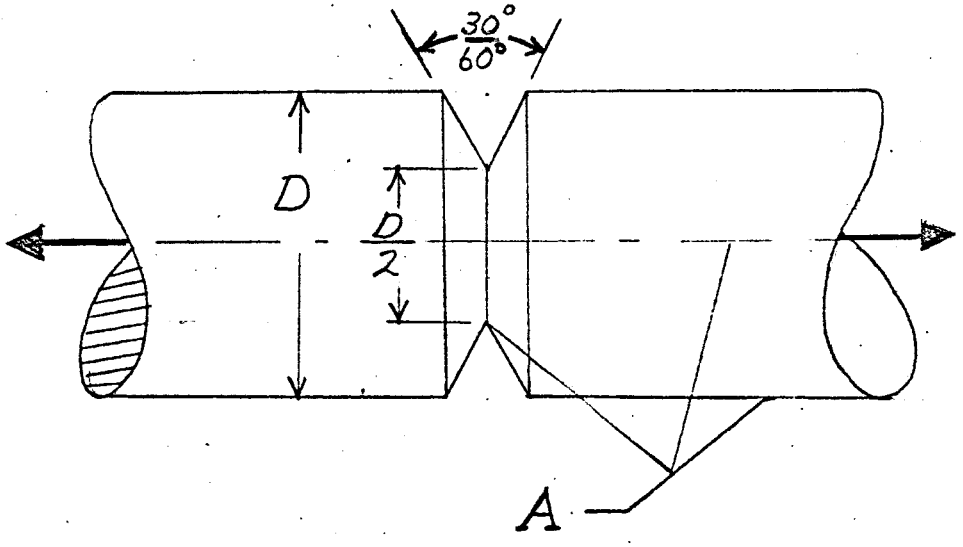

Circumferentially Cracked Round Bar
Radius of Machined Notch = 0.005 in max.

Fig. B-3: Proportions for The Circumferentially Cracked Round Bar.
A - Surfaces must be Concentric with The Load Axis to within $\frac{D}{1000}$

Preferred Range of Thickness $\frac{W}{2}$ to $\frac{W}{4}$

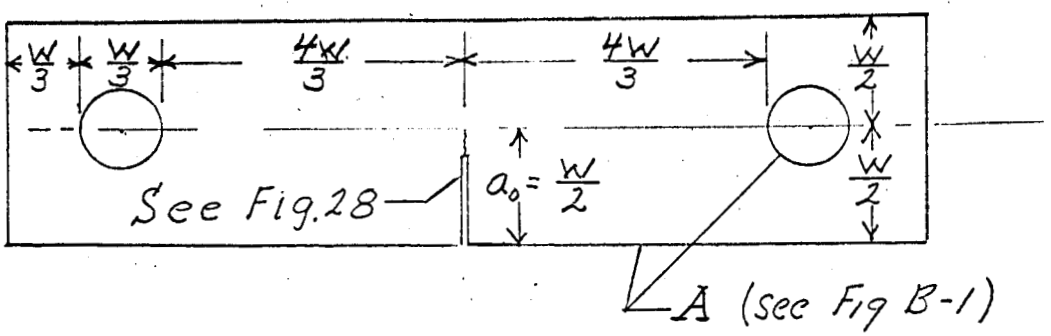

Single Edge Cracked Plate (Tension)

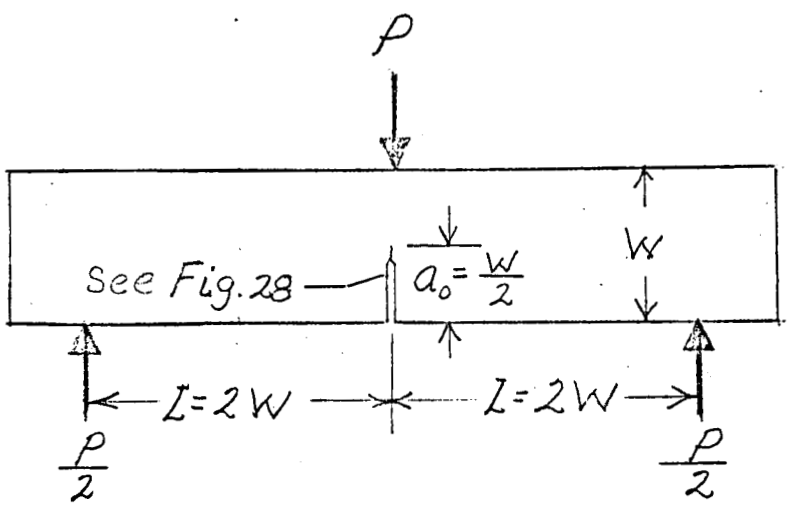

Single Edge Cracked Bend Specimen
(Three point loaded)

Fig. B2 Proportions for Single Edge Cracked Tension & Bend Specimens

Preferred Range of Thickness $\frac{W}{2}$ to $\frac{W}{4}$

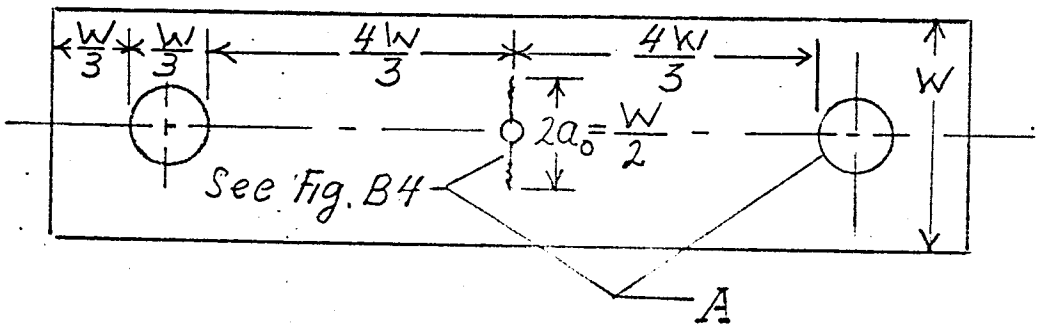

Center Cracked Plate

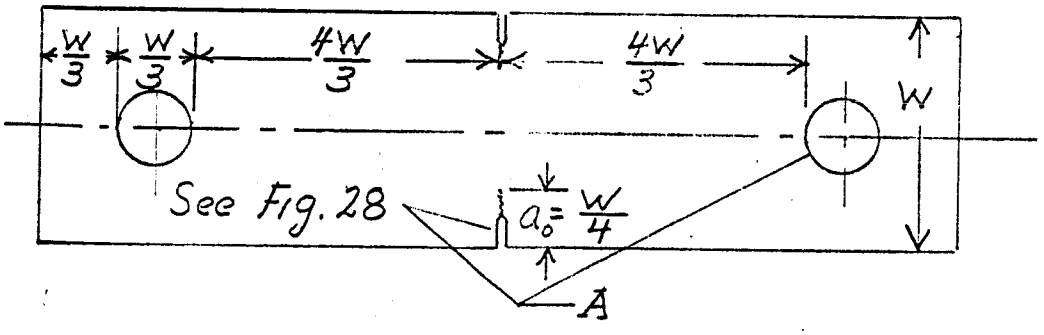

Double Edge Cracked Plate

Fig. B1: Proportions for Center & Double Edge Cracked Plate Specimens
A - Surfaces must be Symmetric to Specimen Centerline within $\frac{W}{1000}$

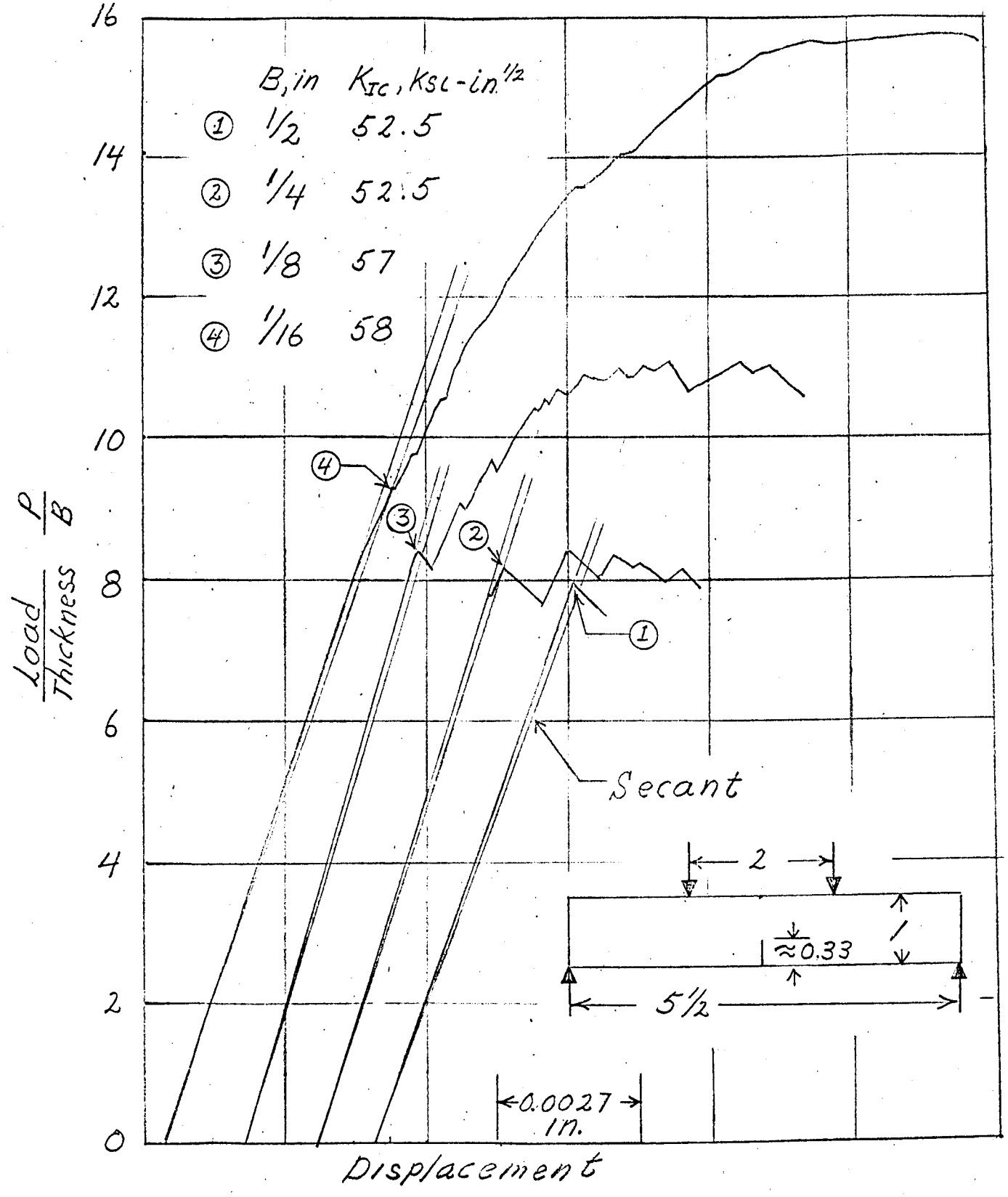

Fig. A-3: Examples of Analyses of Load-Displacement Records for Several Thicknesses of SAE 4340 Bend Specimens

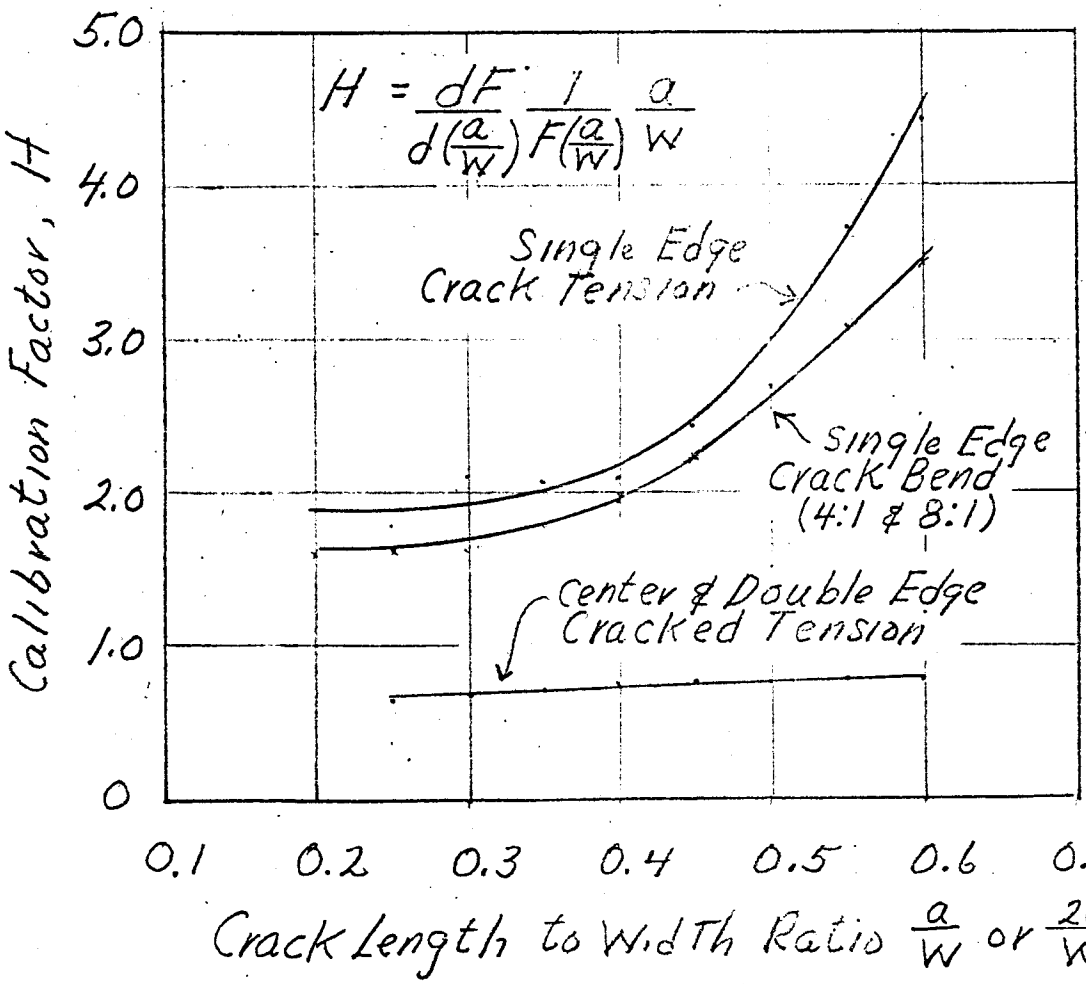

Fig. A-2: Calibration Factors For Use in Analysis of Load Displacement Records

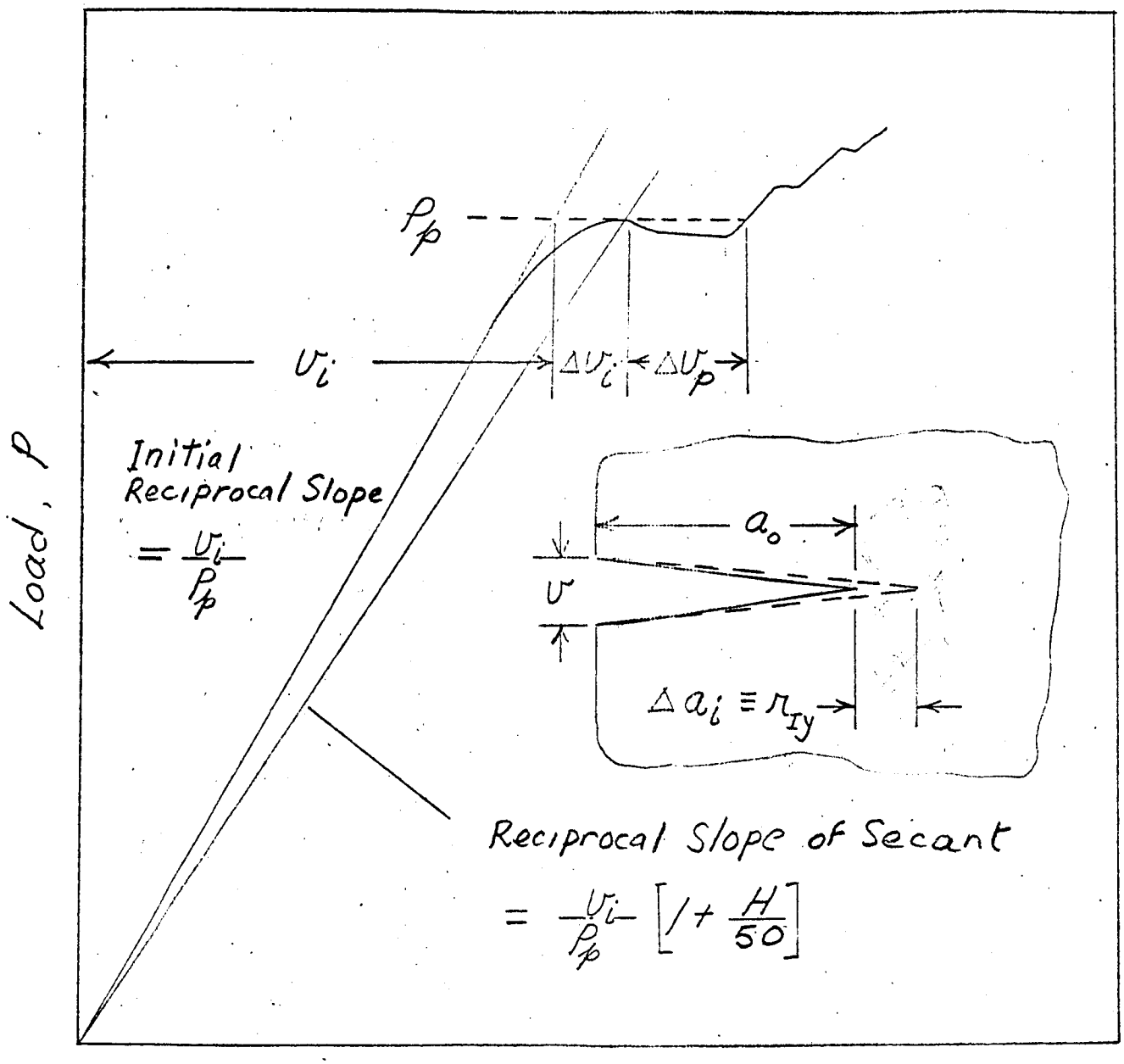

Fig. A-1: Typical Load Displacement Record Showing Quantities Involved in Development of a Procedure for Load-Displacement Record Analysis.

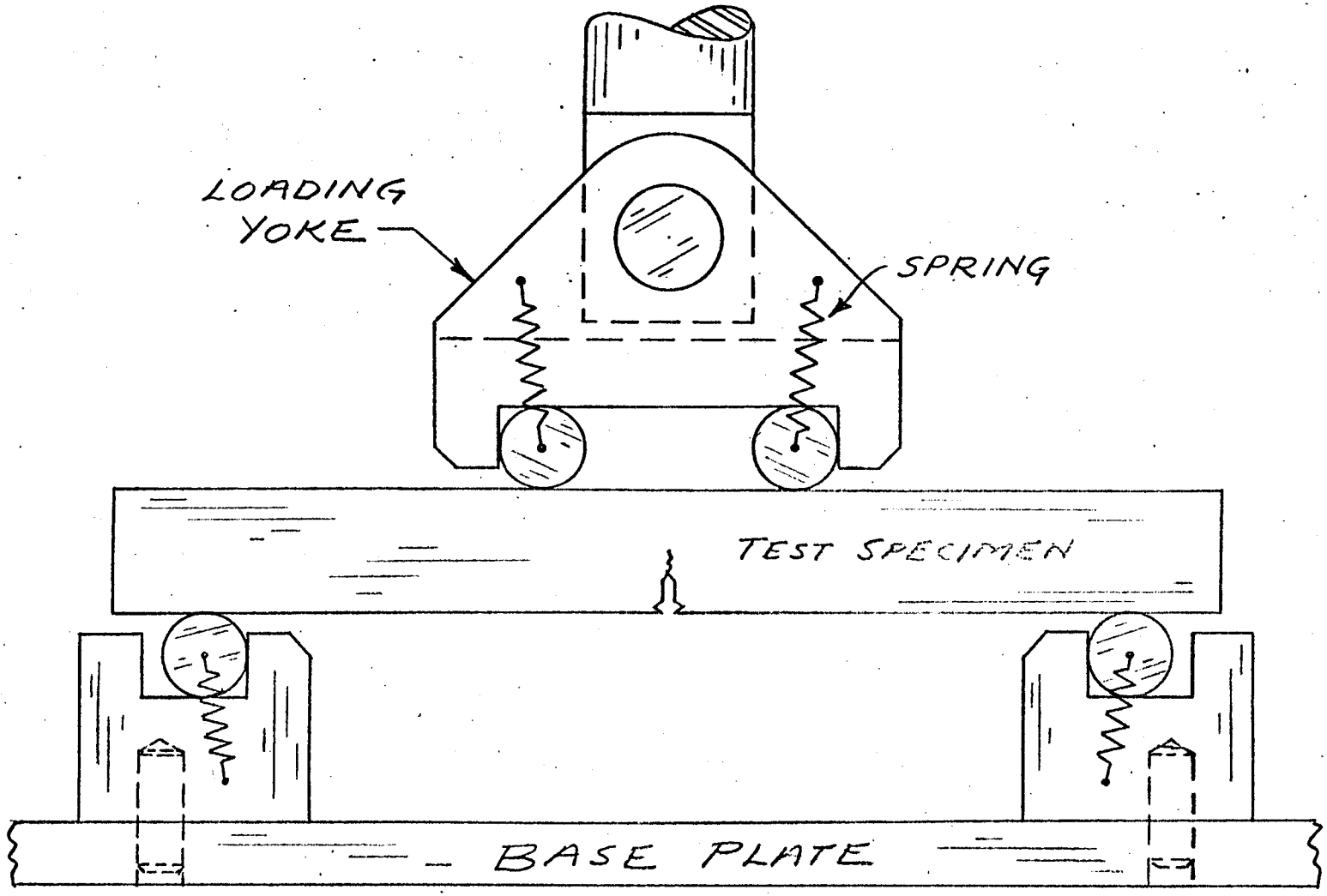

FIG. 38: SUGGESTED DESIGN OF BEND FIXTURE PERMITTING PIN MOVEMENT.

FIG. 38

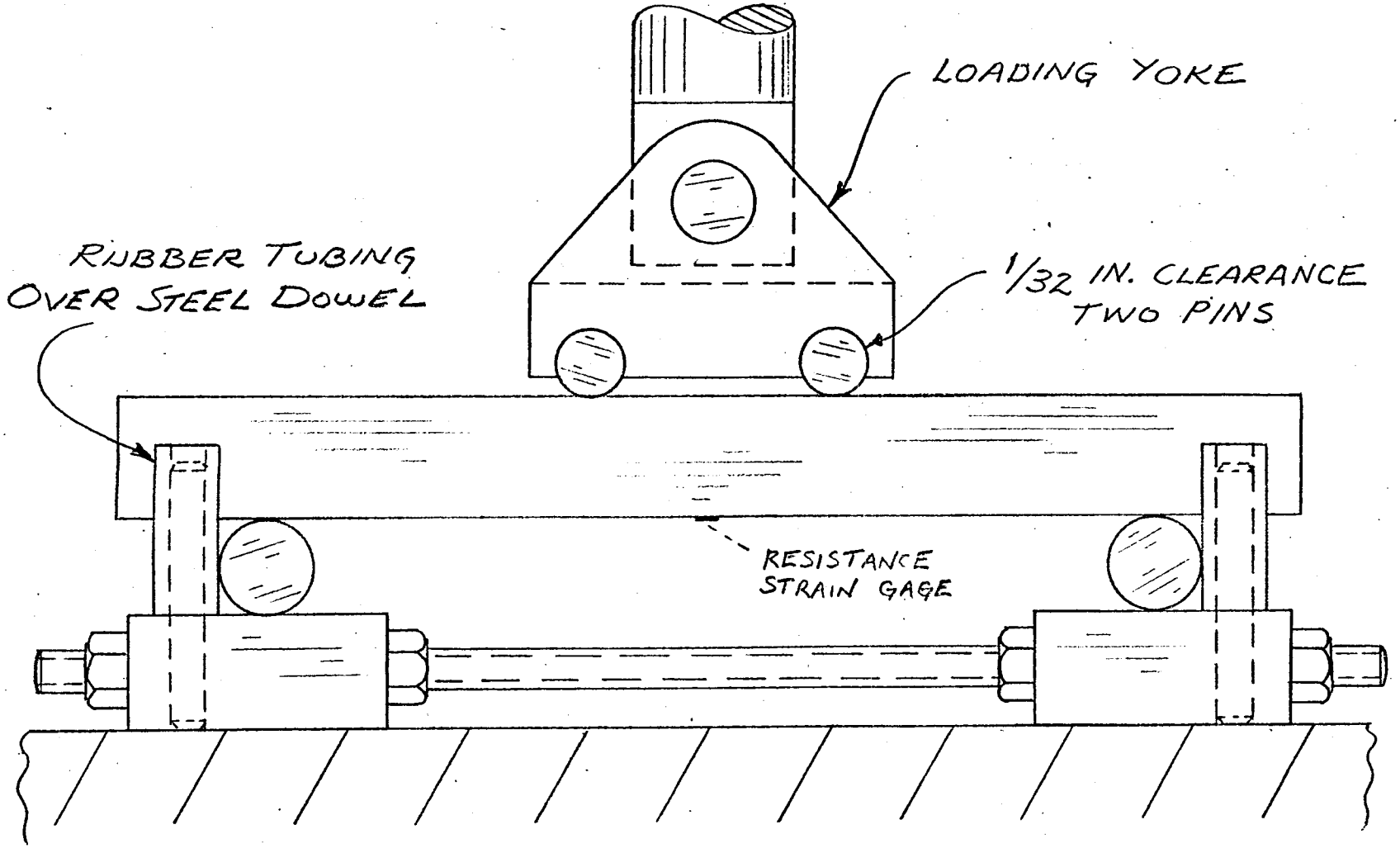

FIG 37: MODIFIED BEND FIXTURE.

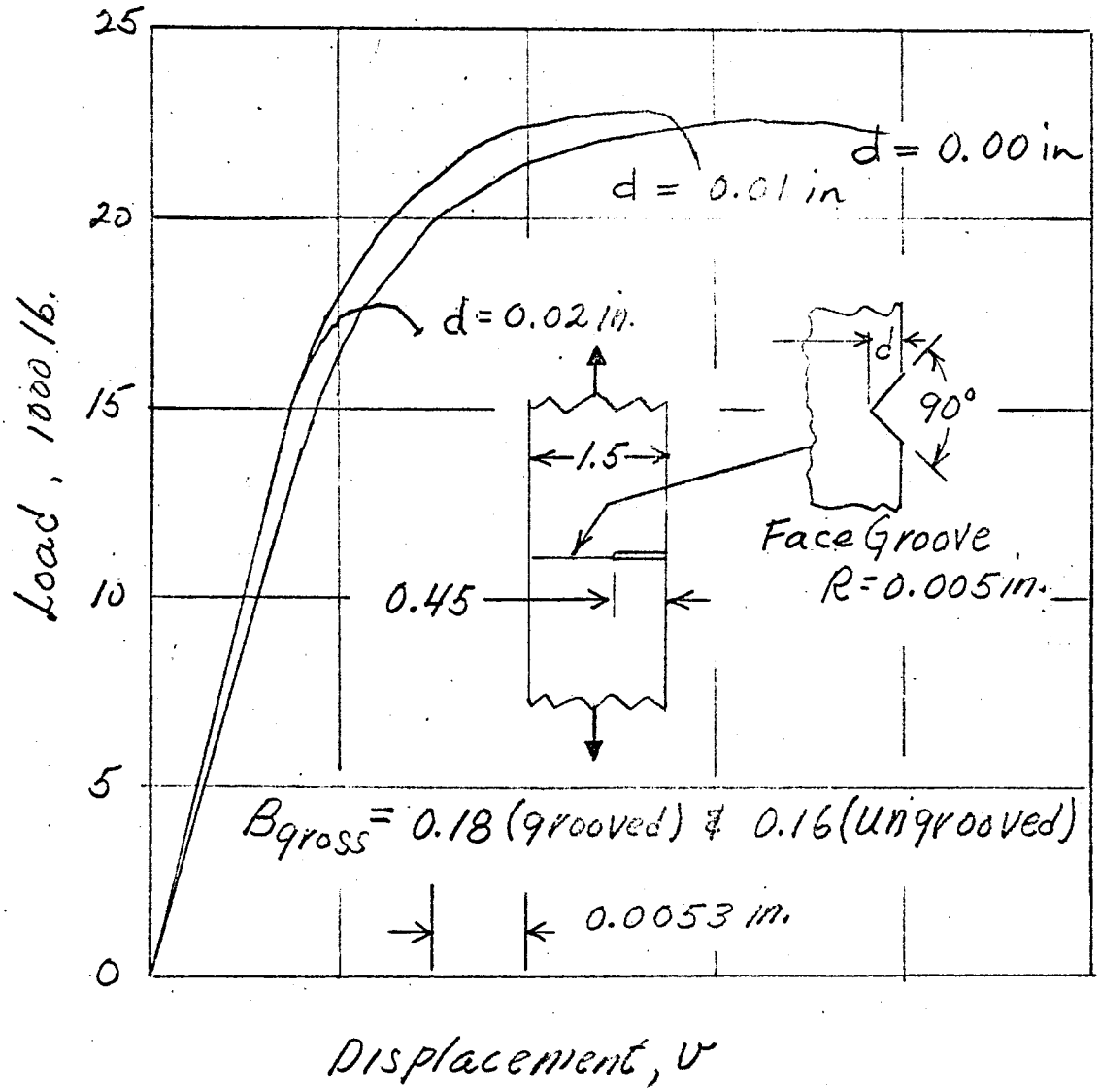

Fig. 36: Load-Displacement Records from Single-Edge Crack Tension Specimens With and Without Face Grooves (195 ksi Yield Strength Maraging Steel)

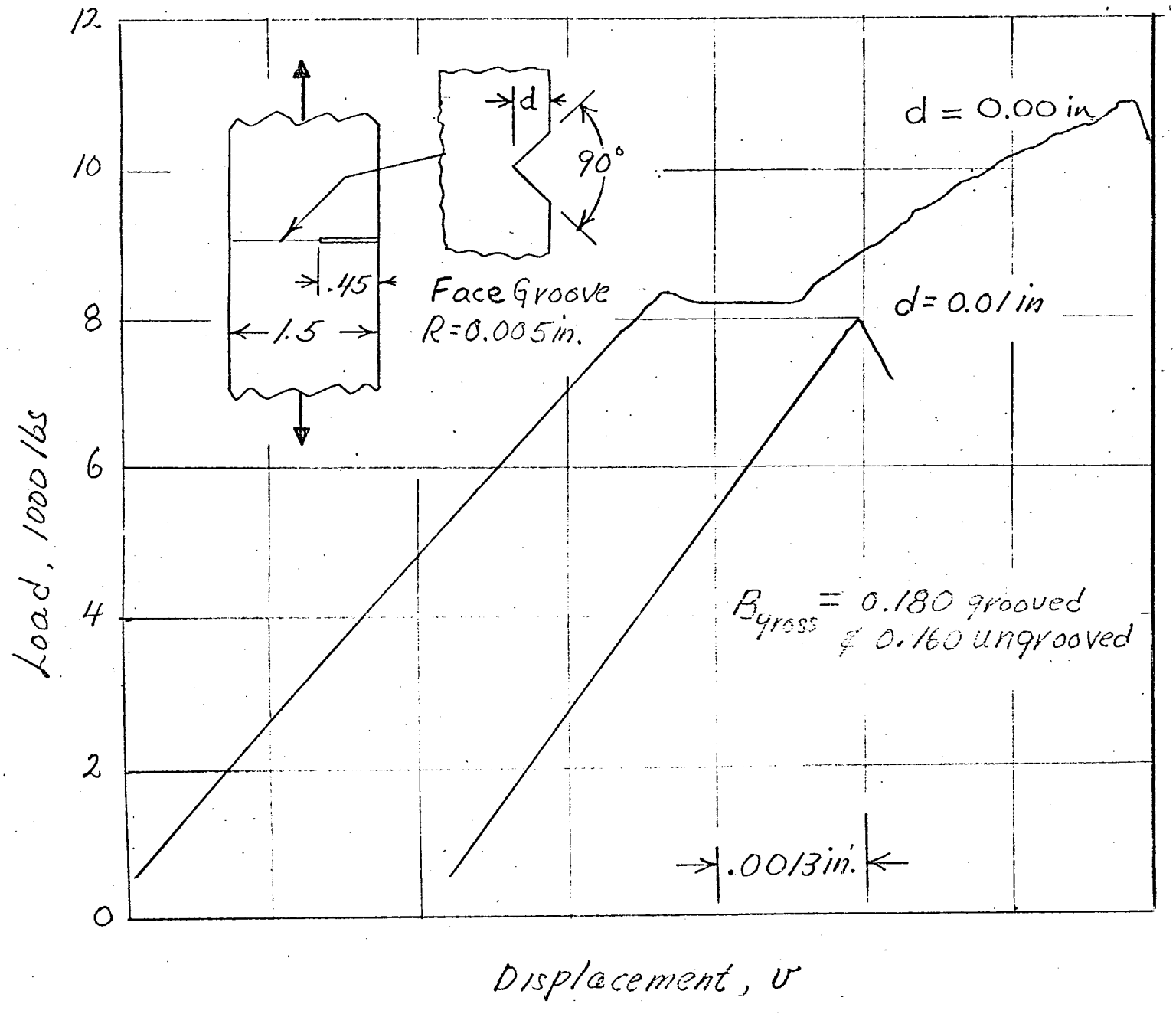

Fig. 35: Load-Displacement Records from Single-Edge Crack Tension Specimens with and without Face Grooves (280 ksi Yield Strength Maraging Steel)

Fig. 35

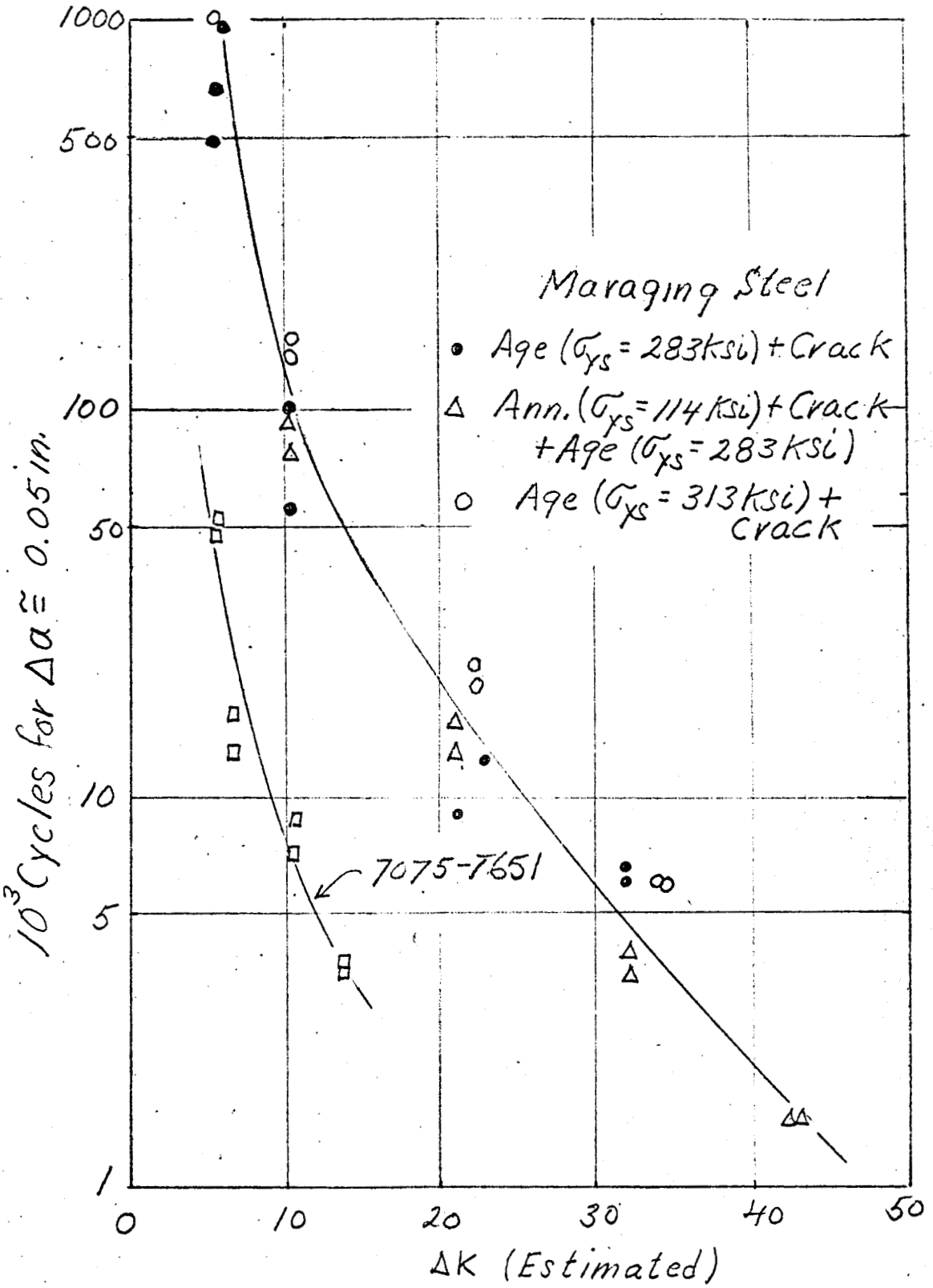

Fig. 34: Influence of ΔK on The [illegible] Number of Tension-Tension Fatigue Cycles to Produce a Total Crack Extension of 0.050 in. in Bend Specimens.

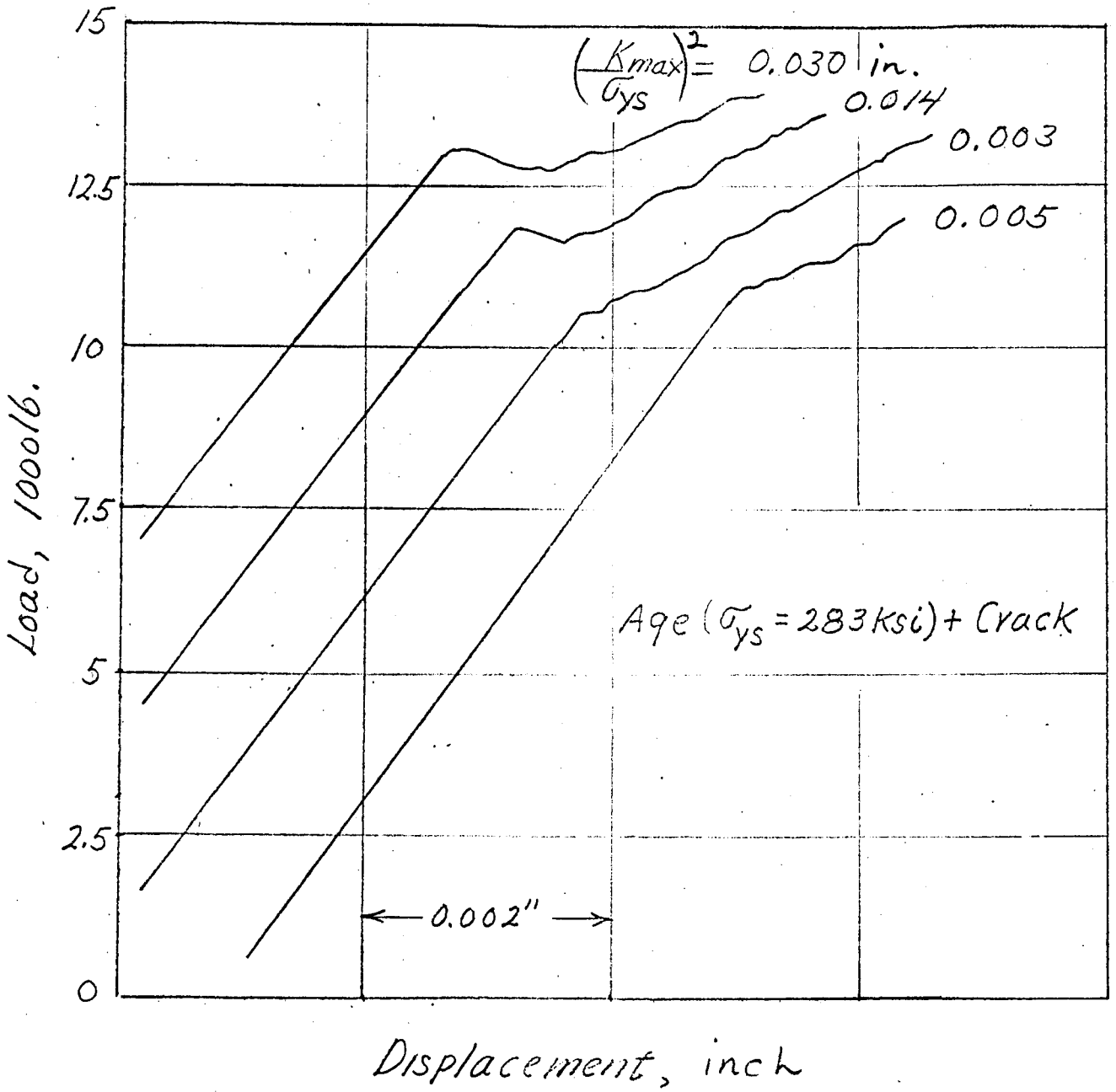

Fig. 33: Effect of Estimated $\left(\frac{K_{max}}{\sigma_{ys}}\right)^2$ on The popin Behavior of Maraging Steel Bend Specimens Cracked after Aging.

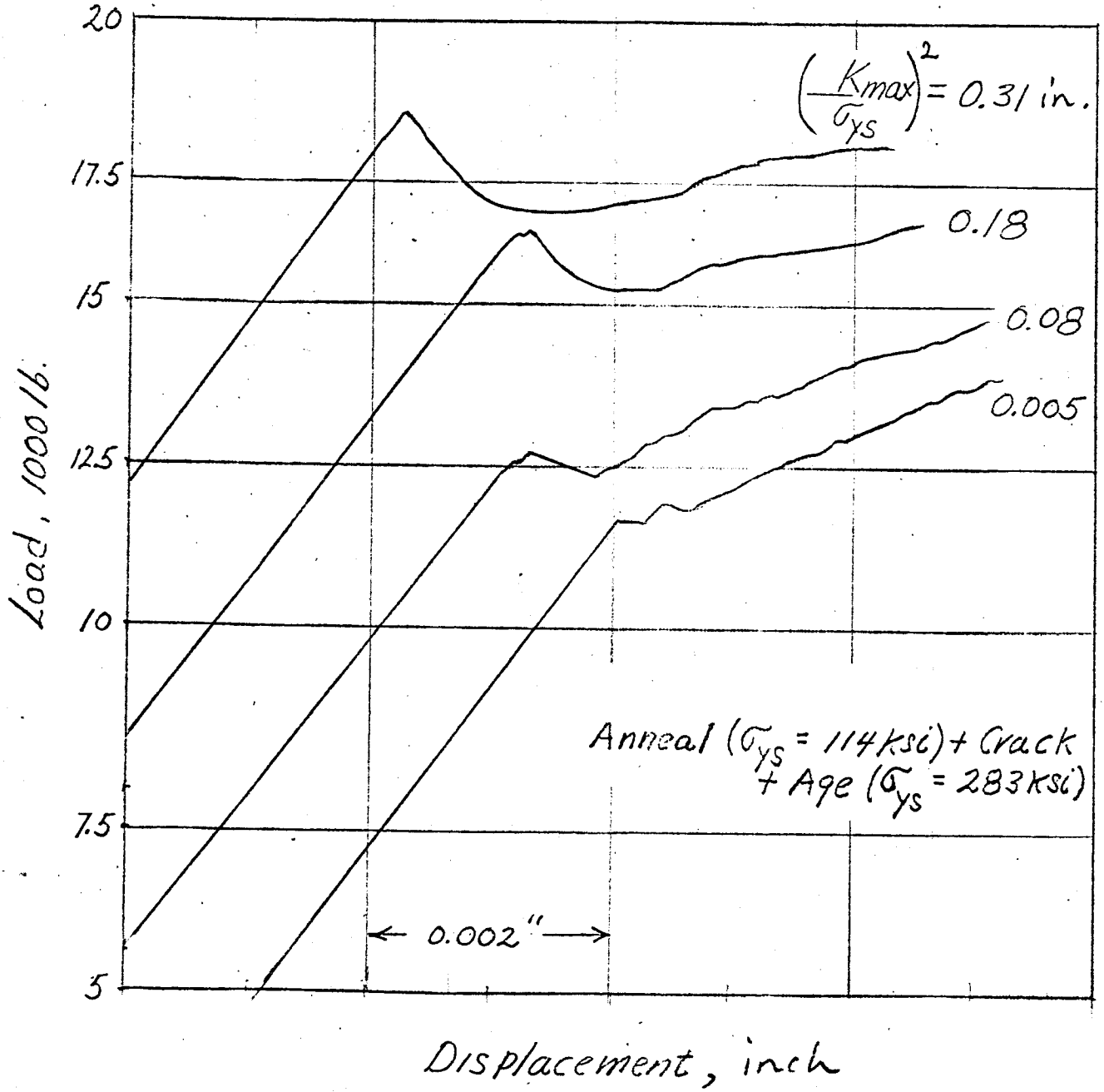

Fig. 32: Effect of Estimated $\left(\frac{K_{max}}{\sigma_{ys}}\right)^2$ on The Pop-in Behavior of Maraging Steel Bend Specimens Cracked before Aging

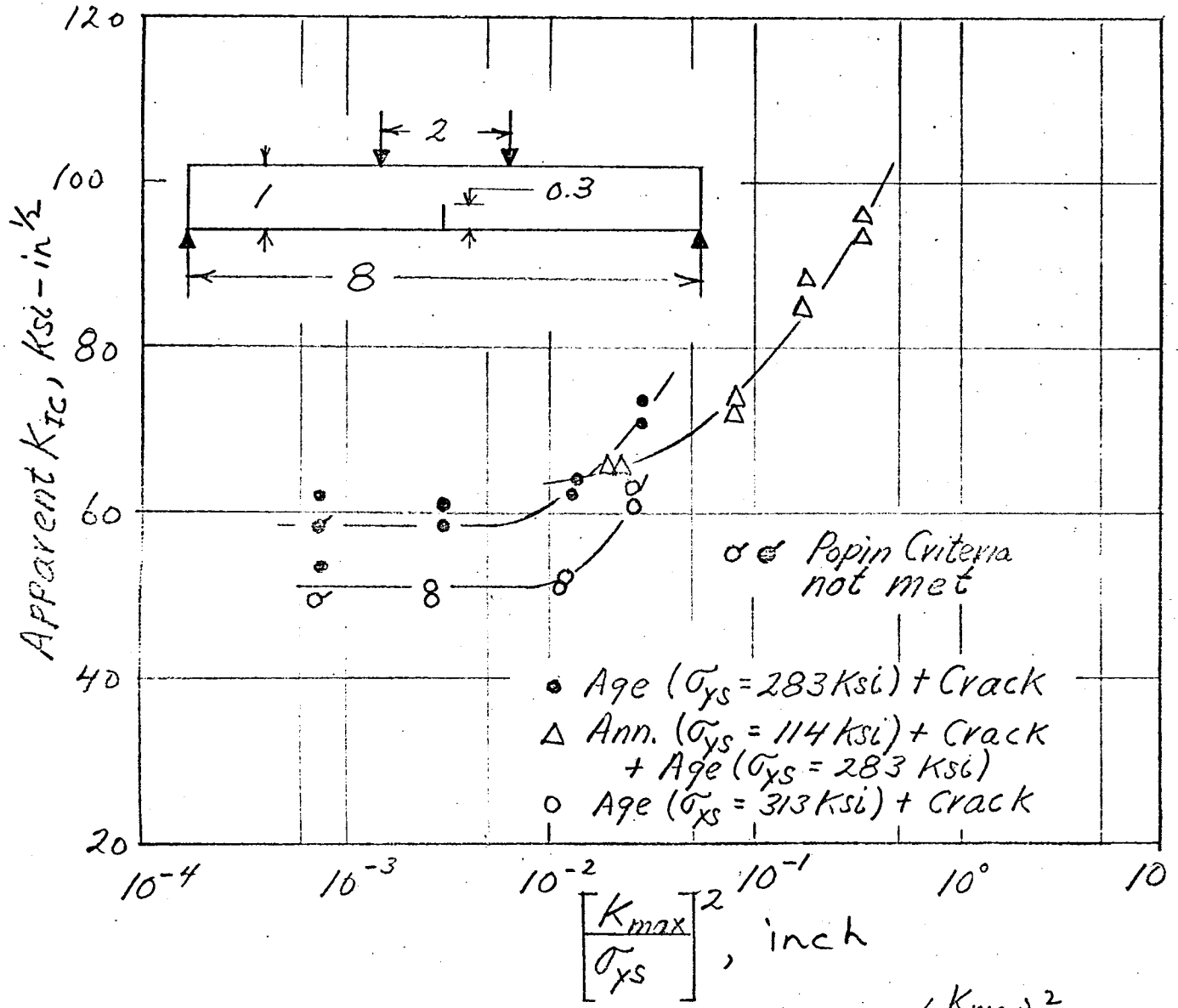

Fig. 31: Effect of Estimated $\left(\frac{K_{max}}{\sigma_{ys}}\right)^2$ During Fatigue Cracking on Apparent K_{IC} of Maraging Steel Cracked Before or After Aging

Fig. 31

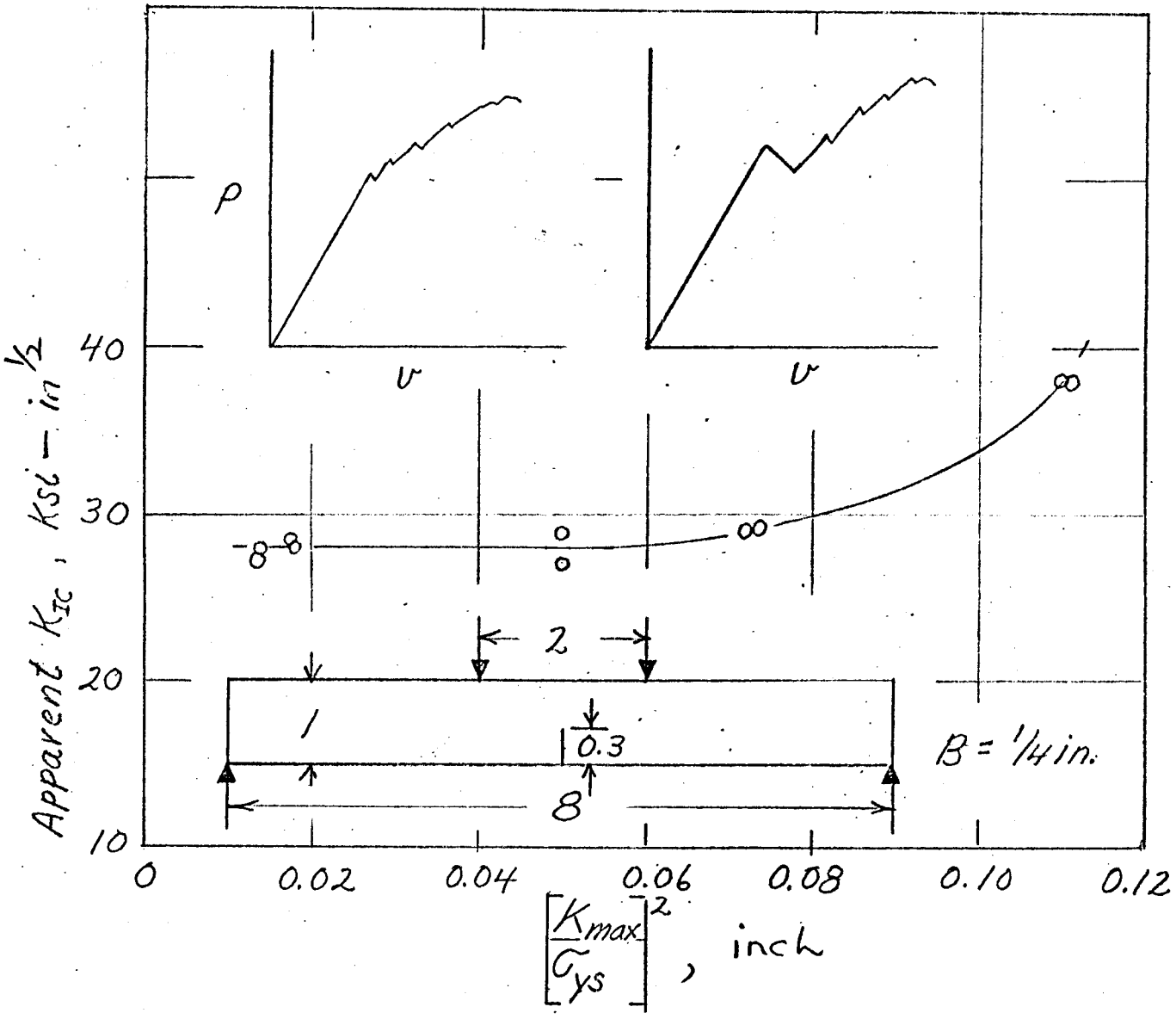

Fig. 30: Effect of Estimated $\left(\frac{K_{max}}{\sigma_{ys}}\right)^2$ During Fatigue Cracking on The Apparent K_{Ic} and Popin Behaviour for 7075.T651

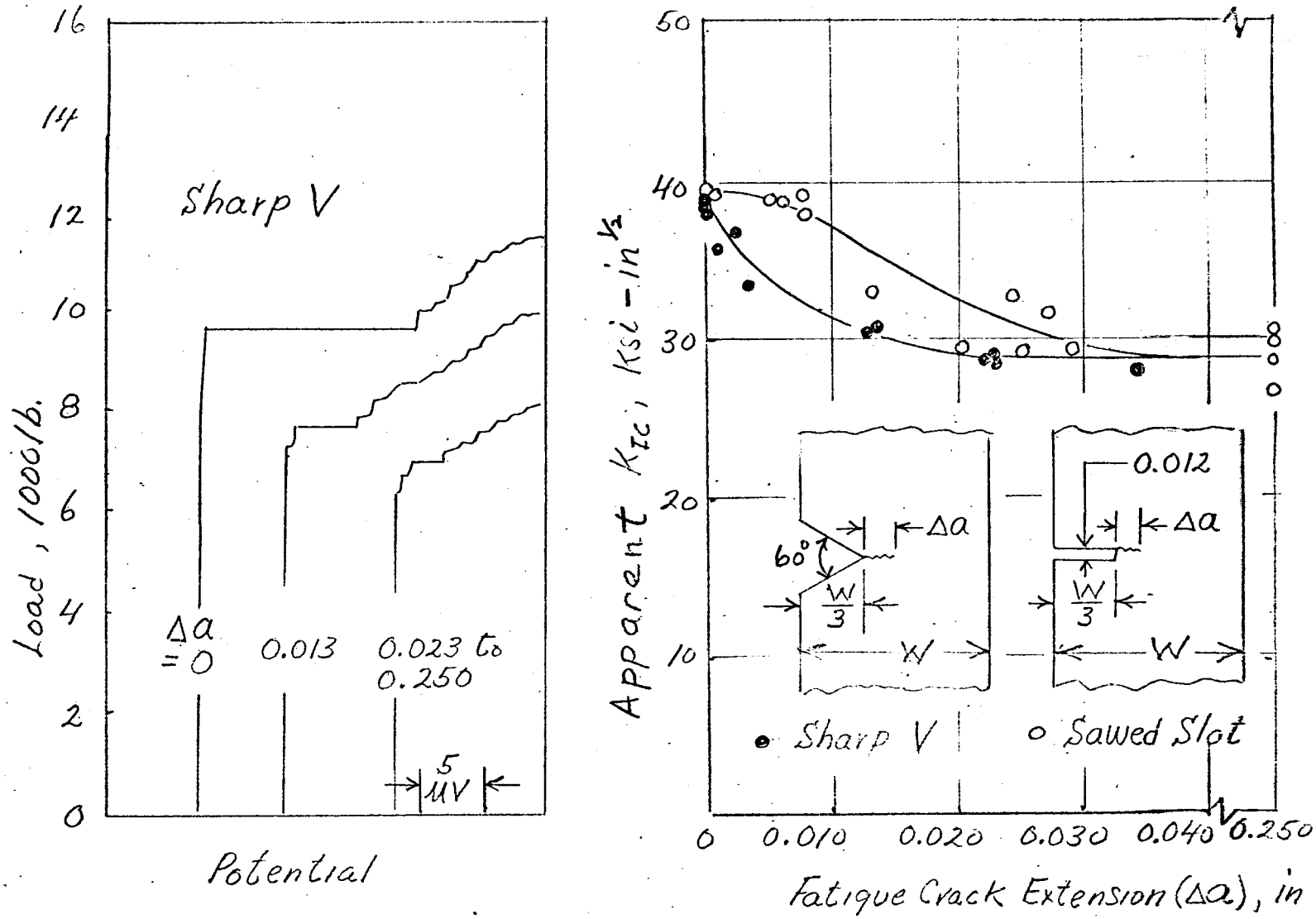

Fig. 29: Influence of Amount of Fatigue Crack Extension From Starter Notches on Apparent K_{Ic} & Pop-in Behavior for 7075-T651 Aluminum Alloy

Fig. 29

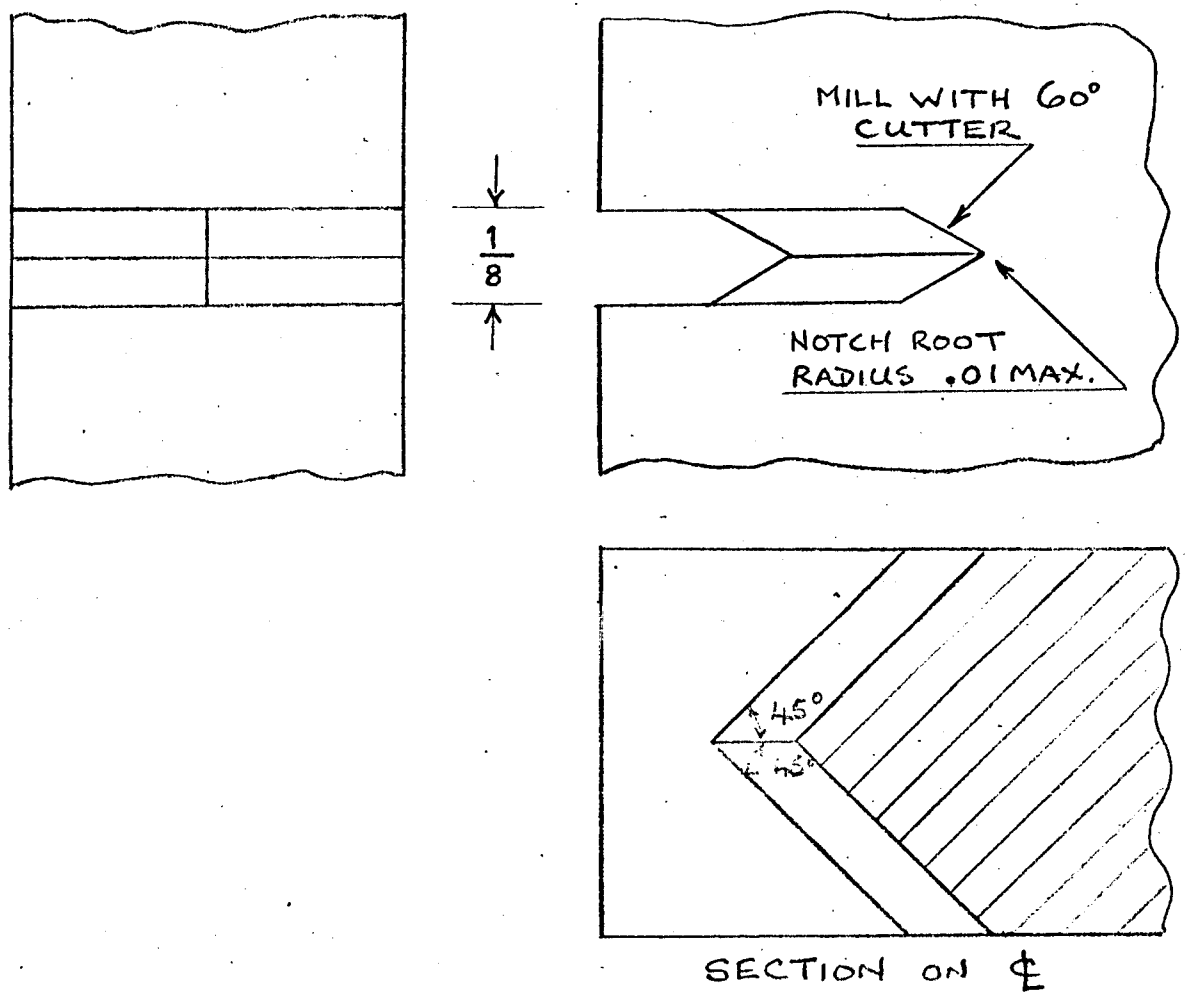

FIG. 28: CHEVRON NOTCH FOR EDGE-CRACK PLATE SPECIMENS.

FIG. 28

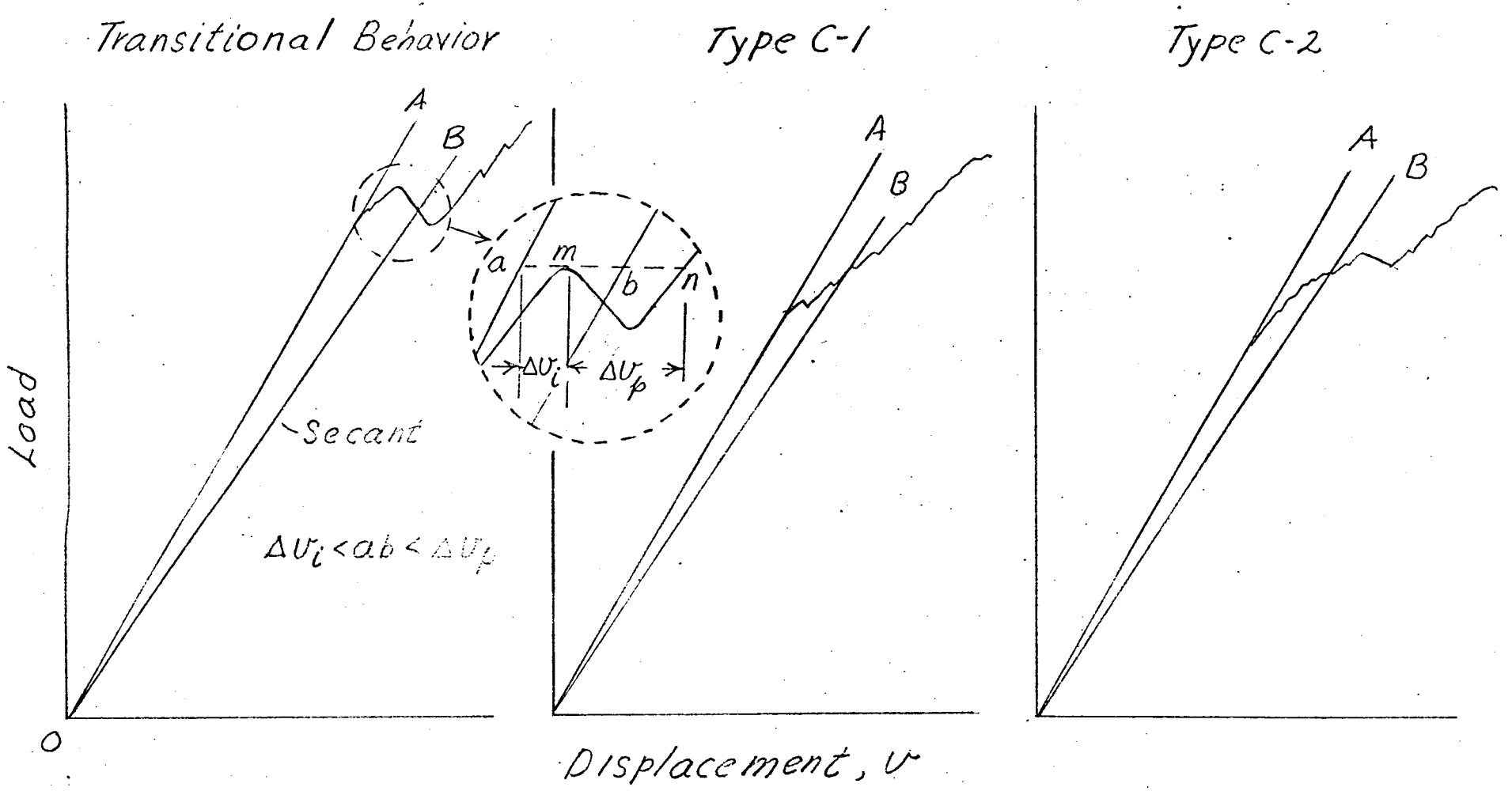

Fig. 27: Examples of Load Displacement Records For Bend Specimens Illustrating Suggested Criteria for Analysis of Popin Records

Fig. 27

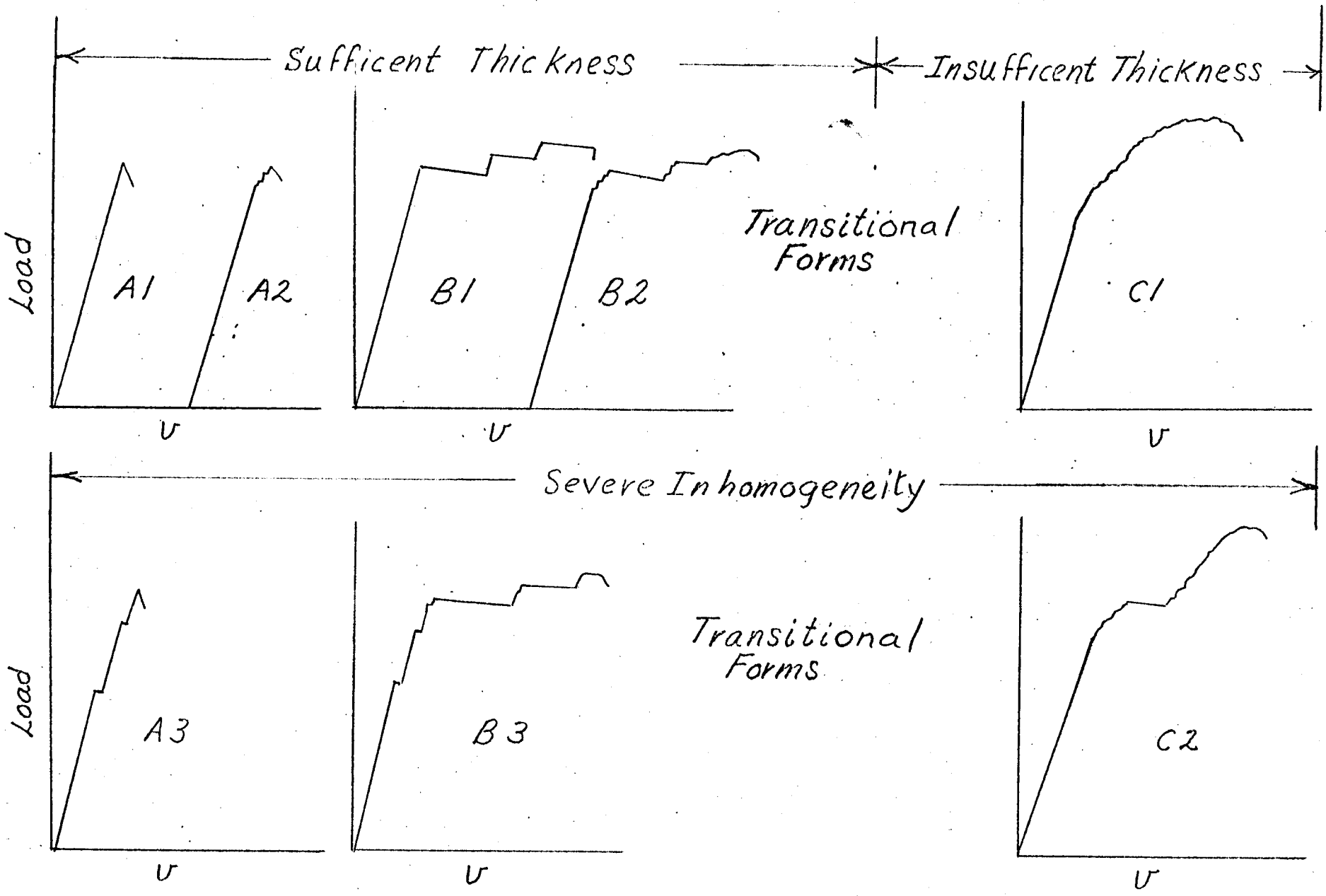

Fig. 26: Typical Load-Displacement Records Illustrating Several Types of Popin Behavior.

Fig. 26

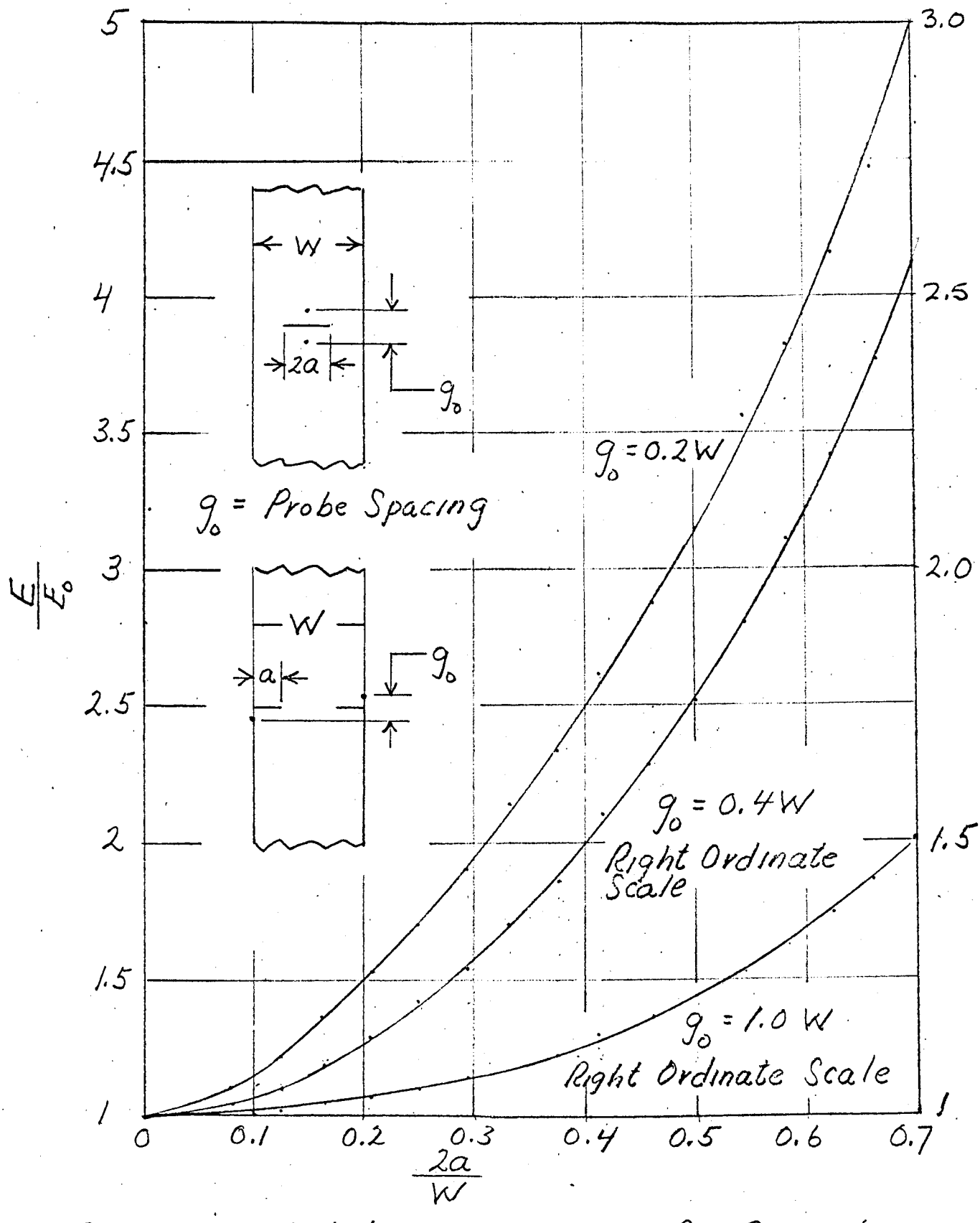

Fig. 25 : Calibration Curves for Converting Electric Potential Measurements to Crack Lengths For Symmetrically Cracked Plate Specimens.

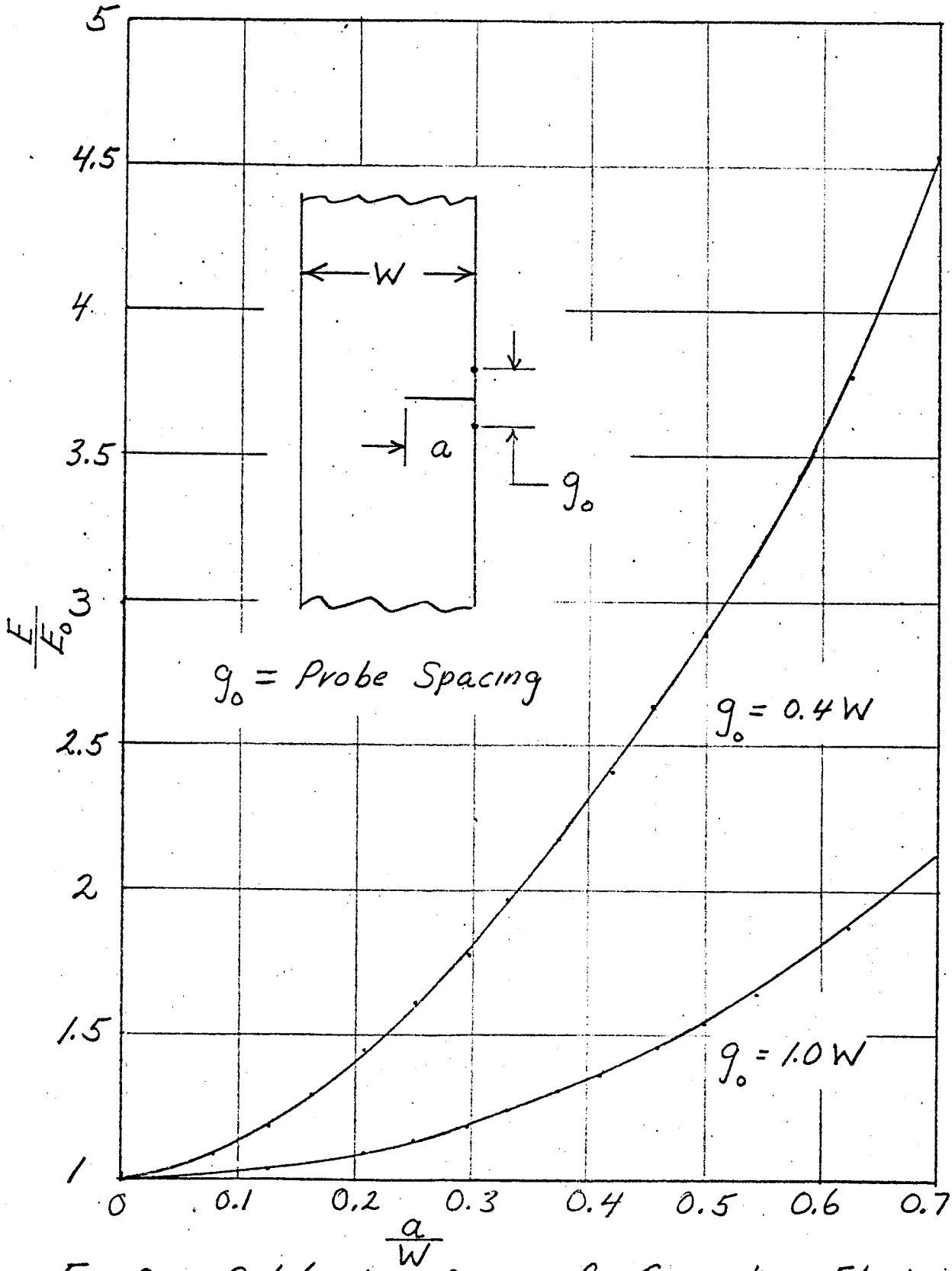

Fig. 24: Calibration Curves for Converting Electric Potential Measurements to Crack Lengths for Single Edge Crack Specimens.

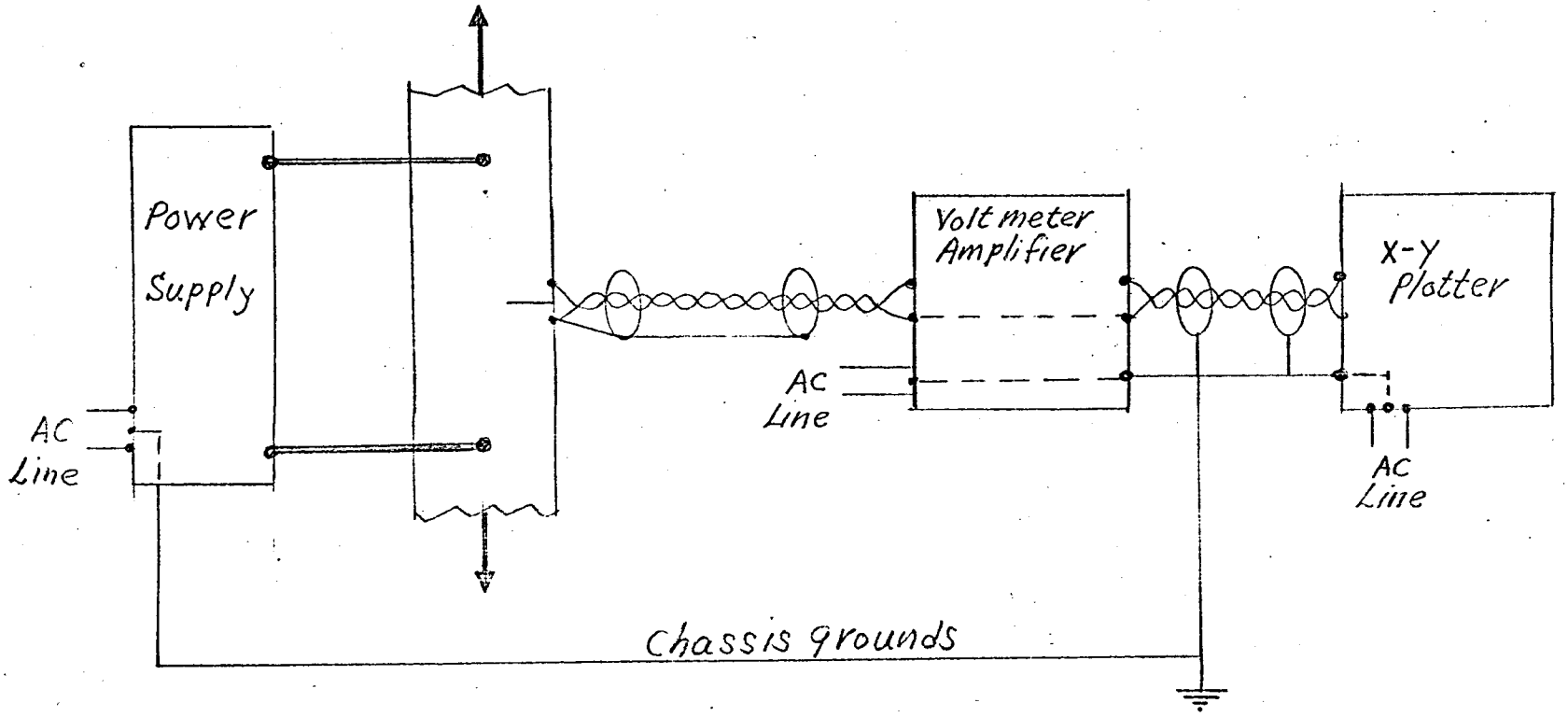

Fig. 23: Block Schematic of Set-up For Measuring Electrical Potential showing arrangement of Shields & Grounds

Fig. 23

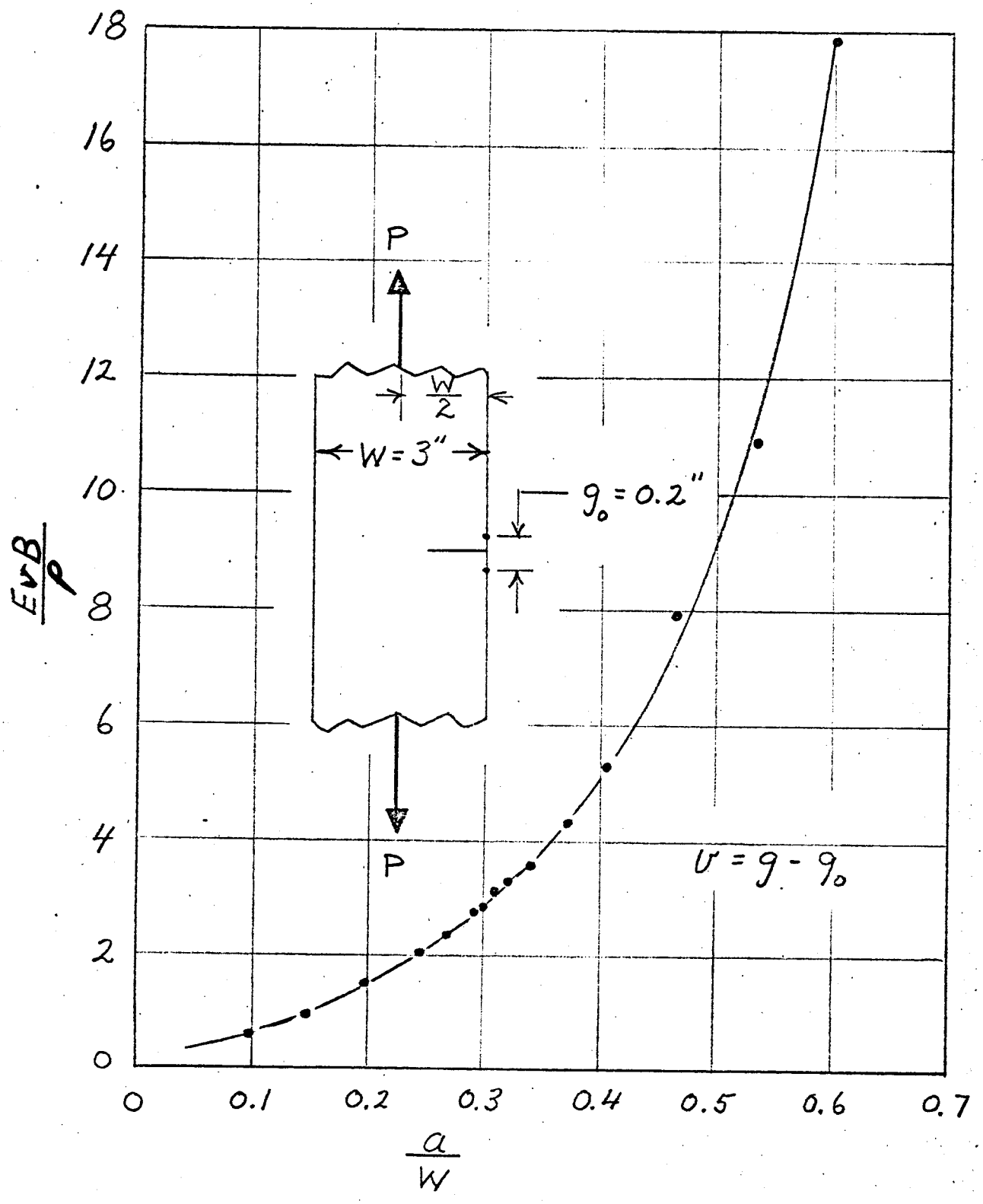

Fig. 22: Calibration Curve for Converting Displacement Measurements to Crack Length for Single Edge Crack Tension Specimens

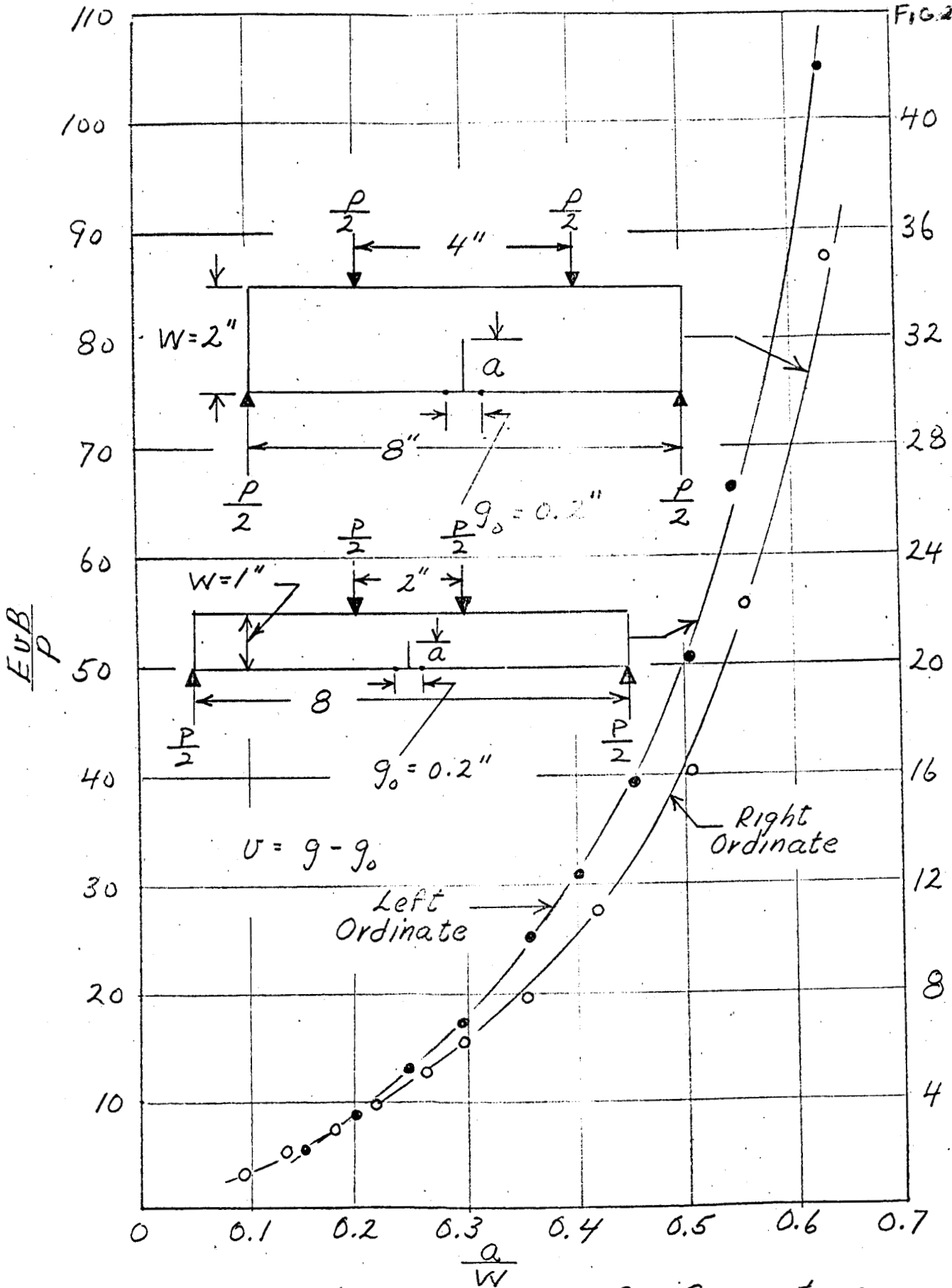

Fig. 21: Calibration Curves for Converting Displacement Measurements to Crack Lengths for Bend Specimens.